Doctor of Philosophy

Towards Predictive Bridge Maintenance: Element Condition, Damage Size, and Repair Cost Estimation

February 2023

Department of Civil and Environmental Engineering

The Graduate School of

Seoul National University

Taeyeon Chang

Towards Predictive Bridge Maintenance: Element Condition, Damage Size, and Repair Cost Estimation

A dissertation submitted to the Graduate School of
Seoul National University
in partial fulfillment of the requirements for the degree of
Doctor of Philosophy

By
Taeyeon Chang

December 2022

Approval Signatures of Dissertation Committee

_____
Moonseo Park

_____
Seokho Chi

_____
Changbum Ryan Ahn

_____
Seok-Been Im

_____
Seok Kim

Towards Predictive Bridge Maintenance: Element Condition, Damage Size, and Repair Cost Estimation

지도교수 지 석 호

이 논문을 박사학위논문으로 제출함

2022 년 10 월

서울대학교 대학원

건설환경공학부

장 태 연

장태연의 박사학위논문을 인준함

2022 년 12 월

위 원 장 박 문 서 (인)

부 위 원 장 지 석 호 (인)

위 원 안 창 범 (인)

위 원 임 석 빈 (인)

위 원 김 석 (인)

DEDICATION

To all of my family

ACKNOWLEDGEMENT

It is an honor to express my gratitude to those who have shown support and encouragement to me during my Ph.D. study.

First, I sincerely appreciate my supervisor, Prof. Seokho Chi, for his invaluable support and advice. He seriously pondered my concerns about research and life and gave me meaningful advice or clear direction. Thanks to his guidance, I was able to focus on my research and eventually complete my doctoral course. I also appreciate my Ph.D. committee members, Prof. Moonseo Park, Prof. Changbum Ahn, Dr. Seok-Been Im, and Prof. Seok Kim. I was able to improve the quality of my whole dissertation with their insightful comments and practical considerations.

Next, I would like to express gratitude to Dr. Kyung-Hoon Park and Dr. Jong-Wan Sun of the Korea Institute of Construction Technology, and Byung-Chul Lee, the director of G3WAY, for their kind advice on practice and data processing.

Many thanks to C!LAB members. The funny and happy time in the lab is an unforgettable memory for me. Especially, thanks to my lab seniors, Dr. Soram Lim, Dr. Jinwoo Kim, and Dr. Seonghyeon Moon, for giving me generous help with my research, coding, and graduate school life. I am thankful to my team colleagues, Gyueun Lee, Sihoo Yoon, and Geonwoo Kim, for their valuable time in meetings, discussions, and business trips.

I am also grateful to my undergraduate school friends, Minsun, Eunsun, and Youngkyung. Chattings and cheerings with you guys made it possible for me to continue studying civil and environmental engineering.

Finally, I extend my greatest gratitude to my beloved family, my father, Yangwon Chang, my mother, Eunok Lee, my only sister, Yunjung Chang, and my only brother-in-law, Seungbeom Woo. Their endless love and support were the driving force for me to study and research in good health. In particular, the love and wisdom that my father and mother taught me are the most precious assets in my life.

Once again, thank you all.

ABSTRACT

Towards Predictive Bridge Maintenance: Element Condition, Damage Size, and Repair Cost Estimation

Taeyeon Chang

Department of Civil and Environmental Engineering

The Graduate School of Seoul National University

To maintain bridges in an appropriate condition, bridge managers in many countries periodically inspect the condition and damage on bridge elements and establish a proper maintenance plan (e.g., repair or rehabilitation) and annual repair works with a limited budget. In this process, it is essential to detect the repair-required damage size on each element as the construction cost calculation method is defined as the product of the quantity and unit cost. Bridge maintenance practices, however, have difficulty in identifying repair-required damage size on bridge elements at a future time when maintenance is to be performed and estimating repair costs based on the expected damage size. This is because condition and damage on bridge

elements have a divergent phase over time since bridges have different characteristics, such as age, identification, and inspection history. Therefore, it is necessary to provide managers with three types of predictive information at a future time: where to undertake repair; how much repair-required damage there will be; and what the repair cost will be. It enables predictive bridge maintenance to maintain proper bridge condition by responding to future maintenance demands in advance. To do this, researchers have conducted data-driven studies using the bridge management system (BMS) data to estimate the future condition of bridge elements, identify the occurrence and severity of damage on each element, and analyze the future bridge repair costs at once. Despite the existing efforts, there are difficulties in anticipating the repair-required damage size and estimating the exact repair cost based on it; that is, it is still challenging to concretely determine the three types of predictive information.

Therefore, the primary objective of this research presented in this dissertation is to provide bridge managers with predictive maintenance information based on element condition, damage size, and repair cost estimation. To accomplish this objective, first, an optimized model is developed to estimate the element condition based on the outstanding algorithm and the influential variables using bridge information, environmental information, and inspection records. Second, to estimate the repair-required damage size on bridge elements, this study develops and compares the regression and classification models using bridge information, environmental information, and inspection records, including damage details. Last, this study proposed the estimation method of repair costs for the expected damage according to damage size and unit cost by repair method using bridge information, environmental information, inspection records, and repair records.

To validate the proposed methodology, the author implemented the experiment to conduct performance verification and demonstrate the superiority in providing predictive maintenance information by comparing with existing approaches. The results showed that the proposed methodology

could provide three types of information about predictive maintenance and estimate bridge repair costs more specifically and accurately in line with the construction cost calculation method. The predictive information can be used as a basis for bridge managers to prepare details and costs for repair works and establish a reasonable repair plan, including repair methods, priorities, and budgets.

In conclusion, this dissertation proposed the research methodology to enable predictive bridge maintenance based on element condition, damage size, and repair cost estimation. In particular, this research determined three specific types of information about predictive bridge maintenance based on the practical calculation method of repair costs. The author also scrutinized BMS data and determined data-driven approaches (e.g., an optimal algorithm and combination of variables) that fit the data to derive three specific types of information. To the best of the author's knowledge, this is a pioneering attempt to estimate specific damage size on bridge elements and identify future repair costs based on the estimated damage size and unit cost by repair method for predictive maintenance in the bridge management field. The developed methodology can assist in maintaining proper bridge condition by responding to future elements' damage and repair costs in advance. In addition, bridge managers can obtain a reasonable range for damage size and repair costs that may occur on elements in the future. It can help restrict unnecessary repair activities or exorbitantly high repair costs in bridge maintenance practices. Eventually, this research contributes to reducing bridge life-cycle costs and making society safer by preventing bridge safety accidents.

Keyword: Urban infrastructure management; Predictive maintenance; Bridge management system (BMS); Condition estimation; Bridge damage size; Bridge repair cost; Unit cost by repair method; Data-driven approaches

Student Number: 2017-27720

CONTENTS

LIST OF TABLES

LIST OF FIGURES

Chapter 1. Introduction

1.1. Research Background

Ensuring urban infrastructures are in reasonable condition is fundamental for public safety and the economy. In the case of bridges, damage and maintenance delays worldwide have caused catastrophic safety accidents, such as the Mississippi River Bridge collapse in 2007, which caused over 100 casualties (National Transportation Safety Board 2008). Bridge deterioration due to damage is also prone to progress more rapidly over time (Alsharqawi et al. 2018). For this reason, it is vital to maintain bridges in an appropriate condition through timely maintenance (Bu et al. 2015; Ellingwood 2010). To do this, bridge maintenance practices in many countries, including the United States and South Korea, take reactive maintenance strategies. Bridge managers inspect the condition and damage on bridge elements periodically and establish a proper maintenance plan (e.g., repair or rehabilitation) and annual repair works with a limited budget. Here, inspection and maintenance records are accumulated along with bridge information (e.g., age, location, structure type) in the bridge management system (BMS) database. Using BMS data can support managers in making

systematic maintenance decisions based on bridge information, inspection records, and maintenance history (Chang and Chi 2019; Morcous et al. 2002).

In particular, to plan repair works performed annually, it is essential to detect the repair-required damage size on each element as the construction cost calculation method is essentially defined as the product of the quantity and unit cost (Gordian 2022; Ministry of Land, Infrastructure and Transport [MOLIT] 2022a). Managers in the United States explore appropriate repair methods in response to the type and size of the inspected damage through an in-depth field inspection and annually allocate repair costs considering the unit cost of each repair method (American Association of State Highway and Transportation Officials [AASHTO] 2021; Federal Highway Administration [FHWA] 2018). South Korean practice also plans repair works and estimates repair costs in the same way by changing the collection method of the inspection records in the BMS database. In other words, the type, size, and expected repair method of the inspected damage and unit cost by the repair method on each element are collected instead of an emphasis on the location and severity of the damage (MOLIT 2019).

However, these practices have difficulty in identifying repair-required damage size on bridge elements at a future time when maintenance is to be performed and estimating repair costs based on the expected damage size.

This is because condition and damage on bridge elements have a divergent phase over time since bridges have different characteristics, such as age, identification, and inspection history (e.g., the latest inspection record). Take, for instance, the case where a bridge manager does not consider deck repair for two bridges (i.e., a bridge inspected three years ago and a bridge inspected one year ago) in the following year because the two decks had no damage according to the latest inspection record. In the following year, however, one of the bridges (i.e., the bridge inspected three years ago) suffered severe damage despite its latest inspection record. In this case, the manager would not have planned timely repair for the deck. Therefore, it is necessary to provide managers with three types of predictive information at a future time when the maintenance is to be performed: 1) where to undertake repair; 2) how much repair-required damage there will be; and 3) what the repair cost will be. It enables predictive bridge maintenance which is a decision-making strategy for maintenance plans and actions considering the forecasted future condition to maintain proper bridge condition by responding to future maintenance demands in advance (Hadjidemetriou et al. 2021).

To provide managers with information about predictive maintenance, researchers have conducted data-driven studies using BMS data. First, many researchers have developed models to estimate the future condition or

deterioration of bridge elements over time, such as condition rating 7 of the deck after three years (Bektas et al. 2013; Bolukbasi et al. 2004; Kim and Yoon 2010; Liu and Zhang 2020; Morcous 2005; Shan et al. 2016). In practice, BMS tried to estimate future repair costs by applying the average repair cost by element condition to the estimation result of the developed model. Although these practical efforts can provide repair-required elements and approximate repair costs by element, they have a limitation in accurately estimating repair costs based on the repair-required damage size. Second, at the damage level, BMS data-driven studies have been conducted to estimate the type, location, and severity of damage on each element, for example, two crackings in condition grade 'C' on the center of the deck (Chang and Chi 2019; Lim 2019; Lim and Chi 2021). Nevertheless, it is difficult to provide information on repair costs based only on the occurrence and severity of damage because the size and applied repair method are different for each instance of damage. Last, attempts have been made to estimate maintenance costs, including repair costs, based on bridge condition changes or environmental effects (Ghahari et al. 2019; Ghodoosi et al. 2017; Shi et al. 2019). However, it was difficult for these attempts to provide concrete information about which element to undertake repair on and how much repair-

required damage there would be. Table 1.1 summarizes the predictive information that the three existing approaches can provide.

Table 1.1 Summary of information provided by existing approaches

Category of predictive information	Existing approach		
	Element condition estimation	Damage identification	Repair cost estimation
Where to undertake repair	*	*	
How much repair-required damage there will be			
What the repair cost will be	**		*

Note: (*) indicates the approach provides the information; and (**) indicates the approach provides approximate information based on the average repair costs by element condition in practice.

1.2. Problem Statement

For predictive bridge maintenance, it is necessary to detect how much damage will need to be repaired on each bridge element at a future time according to the construction cost calculation method, which is defined as the product of the quantity and unit cost. Repair cost can then be estimated based on the expected damage size and unit cost by repair method. To provide bridge managers with information about predictive maintenance, many researchers have attempted to estimate the future condition or deterioration of bridge elements (e.g., condition rating 7 of the deck after three years), to identify the occurrence, location, and severity of bridge damage (e.g., two crackings in condition grade 'C' on the center of the deck), and to estimate the future bridge repair costs at once by using BMS data. Despite promising results in the existing studies, they share difficulties in anticipating the repair-required damage size and estimating the exact repair cost based on it. That is, it is still challenging to concretely determine for predictive bridge maintenance: 1) where to undertake repair; 2) how much repair-required damage there will be; and 3) what the repair cost will be.

1.3. Research Objectives and Scope

This dissertation aims to provide bridge managers with predictive maintenance information based on element condition, damage size, and repair cost estimation. Three specific objectives were established to address the three challenges presented above. The overall research framework is illustrated in Figure 1.1.

Objective 1: To estimate the bridge elements' condition based on outstanding algorithm selection and influential variables identification by using bridge information, environmental information, and inspection records to provide information on where to undertake repair.

Objective 2: To estimate the repair-required damage size on bridge elements through a comparison of the regression model and the classification model by using bridge information, environmental information, and inspection records to provide information on how much repair-required damage there will be.

Objective 3: To estimate bridge repair costs for the expected damage according to damage size and unit cost by repair method by using bridge

information, environmental information, inspection records, and repair records to provide information on what the repair cost will be.

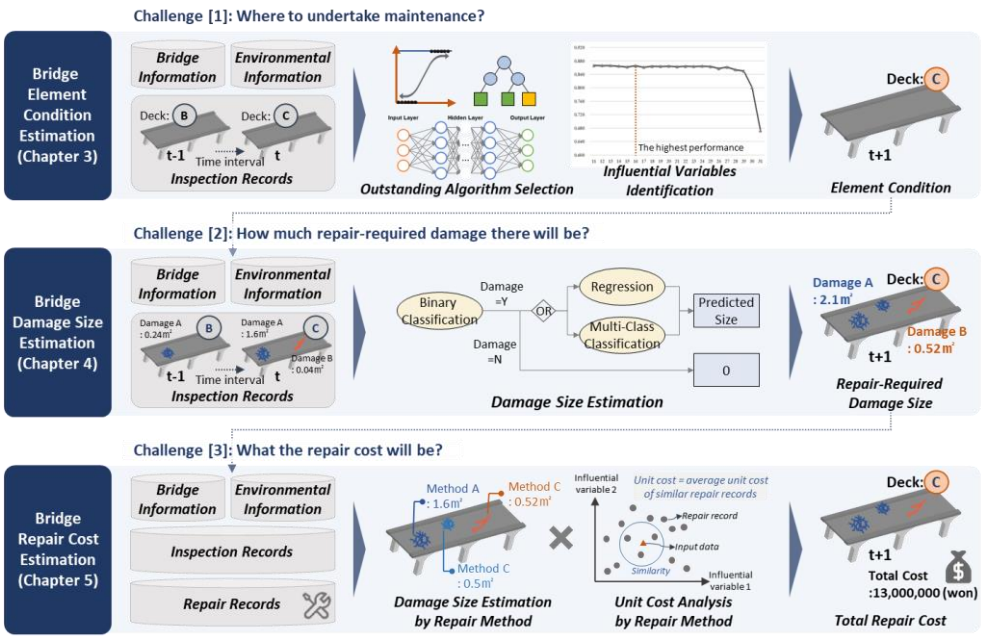

Figure 1.1 Research Framework

This dissertation focused on concrete-girder bridges with pre-stressed concrete (PSC) girders or reinforced concrete (RC) girders as the main superstructure types because concrete-girder bridges made up the largest proportion (47.4%) among the bridges managed by the Korean Bridge Management System (KOBMS) in 2021, compared to other main structure types, such as ramen bridges (24.4%) and steel bridges (21.0%). Among the

major bridge elements, the author also focused on the deck, which directly supports the load on the bridge and is also known as a structural element that shows the fastest deterioration (Huang 2010; Lim and Chi 2019; Morcous et al. 2002). Because of this, the deck plays the most crucial role in bridge safety and serviceability. Deck repair costs in the KOBMS accounted for the highest proportion (55.0%) of repair costs for structural elements of concrete-girder bridges from November 2012 to December 2021.

1.4. Dissertation Outline

This dissertation consists of seven chapters. The details of each chapter are presented below.

Chapter 1. Introduction: This chapter introduces the research background, problem statement, research challenges, objectives, framework, and scope.

Chapter 2. Literature Review: This chapter provides information about bridge maintenance practice and BMS. Existing approaches and practical efforts using BMS data are also reviewed for predictive bridge maintenance related to the research challenges.

Chapter 3. Bridge Element Condition Estimation: This chapter presents a research process to develop an optimized model to estimate bridge elements' condition using BMS data. A deck condition estimation model is developed, and the results of this chapter are discussed in terms of outstanding algorithm selection, influential variable identification, model evaluation, and model validation.

Chapter 4. Bridge Damage Size Estimation: This chapter presents a research process to estimate repair-required damage size on bridge elements using BMS data. The regression and classification models are developed and compared in terms of strength, weakness, and performance. The final estimation model is then selected based on the model performance.

Chapter 5. Bridge Repair Cost Estimation: This chapter presents a research process to estimate bridge repair cost according to damage size and unit cost by repair method using BMS data. The author conducts data exploration and develops a damage portion estimation model by each damage type to estimate damage size by repair method. The unit cost is also identified based on the influential variable's similarity by repair method.

Chapter 6. Experimental Results and Discussions: In this chapter, experiments are implemented to conduct performance verification and validate the superiority of the proposed methodology for predictive bridge maintenance by comparison with existing approaches. The practical applications and contributions of this study are discussed through the experimental results and discussions.

Chapter 7. Conclusions: This chapter summarizes and discusses the objectives, achievements, findings, and contributions of this research. Recommendations for future research are also provided.

Chapter 2. Literature Review

This chapter introduces bridge maintenance practices in which research challenges are identified. Also, an overview of a bridge management system (BMS) is described, including specific information on BMS data with examples for South Korea and the United States. This chapter then reviews existing studies for predictive bridge maintenance using BMS data related to the research challenges and provides the limitation of the previous studies.

2.1. Bridge Maintenance Practice

Bridge maintenance to preserve bridges in the appropriate condition is performed according to inspection, plan, and action. Bridge maintenance practices in many countries, including the United States and South Korea, commonly take reactive maintenance strategies. The maintenance process includes inspecting repair-required condition and damage on bridge elements and establishing a proper repair plan (e.g., repair size, method, cost, and time) within a limited budget based on the inspected information (Bu et al. 2015; Chang and Chi 2019; Ellingwood 2010; Morcous et al. 2002). Specifically, the details and costs of repair works are established in line with the construction cost calculation method. The method is essentially defined as the

product of quantity and unit cost (Gordian 2022; MOLIT 2022a), as represented in Equation 2.1.

$$Construction\ \ cost = (Quantity) \times (Unit\ \ cost) \times (Unit) \quad (2.1)$$

It is thus essential to detect the repair-required damage size on each element and unit repair cost to plan and estimate repair works performed. In this aspect, the bridge maintenance practices 1) inspect and diagnose the condition and damage on each element (e.g., deck, girder, abutment/pier) through an periodic in-depth field inspection, 2) explore proper repair methods in response to the type and size of the inspected damage, and 3) annually allocate repair costs considering the unit cost of each repair method. Specific practices in South Korea and the United States are as follows.

In South Korea, bridge managers conduct an in-depth inspection periodically for each bridge every two to six years depending on the condition grades of bridges, according to the Special Act on the *Safety Control and Maintenance of Establishments* by Ministry of Land, Infrastructure, and Transport (MOLIT). Certified inspectors survey repair-required damage size, investigate the expected repair methods for each damage, and synthetically diagnose the condition grade of the element. Every year, Korean managers

also identify repair-required elements' condition (e.g., decks with condition grade 'C' or 'D') and repair-required damage size (e.g., $2.1m^2$ cracking in a deck) by examining the latest inspection history from the KOBMS database (MOLIT 2021). Managers then estimate the repair cost for each repair-required element by applying the repair-required damage size to the unit cost for each expected repair method (Korea Institute of Civil Engineering and Building Technology [KICT] 2022b). To estimate the repair cost, the KOBMS recently changed its inspection record collection method to record the type, size, expected repair method, and unit cost by repair method instead of the location or severity of damage. Figure 2.1 describes the concept and example of bridge repair cost estimation in Korean practice.

● **Concept of Repair Cost Calculation in Korean practice**

Bridge Repair Cost

$= \alpha \times \beta \times$ ***(Repair-Required Damage Size)***

Element Condition (e.g., Grade 'A' or 'C') ***Unit Cost by Repair Method***

● **Example of Repair Cost Estimation using the KOBMS Database**

Bridge No.	Inspection Year	Element	Condition Grade	Damage Type	Damage Size	Repair Method	Unit Cost	Allocated Repair Cost (1,000won)
000078	2019	Deck	C	Map Cracking	0.30 (m^2)	Surface Repair	42.0 (m^2/1,000won)	**12.6**
000078	2019	Deck	C	Cracking	98.00 (m)	Grouting	90.0 (m/1,000won)	**8,820.0**
000090	2019	Deck	D	Breakage	1.00 (m^2)	Section Repair	450.0 (m/1,000won)	**450.0**
...	...	...	...	...	...	...	...	...

Figure 2.1 Concept of bridge repair cost calculation in practice

Practice in the United States is similar to that in South Korea. An in-depth inspection is periodically performed within two years, according to the *National Bridge Inspection Standards* by Federal Highway Administration (FHWA). At the element level, the condition states are assessed based on the type, size, and severity of damage (i.e., defect) (AASHTO 2010). The appropriate repair methods (i.e., activities) are then taken in response to the type and severity of the inspected damage. Repair costs are estimated, considering which repair method will be performed and the unit cost of the repair method (AASHTO 2021; FHWA 2018).

However, these practices have difficulty in identifying repair-required damage size on bridge elements at a future time when maintenance is to be performed and estimating repair costs based on the expected damage size. Since bridges have different characteristics, such as age, identification, and inspection history (e.g., the latest inspection record), the latest inspection record, which is the basis for bridge maintenance process in practice, may not be consistent with the elements' condition and damage at a future point in time. For this reason, it is still problematic to identify repair-required damage size on bridge elements at a future time and estimate the repair costs based on the expected damage. Thus, it is necessary to provide managers with three types of predictive information at a future time when the maintenance is to be performed: 1) where to undertake repair; 2) how much repair-required damage there will be; and 3) what the repair cost will be. It enables predictive bridge maintenance which is a decision-making strategy for maintenance plans and actions considering the forecasted future condition to maintain proper bridge condition by responding to future maintenance demands in advance (Hadjidemetriou et al. 2021)..

2.2. Bridge Management System (BMS)

A bridge management system (BMS) is a systematic and computerized approach to managing a network of bridges (Scherer and Glagola 1994; Zhao and Tonias 2013). Many countries, including South Korea and the United States, have established BMS to make strategic and cost-efficient maintenance plans within a given budget (Gralund and Puckett 1996; Morcous 2005). For that purpose, the BMSs generally 1) accumulate bridge information, periodic inspection records, and maintenance records into a database, 2) analyze and predict the deterioration and degradation of the bridge condition, and 3) optimize bridge maintenance decisions (Chang and Chi 2019; MOLIT 2019; Morcous et al. 2002).

Using the data accumulated in the BMS databases supports bridge managers in making systematic maintenance decisions. The data accumulated in the BMS database generally contain basic inventory information, inspection information, and intervention information based on the report investigating 35 BMSs (Mizaei et al. 2014). Basic inventory information includes general information on a bridge (e.g., location and management agency) and structural information (e.g., material and structural type for each bridge element). Inspection information is collected from periodic inspection records at the level of entire bridge, main component, element, and damage

(e.g., inspection date, inspection type, and inspection results for each level). Intervention information is collected from maintenance and preservation records. They include repair period, methods, and cost information.

In South Korea, since 1995, the Korean Bridge Management System (KOBMS), which is operated by the Korea Institute of Civil Engineering and Building Technology (KICT), was developed to accumulate data concerning bridge information (i.e., general and structural information) and bridge inspection records and to establish maintenance strategies using the data. As of 2021, the KOBMS had managed and updated data of more than 9,000 bridges located in the Provinces of South Korea (except Seoul) that were built from 1962 to 2021. The data contain basic inventory information, including general information (e.g., bridge class, location, and length) and structural information (e.g., element structure type and material for each span or support). The inspection records of the KOBMS include information collected from bridge element-level in-depth inspections that have been performed periodically since 1994. The inspection information mainly consists of the inspection date, bridge elements' condition, type and size of repair-required damage, and the expected repair methods for each damage, as illustrated in Figure 2.1. Particularly, the bridge condition at the element level is graded into five categories ranging from 'A' (best condition) to 'E' (worst

condition), comprehensively reflecting the inspection results in terms of visual damage, structural integrity, and safety of the bridge. Among the five grades, 'C,' 'D,' and 'E' indicate damaged condition that has to be repaired. In addition, repair records of the KOBMS include information collected from bridge repair constructions that have been performed after 2012. The repair information (as known as intervention information) contains repair construction start/end date, method, size, and cost.

In the United States, the National Bridge Inventory (NBI), which is a representative BMS database, has accumulated data of more than 600,000 bridges with 116 items of information collected in accordance with the *National Bridge Inspection Standards* by FHWA (Bolukbasi et al. 2004; Jootoo and Lattanzi 2017). According to the *Recording and Coding Guide for the Structure Inventory and Appraisal of the Nation's Bridges* by FHWA (1995), the accumulated data include basic inventory information, inspection information, and intervention information. Basic inventory information contains general information (e.g., bridge length and the number of spans) and structural information (e.g., design load and structure type). Inspection information includes inspection date, condition ratings at the major component level (e.g., deck, superstructure, and substructure), and proposed type of maintenance work. The condition ratings of major components are

assigned on the 10 scales ranging from 0 (worst condition) to 9 (best condition), as provided in NBI Item No. 58-62. In addition, condition and damage (i.e., defect) at the element level are inspected and collected as inspection information by AASHTO (1997). Intervention information also contains date and cost related to repair, improvement, and reconstruction that were taken in response to the type and severity of the inspected damage (AASHTO 2021; FHWA 2018).

2.3. Existing Studies for Predictive Bridge Maintenance

Predictive bridge maintenance is a decision-making strategy for maintenance plans and actions considering the forecasted bridge condition (Hadjidemetriou et al. 2021). As a large amount of data in a BMS database have been accumulated and updated, many researchers have conducted data-driven studies using BMS data to support predictive bridge maintenance for managers. A data-driven approach makes knowledge or decisions based on data instead of intuition. These studies can be categorized into three groups: element condition estimation, damage identification, and maintenance cost estimation. The detailed reviews and limitations of the three groups are as follows.

2.3.1. Element Condition Estimation

The researchers have tried to estimate the future condition of bridge elements by utilizing diverse algorithms and identifying influential factors that affect the bridge element's condition. The algorithms applied in existing studies can be grouped into deterministic, stochastic, and artificial intelligence (AI) algorithms (Morcous et al. 2002). First, deterministic algorithms, represented by regression methods, have been commonly applied to predict the deterioration rate of elements over time by defining the

relationships between the bridge condition and selected variables, including the bridge age (Bolukbasi et al. 2004). Kim and Yoon (2010) conducted a regression analysis to derive the deterioration rate of bridge deck, in which the condition rating of the deck ranged from 0 (poor) to 9 (good), and to explore critical variables influencing bridge decks' deterioration in cold regions using the NBI database. Shan et al. (2016) also applied logistic regression to estimate the probability of deterioration of bridge superstructure based on bridge information (i.e., age, design load, and structure length) using the 2013 NBI database. Second, stochastic algorithms are represented by Markovian chains, which are used in the Pontis BMS in the United States. Previous studies estimated the probability of future condition transitions based on the current condition at the levels of the major structures (e.g., deck, superstructure, and substructure) (Agrawal et al. 2021; Cesare et al. 1993; Morcous 2006; Scherer and Glagola 1994).

Last, many studies have recently used AI algorithms, which include tree-based algorithms and neural network algorithms. By utilizing the decision tree, which is one of the common tree-based algorithms, for instance, elements' condition can be estimated according to the classification rules generated from input variables such as general and structural bridge information and inspection history (Bektas et al. 2013). Morcous (2005)

developed a decision tree model for estimating the future condition of concrete bridge decks based on the data from Quebec, Canada. Various types of neural network algorithms have also been widely investigated. Huang (2010) developed an artificial neural network (ANN)-based model to estimate future deck condition states, which were divided into five labels from acceptable to very severe, in the Wisconsin BMS database; a deep neural network (DNN) with multiple hidden layers was adopted to the NBI data for Missouri bridges for predicting the deterioration of deck, superstructure, and substructure (Ali et al. 2020). Liu and Zhang (2020) utilized a convolution neural network (CNN) to classify the condition grades of major components for the immediate next inspection by using the historical data (from 1992 to 2017) for Maryland and Delaware highway bridges sourced from the NBI database.

Meanwhile, the BMS tried to estimate future repair costs by applying the average repair cost by element condition to the result of the element condition estimation model. In South Korean practice, the average repair cost for each condition grade of element is determined based on historical inspection and repair records from the KOBMS database. For instance, Table 2.1 shows the average and median of repair costs by deck condition grades as of June 2021, which is extracted from KICT (2021). Bridge managers

estimate the repair cost for each element by using the average repair cost according to the expected condition grade.

Table 2.1 Example of repair costs by deck condition grades

Condition grade of deck	Repair cost as of June 2021 (1,000won/m^2)	
	Average	Median
A	3.18	0.20
B	5.87	0.74
C	14.45	3.95
D	59.94	35.04
E	68.33	49.46

2.3.2. Damage Identification

Previous studies have estimated bridge condition at the damage level by utilizing the algorithms. Zhao and Chen (2002) estimated the occurrence of cracking and spalling on superstructures and substructures to support a BMS to diagnose the deterioration of concrete bridges. They utilized a probabilistic neural network based on Singapore bridge data. Chang and Chi (2019) developed the estimation model on the occurrence of representative damage types to five elements (i.e., deck, girder, cross beam expansion joint, and pavement) by using logistic regression based on the KOBMS data. The damage types included dirt deposition of an expansion joint, crazing crack of a deck, and steel deformation of a girder.

Lim and Chi (2019) also tried to apply the extreme gradient boost (XGBoost), which is a representative tree-based boosting algorithm, to the KOBMS data to estimate the occurrence of damage on decks. Lim (2019) further developed the AI-based model and system to provide bridge inspectors with the expected type, location, grade, and severity of the damage at the individual bridge and region level. The DNN-based model was also developed to predict the number of damage by condition grade for seven types of damage on the deck (e.g., two crackings in condition grade 'C' on deck) by using the environmental information (Lim and Chi 2021).

2.3.3. Maintenance Cost Estimation

The researchers have analyzed bridge data with a focus on bridge maintenance costs, including repair costs and rehabilitation costs. Previous studies have conventionally attempted to suggest bridge maintenance optimization and the expected costs by analyzing the effects of maintenance activities on the condition of bridge structures in the perspective of the life-cycle (construction, inspection, maintenance, and failure) of deteriorated structures (Frangopol and Kong 2000; Ghodoosi et al. 2017; Kong and Frangopol 2003; Liu and Frangopol 2005). For instance, Ghodoosi et al. (2017) tried to provide the most cost-effective optimal maintenance scenario

in the long term by predicting the deterioration of the superstructure over time and analyzing the effect of each maintenance activity based on the asset inventory along with the maintenance actions list in Canada.

Some researchers have also conducted studies to estimate the maintenance costs by considering various factors, including changes in the bridge condition. Gong and Frangopol (2020) calculated the optimal solution of the utility function to derive the optimal bridge maintenance cost according to factors such as maintenance criteria, external traffic loads, and structural resistance of bridge elements by calculating the optimal solution of the utility function. Ghahari et al. (2019) identified factors influencing bridge repair cost (e.g., traffic loading, annual temperature, and condition ratings of superstructure and substructure) and estimated expected annual repair cost. They used annual repair cost expenditure data sourced from the FHWA's Office of Highway Policy Information and bridge inspection data from the NBI database. Bridge routine maintenance cost was also predicted based on multiple linear regression. The repair cost prediction model utilized traffic factors, bridge age, regional factors, and bridge scale factors (e.g., the length, width, and area of bridge) as independent variables (Shi et al. 2019).

2.3.4. Limitations of Existing Studies

The previous research showed the potential benefits of data-driven approaches using BMS data for estimating the future condition of bridge elements, damage occurrence and severity on elements, and maintenance costs. Nevertheless, existing studies had limitations in providing managers with three types of predictive information about a future time when maintenance will be performed: where to undertake repair (i.e., which element to undertake repair on); how much repair-required damage there will be; and what the repair cost will be.

First, many studies have shown promising results in estimating the future condition of bridge elements by utilizing diverse algorithms and identifying influential factors that affect the bridge element's condition. Furthermore, the practical efforts can provide repair-required elements and approximate repair costs by element. However, they are limited in being able to accurately estimate repair costs based on the repair-required damage size. At the damage level, second, previous researchers conducted data-driven studies to estimate the occurrence and severity of the damage; but they could not offer information on repair costs because the size and applied repair method are different for each instance of damage. Last, the previous studies tried to estimate the maintenance costs, including repair costs, based on the

bridge condition changes and environmental effects. However, it was difficult to derive concrete information about which element to undertake repair on and how much repair-required damage there would be.

Consequently, although it is necessary to detect how much damage will need to be repaired on each element at a future time according to the construction cost calculation method, the existing studies have limitations in anticipating the repair-required damage size and estimating the exact repair cost based on it for predictive bridge maintenance; that is, it is still challenging to determine 1) where to undertake repair, 2) how much repair-required damage there will be, and 3) what the repair cost will be, at a future point in time. To address these research challenges, this research provides bridge managers with predictive maintenance information based on element condition, damage size, and repair cost estimation using BMS data.

Chapter 3. Bridge Element Condition Estimation

This chapter provides a research process for bridge element condition estimation. As described in Section 2.3.1 “Element Condition Estimation,” considerable attempts have shown potential benefits for developing condition estimation models for bridge elements based on the BMS data. However, existing studies had a limitation that the developed models only focused on the BMS data used in each research. It makes it difficult to deal with the BMS data that continuously become heterogeneous and complex by period or country. For this reason, it is still problematic to construct a robust and generally applicable condition estimation model for bridge elements regardless of the characteristics of the BMS data.

To address the problem, the author proposes a research process to develop an optimized and universal model to estimate bridge elements’ condition using data-driven approaches. The target of the estimation model was set as the condition grades of the bridge elements (e.g., condition grade ‘C’ of deck) expected in the next inspection. Figure 3.1 illustrates the proposed research process. First, the KOBMS data for analysis was prepared through data collection and preprocessing. Second, diverse types of data-driven algorithms were explored and trained using training data by tuning

hyperparameters. The outstanding algorithm was then selected based on the results of comparing the performance of the explored algorithms using the testing data. Third, the author identified the combination of influential variables that maximize the performance of the previously selected algorithm by utilizing the recursive feature elimination (RFE) based on permutation importance. Last, an optimized model was developed by combining the two results (i.e., the results of the outstanding algorithm selection and the influential feature identification).

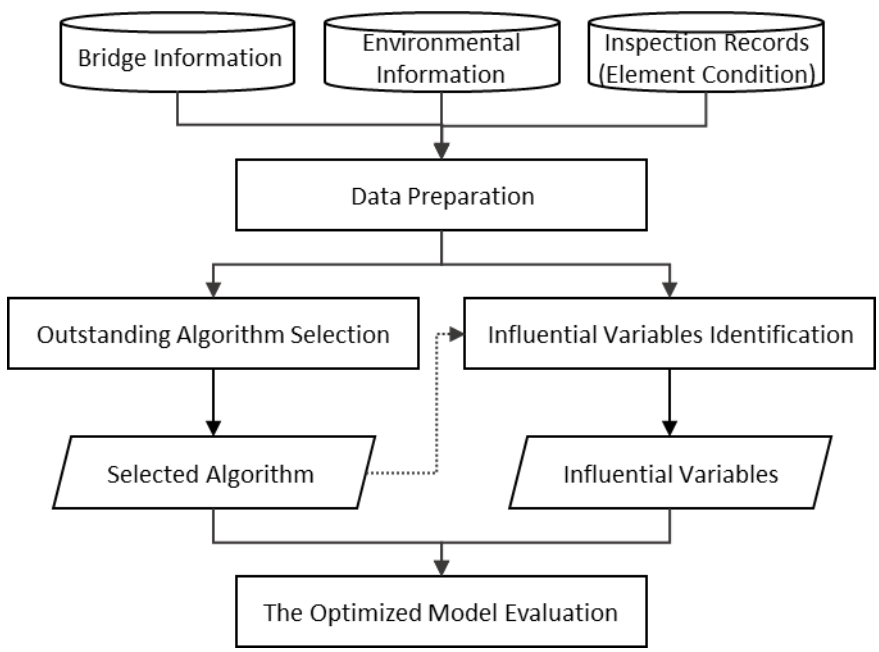

Figure 3.1 Research process of bridge element condition estimation

3.1. Data Preparation

3.1.1. Data Collection

The BMS data for this chapter were collected from the KOBMS database. The collected data include bridge information (i.e., general and structural information) and inspection records for the bridges in South Korea. The general information contains a total of 17 variables (e.g., bridge class, bridge length, and main superstructure type) by bridge. The structural information contains 14 variables regarding the deck and superstructure (e.g., deck thickness, deck rebar strength, material, deck pavement type for each bridge span) and 15 variables regarding the substructure (e.g., abutment/pier type, abutment/pier strength, and the number of bearing for each bridge span).

The inspection records were accumulated through 11,230 in-depth inspections of 4,688 bridges from 2009 to 2021. According to this dissertation scope, the author extracted the inspection records of decks on 4,085 in-depth inspections of 2,064 concrete-girder bridges. The inspection records include inspection year, bridge age, condition grades (CG_t) of deck, and inspection history for each span (or support) of bridge. The condition grades at the element level are categorized into five grades, i.e., 'A' (excellent), 'B', 'C', 'D', and 'E' (poor) (MOLIT 2021). Among the five grades, 'C,' 'D,' and 'E' indicate damaged condition that has to be repaired. The inspection history

contains past condition grades by elements and time intervals between past and current inspections. Since in-depth inspections in South Korea are usually performed every two to six years, past condition grades and time intervals for two past inspections were collected taking into consideration the period in which the inspection records have been accumulated in KOBMS (i.e., from 2009 to 2021). In other words, the inspection history collected for this research included the first past condition grade (CG_{t-1}) of deck, the first past inspection interval (I_{t-1}) (defined as the difference between the current inspection year, t and the first past inspection year, $t-1$), the second past condition grade (CG_{t-2}) of deck, and the second past inspection interval (I_{t-2}) (defined as the difference between the first, $t-1$ and the second past inspection year, $t-2$).

In addition, environmental information was collected from other databases. Many previous studies identified the influence of environmental information, such as traffic volume and weather factors, on the bridge element's condition by utilizing data-driven approaches. For example, Kim and Yoon (2010) explored environmental information (e.g., traffic volume, precipitation, and temperature) influencing bridge decks' deterioration in cold regions by using a regression. Huang et al. (2010) explored significant deterioration factors for RC bridge decks by damage types using a Rough set

theory; for instance, the major factors influencing rebar corrosion were identified as peak monthly rainfall and traffic volume. Several types of environmental information, such as temperature, rainfall, and humidity, were also considered to develop a DNN-based damage prediction model for bridge decks (Lim and Chi 2021).

In this research, traffic and weather information were obtained from the Traffic Monitoring System in Korea (MOLIT 2022b) and the Korea Meteorological Administration (KMA) (KMA National Climate Data Center 2022) to collect environmental information around the bridges entered into the KOBMS. Specifically, the author calculated the average values of the previous three years for each inspection year to obtain environmental information that affected the bridge condition for inspection intervals. The average values were calculated for two types of traffic information—average daily traffic (ADT) and average daily truck traffic (ADTT)—and 11 types of weather information (e.g., annual heatwave days, annual average temperature, and annual precipitation) at the measurement point closest to the bridge location. In particular, since this environmental information changes over time, environmental information based on past inspections was also collected. For example, environmental information included ADT from the past two

inspections (i.e., ADT_{t-1} and ADT_{t-2}) along with ADT based on the current inspection, ADT_t.

3.1.2. Data Preprocessing

The collected data were preprocessed based on data cleaning, integration, reduction, and transformation to raise the completeness of the data to improve a model's performance (Han et al. 2011). First, data cleaning is a step for the treatment of noisy data and missing values. For instance, the author eliminated the inspection records with noisy values other than the five condition grades (e.g., 'X' and 'Q'), and the condition grade 'D' and 'E' were replaced with the grade 'Under C' since the condition grade 'E' for decks accounted for 0.14% in the extracted inspection records. The missing values of less than 20% in the numeric variables were replaced with the median values of the variables. Particularly, in the case of variables related to the inspection history, if the past inspection was not recorded, the values of the past condition grades were represented as 'F,' and the values of the past inspection intervals were represented as zero. Also, since bridge inspections should be carried out within six years according to the inspection guidelines (MOLIT 2021), the values of the past inspection intervals over six years were substituted with the number six. Next, the data within multiple data tables

were integrated to make one dataset so that the data could be input into the model.

In integrated data, data reduction was then performed to remove variables that do not affect analysis results. The removed variables can include the variables with duplicate meanings and those with a high proportion of missing values. For example, ‘construction year’ and ‘inspection year,’ which were variables that had duplicate meanings with ‘bridge age,’ were removed because ‘bridge age’ is defined as the difference between the inspection year and the construction year. The numerical variables with more than 20% missing values, such as ‘deck rebar diameter’ and ‘girder strength,’ were also removed. In the case of a categorical variable, such as ‘region,’ the data with missing values were deleted.

In addition, since the variable redundancy increases the dimension of the input variable and may confuse the analysis results, it is necessary to remove one of the duplicated variables (Huang et al. 2012). In order to examine possible variable redundancies across the integrated data, the author calculated the Pearson correlation coefficient between numeric variables and the Cramer’s V coefficient between categorical variables (Han et al. 2011; Wu et al. 2014). The threshold that indicates the existence of variable redundancy was defined as 0.6 according to previous research (Reddy et al. 2013). The

condition grade with four categories from 'A' to 'under C' were converted into four numbers (i.e., 0.1, 0.2, 0.4, and 0.7) in the correlation analysis with numerical variables (MOLIT 2021). Among two redundant variables with a high coefficient, one variable with a lower correlation with the target variable was then removed.

Based on the results of the Pearson's correlation coefficient analysis of the combinations of numerical variables, 12 combinations of variables with correlation coefficients over 0.6 were investigated; e.g., 'total width – road width (0.97)' and 'total width – number of lanes (up/down) (0.92).' The variables, including 'road width' and 'total number of lanes (up/down),' were then removed. In particular, as a result of the analysis of environmental information, the correlation coefficients between the value based on the current inspection and the value of the past inspection for each variable were all confirmed to be over 0.6; e.g., '$ADT_t - ADT_{t-1}$ (0.99)' and '$ADT_t - ADT_{t-2}$ (0.98).' The variables based on the past inspections, including ADT_{t-1} and ADT_{t-2}, were thus removed. On the other hand, based on the results of the Cramer's V coefficient calculation between categorical variables, the combinations of variables with correlation coefficients over 0.6 were 'region – competent authority (1.00),' 'management agency – competent authority (1.00),' and 'main superstructure type – deck material (0.61).'

‘Competent authority’ and ‘deck material’ were then removed because they had a close to zero correlation coefficient with ‘condition grade (CG_t) of deck.’ Last, the data were transformed into appropriate forms for analysis. Numerical variables were normalized based on z-score normalization, and categorical variables were converted to numbers where necessary.

As a result of the preprocessing steps, the final dataset for developing the deck condition estimation model consisted of a tabular format with 31 explanatory variables (21 numerical variables and 10 categorical variables) and one target variable (i.e., condition grade of deck) and 17,567 of data. Table 3.1 lists the 32 variables included in the final dataset and explains the actual values and the value type by each variable, and Table 3.2 shows the sample of the final dataset for developing the deck condition estimation model. Also, the target variable (i.e., the condition grade of a deck) in the final dataset was distributed as ‘A’ (22.2%), ‘B’ (53.1%), ‘C’ (21.6%), and ‘Under C’ (3.0%) (Figure 3.2).

Table 3.1 Variables of the final dataset for deck condition estimation

Concept	Variable	Actual values (or range)	Value type
General information (12)	Region	4 metropolitan cities and 8 provinces	C
	Facility class	3 class	C
	Management agency	13 main agencies (e.g., Seoul, Busan, and Wonju)	C
	Bridge length	10–1,194.7 (m)	N
	Total width	4.9–56 (m)	N
	Pavement area	19.3–13,756.3 (m^2)	N
	Height	1.2–182.6 (m)	N
	Water depth	0–69 (m)	N
	Maximum span length	8–160 (m)	N
	Main superstructure type	PSC I-shaped, PSC Box, PSC Slab, PSC Hole, RC Slab, RC Hole, RC T-shaped, and RC Box	C
	Main substructure type	18 types (e.g., T-shaped pier, rahmen pier, and wall pier)	C
	Design live load	DB−13.5 (24.3 ton), DB−18 (32.4 ton) and DB−24 (43.2 ton)	C
Structural information for deck (7)	Deck waterproofing type	Asphalt, sheet, mortar, film, none, and etc.	C
	Deck thickness	10–290 (cm)	N
	Deck strength	210–4,000 (kg/cm^2)	N
	Deck rebar strength	30–6,400 (kgf/cm^2)	N
	Deck rebar spacing	1–250 (cm)	N
	Deck pavement type	Asphalt, concrete, LMC, none, and etc.	C
	Deck pavement thickness	2–10 (cm)	N

Environmental information based on the current inspection (7)	Average daily traffic (ADT)	152.8–50,666 (vehicles/day)	N
	Annual freeze-thaw frequency	0–22.3	N
	Annual heatwave days	0–41 (days)	N
	Annual average temperature	7.2–15.3 (℃)	N
	Annual precipitation	760.4–2,082.8 (mm)	N
	Winter snowfall	0–47.3 (cm)	N
	Annual average relative humidity	55.1–82.1 (%)	N
Inspection records (6)	Bridge age	2–47 (years)	N
	Condition grade of deck (CG_t)*	A, B, C, and Under C	C
	First past condition grade of deck (CG_{t-1})	A, B, C, Under C, and F	C
	First past inspection interval (I_{t-1})	0–6 (years)	N
	Second past condition grade of deck (CG_{t-2})	A, B, C, Under C, and F	C
	Second past inspection interval (I_{t-2})	0–6 (years)	N

Note: PSC = pre-stressed concrete; RC = reinforced concrete; LMC = latex modified concrete; (*) = the target variable; C = categorical variable; and N = numerical variable.

Table 3.2 Sample of the final dataset for deck condition estimation

Bridge No.	Span No.	Genenral information (12)		Structural information (7)		Environmental information (7)		Inspection records (6)					
		Region	Bridge length	Deck pave-ment type	Deck thick-ness	ADT	Annual freeze-thaw freqency	Bridge age	CG_t (*)	CG_{t-1}	I_{t-1}	CG_{t-2}	I_{t-2}
002560	1	Seoul	26.8	Asphalt	25	13,870	12.3	27	C	C	2	F	0
002560	2	Seoul	26.8	Asphalt	25	13,870	12.3	27	B	B	2	F	0
029882	1	Jeolla-nam-do	120.3	Asphalt	25	4,222	2.0	11	B	B	2	A	4

Note: ADT = average daily traffic; CG_t(*) = condition grade of deck (target variable); CG_{t-1}= the first past condition grade of deck; I_{t-1}= the first past inspection interval; CG_{t-2}= the second past condition grade of deck; and I_{t-2}= the second past inspection interval.

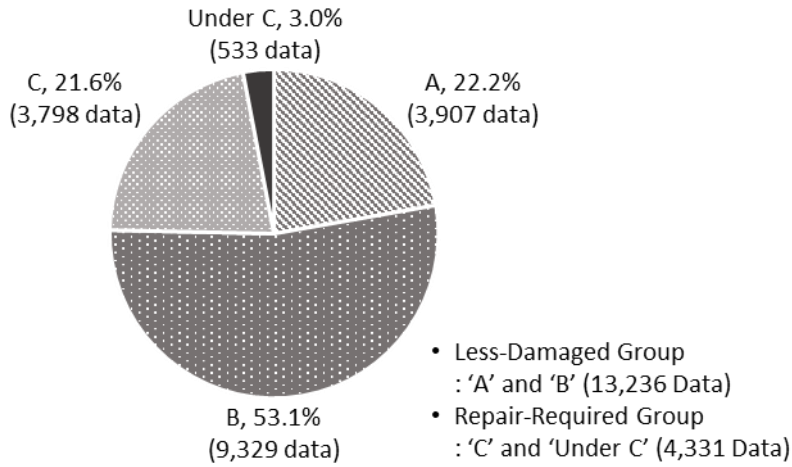

Figure 3.2 Data distribution for the deck condition grades

3.2. Outstanding Algorithm Selection

Since the condition grade of deck, which is the target variable for this research, is divided into four classes, it was necessary to implement a multi-class classification that could predict multiple classes at the same time. However, owing to the severity of the data imbalance between the classes in the final dataset, as represented in Figure 3.2, it is difficult to train the minority class (i.e., condition grade 'Under C' accounting for 3% of the total data) and achieve a good performance for classifying four classes at once in a multi-class classification. Thus, as shown in Figure 3.3, the author tried to conduct several independent binary classifications to estimate the final condition grade of the deck: 'Sub-model (1),' which classified the entire preprocessed data into two classes (i.e., a less-damaged group including condition grade 'A' and 'B' and a repair-required group from condition grade 'C' to 'E'); 'Sub-model (2),' which classified the data belonging to the less-damaged group into condition grade 'A' and 'B'; and 'Sub-model (3),' which classified the data belonging to the repair-required group into condition grade 'C' and 'Under C.' According to the research process in Figure 3.1, the author implemented the detailed steps to develop and evaluated each sub-model.

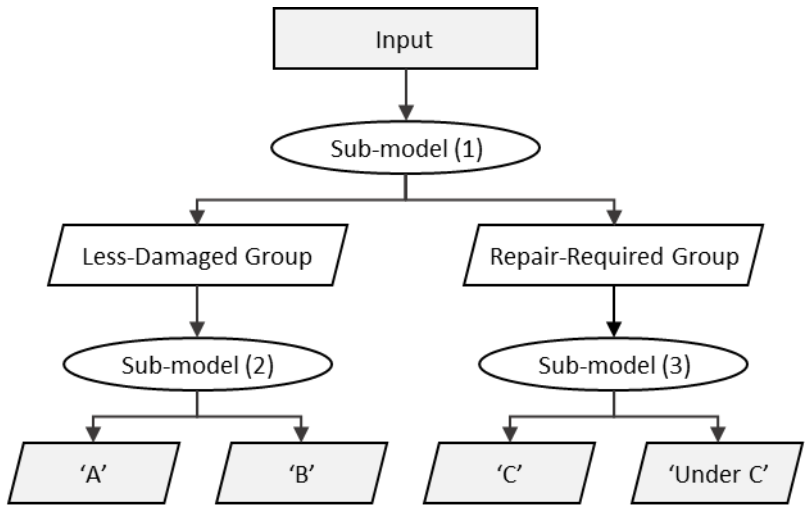

Figure 3.3 Model design for deck condition estimation

3.2.1. Proposed Method: Comparison of Classification Algorithms

Classification Algorithms Exploration

Previous studies have generally utilized six algorithms—logistic regression, k-nearest neighbors (KNN), decision tree, XGBoost, DNN, and CNN—to classify and estimate infrastructure condition states. To select an outstanding algorithm, the author applied and compared these algorithms by using the scikit-learn 0.24.2, the xgboost 1.5 Python libraries, and Tensorflow version 2.0 by Google.

(1) Logistic Regression

Logistic regression is a statistically appropriate algorithm to explain binary outcomes with multiple independent features (Shmueli et al. 2010). Some studies have conducted logistic regression analysis to estimate the occurrence of condition states transition, damage, or deficiencies on bridge elements using bridge information (e.g., length of maximum span, bridge width, and age) (Chang and Chi 2019; Chang et al. 2019; Shan et al. 2016). The occurrence probability (p) of an event, which is a specific condition grade in this research, can be determined by the standard logistic regression represented in Equation 3.1:

$$log\left(\frac{p}{1-p}\right) = \beta_0 + \beta_1 x_1 + \cdots + \beta_i x_i + \cdots + \beta_n x_n \qquad (3.1)$$

where x_i = the value of i-th ($i = 1, \ldots, n$) explanatory variable; and β_i = the estimate of i-th explanatory variable. The left side of the equation (i.e., logit) has a value from -∞ to ∞.

(2) K-Nearest Neighbors (KNN)

When given unknown data, the KNN classifier searches the outcome of the unknown data based on the information of the k-neighbors closest to the

unknown data in the training data (Shmueli et al. 2010). It is widely recognized as a basic classification algorithm only by setting k, which is the number of neighbors, and the distance metric between the data. This method has been utilized for infrastructure management, such as bridge condition index estimation and potential dam hazard level predictions (Assaad and El-Adaway 2020; Martinez et al. 2020). This research calculated the distance between the data using the Euclidean distance, which is the most prominent distance metric.

(3) Decision Tree

A decision tree classifier classifies the data according to the decision rule, like the hierarchical tree structure. The decision tree starts with the first classification criterion, called the root node, branches to the internal nodes according to the outcome of the criterion, and finally ends at the leaf nodes containing the final label of the target variable (Shmueli et al. 2010). The classification criterion in each node is composed of the combinations between the characteristics of the explanatory variables. Given the decision tree method has shown high predictive power in classification and can confirm the decision rules for prediction, previous studies have used it to estimate bridge deck conditions and examine the influence of the explanatory variables

in the classification process. This research utilized the classification and regression tree (CART) algorithm, which is the most widely used decision tree algorithm. In this algorithm, the impurity of a node is calculated using the Gini coefficient, and one node branches to two other nodes to reduce the impurity (Breiman et al. 1984; Lim et al. 2017).

(4) Extreme Gradient Boosting (XGBoost)

Boosting is an ensemble method to generate a classifier with high performance (i.e., strong classifier) by combining several decision tree classifiers with low performance (i.e., weak classifiers) while adjusting the weights of the weak classifiers considering the misclassification of the classifiers (Shmueli et al. 2010). Gradient boosting generates a strong classifier by tuning parameters of the weak classifiers to reduce the gradient of loss function (Friedman 2001). XGBoost is based on the gradient boosting combined with the CARTs (Chen and Guestrin 2016). It has recently gained a lot of popularity with data analysts and machine runners because of its high accuracy and speed by decreasing the risk of overfitting and increasing resource efficiency. Considering these advantages, XGBoost has also been utilized in the field of infrastructure management to predict the condition

status of water pipes and to estimate the occurrence of bridge damage (Darmatasia and Arymurthy 2016; Lim and Chi 2019).

(5) Deep Neural Network (DNN)

A deep neural network (DNN) refers to a neural network with two or more hidden layers between the input and output layers. In order to classify or predict a target using data with high complexity, the optimal weight and bias can be identified by sophisticatedly processing the input signal through deep hidden layers. Recently, previous research using BMS data has applied a DNN to predict the condition ratings of bridge elements or the damage severity of bridge decks using several explanatory variables (Ali et al. 2020; Lim and Chi 2021). When considering the risk of overfitting due to the algorithm complexity for the structured BMS data, this research limited the number of hidden layers to three and applied batch normalization that reduces the weight range through normalization using the mean and variance of each batch. The author also added a dropout layer that lowered the model complexity by omitting a part of the network (Buduma and Lacascio 2017).

(6) Convolution Neural Network (CNN)

A convolution neural network (CNN) indicates a DNN that includes convolution layers between the input and output layers. CNNs have shown superior performance in classification problems for unstructured data with a complex data structure, such as images and texts, because they can extract the features of the input data and identify patterns to classify or predict a target through the convolution processes. In the case of classifying structured data such as BMS data, a CNN basically includes a (1×1) convolution layer and a pooling layer that resizes the convolution layer to maintain the network's simplicity. Liu and Zhang (2020) confirmed good performance of a CNN model in classifying the condition ratings of bridges' major elements for the immediate next inspection. Referring to this, this research constructed a CNN by adding three convolution layers, a maxpooling layer that extracts the maximum value within a specified range, and a dropout layer to reduce the risk of overfitting (Goodfellow et al. 2016).

Data Sampling

The preprocessed data were split into training data and testing data. As the target variable in this study (i.e., the condition grades of elements) had a very high proportion of the normal condition state (e.g., the condition grade

‘B’ in KOBMS), a data imbalance problem occurred in that the distribution of training data was biased into some classes (i.e., majority classes). To solve this problem, data sampling techniques including over-sampling and under-sampling were used to prevent the degradation of algorithm performance because only the data in the majority classes are trained (He and Ma 2013).

It is known that over-sampling, which increases the number of data by duplicating the data belonging to classes with a small number of data (i.e., minority classes), is suitable for training a dataset that is not large in size. Among the over-sampling techniques available, the synthetic minority over-sampling technique (SMOTE) is generally utilized to avoid overfitting caused by simple duplication. SMOTE is a technique used to generate new similar data by extracting a subset of data in the minority classes (Chawla et al. 2002). In this research, borderline-SMOTE was conducted to generate data using the subset located at the boundary between the majority and minority classes where misclassification can frequently occur (Han et al. 2005). In addition, when the data imbalance is not resolved even after over-sampling, a random under-sampling technique can also be implemented to randomly reduce the amount of data in the majority classes (Chawla et al. 2002). These data sampling steps were conducted using the scikit-learn 0.24.2 and imbalanced-learn 0.8.1 Python libraries.

Algorithm Evaluation and Selection

To find the combination of parameters with the best performance by the explored algorithms, the hyperparameters were determined based on a grid search by using 5-fold cross-validation among several potential combinations specified by the authors. The author tuned the hyperparameters of the six algorithms using the training data according to the types of hyperparameters and the grid search values described in Table 3.3. The performance for the cross-validation was measured with an average accuracy index, which is the most popular criterion in classification. Accuracy is defined as the number of correctly predicted data among the total number of testing data. Each algorithm was then trained with the determined optimal hyperparameters.

Table 3.3 Hyperparameters for algorithms

Algorithm	Hyperparameter	Description	Values for grid search
Logistic Regression	Penalty	The type of regularization	L1, L2
	C	The inverse of regularization strength	1e-7–1e-0 (interval: 1e-1)
KNN	k	The number of neighbors	1–20 (interval: 1)
Decision Tree	Max_depth	The maximum number of branches from root node to leaf node	4–10 (interval: 2)
XGBoost	Max_depth	The maximum of number of branches from root node to leaf node	4–10 (interval: 2)
	Min_child_weight	The minimum sum of weights of all data required in a child	1, 5, 10
	Subsample	The ratio of data for sampling to construct each tree	0.6, 0.8, 1.0
	Colsample_bytree	The ratio of columns (variables) for sampling to construct each tree	0.6, 0.8, 1.0
	Gamma	Minimum loss reduction required to do a split	0, 0.1, 0.3
	Learning rate	The amount to change weights	0.05–0.1 (interval: 0.01)
DNN, CNN	Optimizer	The algorithm for updating the parameter weights to minimize the loss function	Adam, RMSprop
	Epoch	The number of iterations for training	50, 100, 150
	Batch size	The number of training data for each iteration	32, 64, 128
	Learning rate	The amount to change weights	0.001, 0.01, 0.1

Note: Adam = adaptive moment estimation; and RMSprop = root-mean-square prop.

The trained algorithms were evaluated based on the accuracy achieved in testing. However, it may have been difficult for the value of accuracy to sufficiently reflect the predictive power of the algorithms since the testing data were imbalanced. For this reason, the author also measured the weighted average F1 score, which indicates an index to consider precision, recall, and support values for each class of target variable. For the i-th ($i = 1, \dots, N$) class of the target variable, $Precision_i$ refers to the ratio of correct results from the predicted i-th class; $Recall_i$ refers to the ratio of those predicted as the i-th class over those in the actual i-th class; $Support_i$ refers to the number of data belonging to the i-th class in the test dataset. The F1 score is then defined as the harmonic average of precision and recall, and the weighted average F1 score can be calculated as an average of the F1 scores for each class considering the support of each class as a weight, as represented in Equation 3.2.

$$Weighted\ \ average\ \ F1\ \ score = \frac{1}{N}\sum_{i=1}^{N} Support_i \times \frac{2}{\left(\frac{1}{Precision_i}\right)+\left(\frac{1}{Recall_i}\right)} \quad (3.2)$$

The algorithm with the highest performance based on the weighted average F1 score was finally selected as the outstanding algorithm.

3.2.2. Results of the Optimal Algorithm Selection

The preprocessed data for each sub-model were first split into training data (80%) and testing data (20%) in accordance with the data distribution by classes of the target variable. Next, in consideration of the severity of the data imbalance between the two classes in the training data, the data in the minority class (e.g., repair-required group in sub-model (1)) were generated using borderline-SMOTE. Random under-sampling was then implemented so that the data size in the majority class (e.g., the less-damaged group in sub-model (1)) was 1.25 times the data size in the minority class for each sub-model.

The six algorithms were tuned according to the grid search, while 5-fold cross-validation was conducted to find the optimal hyperparameter combination with the highest average accuracy. For instance, for the sub-model (1), the optimal combinations were determined with six neighbors for KNN; eight maximum depth, 1.0 minimum child weight, 0.6 subsample, 0.6 colsample by tree, 0.0 gamma, and 0.05 learning rate for XGBoost; and Adam optimizer, 64 batch size, 150 epochs, and 0.001 learning rate for DNN.

The algorithms trained with the optimal hyperparameters were then evaluated using the testing data for the three sub-models; the accuracy and weighted average F1 score for each algorithm is shown in Figure 3.4. As a

result of comparing the weighted average F1 scores for the algorithms, XGBoost was selected as the outstanding algorithm in all sub-models.

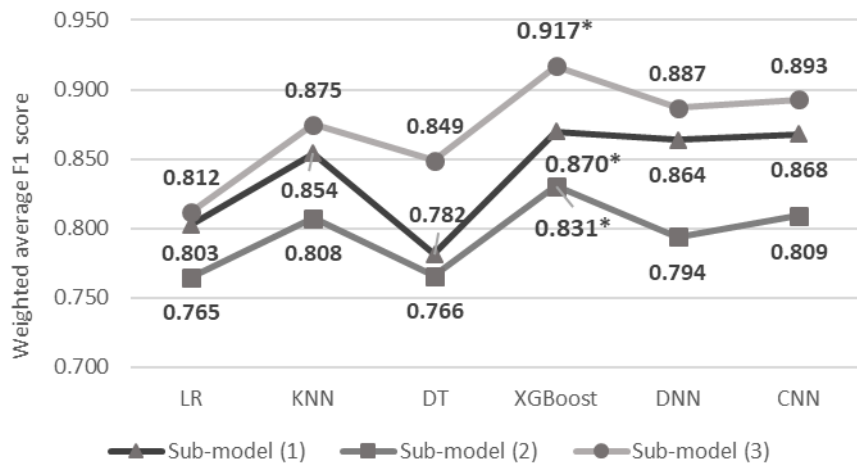

Note: LR = logistic regression; DT = decision tree; and (*) = the highest score by sub-models.

Figure 3.4 Results of the algorithm performance comparison

3.3. Influential Variables Identification

3.3.1. Proposed Method: Recursive Feature Elimination Based on Permutation Importance

Recursive Feature Elimination (RFE)

To improve model performance and practical usability, it is necessary to identify the critical explanatory variables that affect the target variable. Many studies have used feature selection techniques, commonly including filter, wrapper, and embedded methods (Hsu and Hsieh 2010). The filter method is useful for reducing variable redundancies by examining the intrinsic characteristics of variables through correlation measures or information measures when the original data have a large number of explanatory variables (Huan and Yu 2005). In this study, the filter method was specifically applied to remove redundant variables by calculating the correlation coefficient between explanatory variables in the data preprocessing step. The variables selected through the filter method, however, may not be optimal for the selected outstanding algorithm to estimate the condition grades of bridge elements.

The embedded method is a technique that uses a tool embedded into a specific algorithm (e.g., tree-based algorithms) to evaluate the importance of variables. Although it has the advantage of easily extracting influential

variables from an algorithm that has already been trained, it is difficult to utilize for algorithms that do not have such embedded tools. On the other hand, the wrapper method is a technique used to select the subset (i.e., combination) of explanatory variables with the best model performance by continuously generating the variable subsets and testing the algorithm trained with each subset. To prevent the inefficiency of having to test all variable subsets, most research has added significant variables, called forward selection, or removed insignificant variables after setting the reference subset, called backward selection. The author utilized the RFE method, which is an intuitive wrapper method and a popular backward-selection method (Chen and Jeong 2007). In the RFE, the least significant variables are continuously eliminated to determine the optimal subset of explanatory variables when the model has the best performance, regardless of the types of algorithms utilized.

In this research, the RFE was carried out by following the specified steps, as illustrated in Figure 3.5. The author first trained and tested the initial model utilizing the selected outstanding algorithm with all explanatory variables and calculated the importance of each variable. Next, the variable with the least importance was eliminated from the resampled training data. Then, the model without the least important variable was trained and tested, the importance of variables was evaluated, and the variable with the least

importance was again eliminated. This series of steps were iterated until every variable was eliminated. As a result of comparing the model performance based on the weighted average F1 score in model testing, the explanatory variables in the model with the highest performance score could be determined as the influential variables.

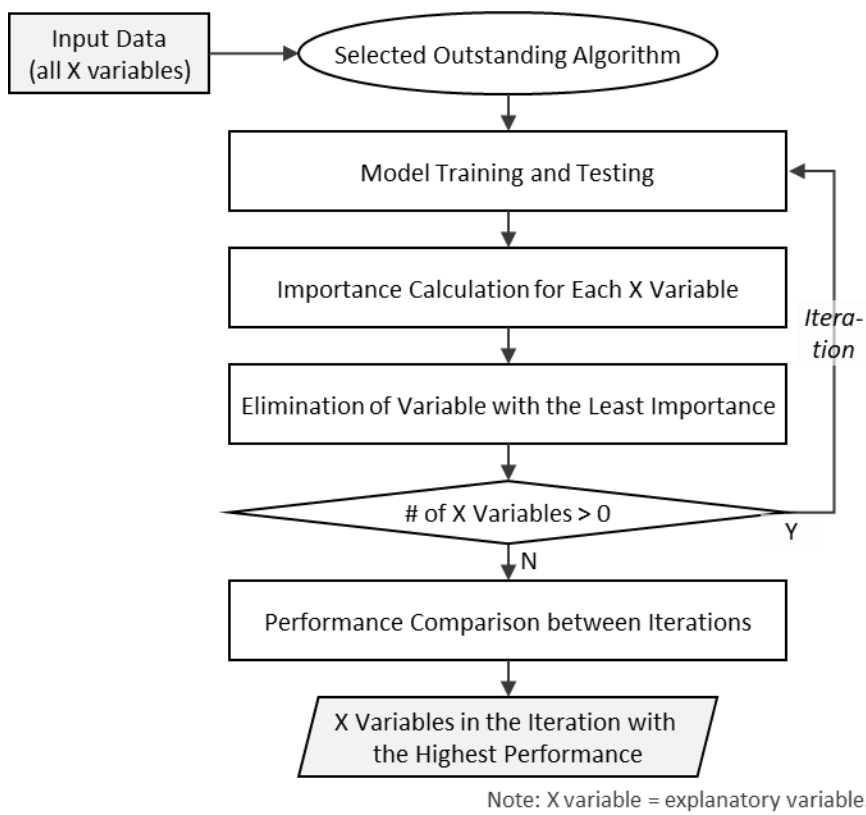

Figure 3.5 Detailed steps of RFE

Permutation Importance

In the RFE steps mentioned above, the importance of variables was evaluated based on the value of permutation variable importance. Permutation importance is defined as the decrease in model performance when one explanatory variable is disconnected from the target variable, and its advantages can be described as applicability to any algorithm and fast computing speed (Fisher et al. 2019). In this study, the permutation importance of the j-th explanatory variable, x_j, PI_j, was calculated according to Equation 3.3:

$$PI_j = F(X) - F(X_j^{perm}) \tag{3.3}$$

where $F(X) =$ the weighted average F1 score of the original model trained with X, which indicates a set of explanatory variables; and $F\left(X_j^{perm}\right) =$ the weighted average F1 score of the model trained with X_j^{perm}, which indicates a set of explanatory variables in which only x_j is randomly shuffled. The large value of PI_j means that the model depends on x_j, which has a role as an influential model variable. The computation of permutation importance was implemented using the ELI5 0.11 Python library.

3.3.2. Results of the Influential Variables Identification

To identify influential variables for each sub-model, the series of steps in the RFE were iterated 31 times for the sub-models until all explanatory variables were eliminated. Figure 3.6 visualizes the change in model performance (i.e., weighted average F1 score) as the 31 iterations were conducted. As a result of the model performance comparison, sub-model (1) represented the highest performance in iterations 1, 3, and 7; sub-model (2) represented the highest performance in iteration 5; and sub-model (3) represented the highest performance in iteration 20. In the case of sub-model (1), the models showed the highest performance (0.870) in three iterations, but the authors determined that the model in iteration 7 had better performance because it was trained with fewer variables in consideration of the computer resource and training efficiency. Therefore, the influential variables for the sub-models were identified as follows in order of importance:

- Sub-model (1): 25 variables – Bridge age, ADT, First past condition grade of deck, Bridge length, Annual Freeze-thaw frequency, Deck rebar spacing, Height, Annual precipitation, Total width, Pavement area, Annual average relative humidity, Deck pavement thickness, Annual average temperature, Water depth, Second past condition grade of deck, Maximum span length, Main substructure type,

Annual heatwave days, Deck thickness, Winter snowfall, Deck Pavement type, First past inspection interval, Region, Deck waterproofing type, Deck rebar strength.

- Sub-model (2): 27 variables – First past condition grade of deck, Bridge age, First past inspection interval, ADT, Annual heatwave days, Pavement area, Total width, Height, Bridge length, Annual average relative humidity, Annual average temperature, Second past inspection interval, Annual Freeze-thaw frequency, Deck thickness, Region, Annual precipitation, Water depth, Deck rebar spacing, Winter snowfall, Maximum span length, Main substructure type, Deck pavement thickness, Deck waterproofing type, Management agency, Second past condition grade of deck, Deck Pavement type, Deck strength.
- Sub-model (3): 12 variables – ADT, Bridge age, First past condition grade of deck, Deck rebar spacing, Bridge length, Annual precipitation, Total width, Annual average temperature, Maximum span length, Winter snowfall, Annual Freeze-thaw frequency, Management agency.

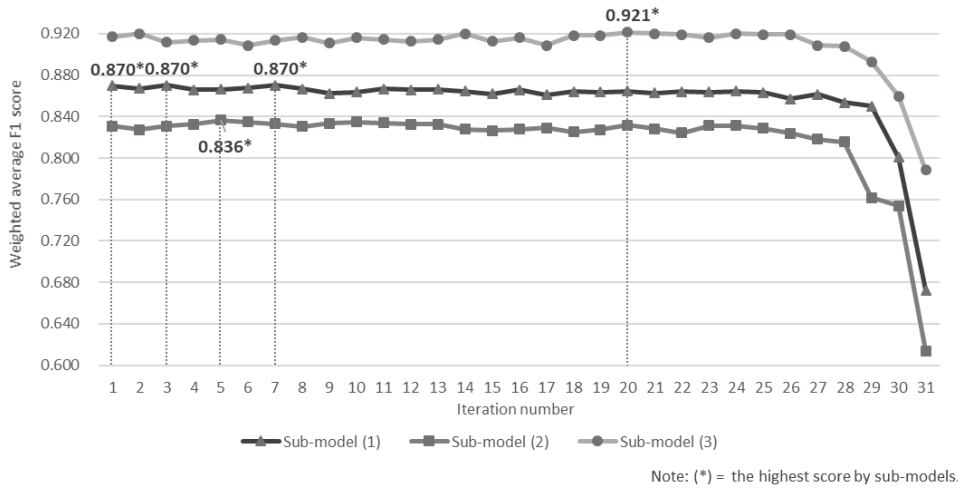

Figure 3.6 Model performance for iterations in the RFE

3.4. Results and Discussions

3.4.1. The Optimized Model Evaluation

An optimized model was finally developed using three sub-models based on the XGBoost selected as an outstanding algorithm and the identified influential variables. As a result of the model training, the optimal XGBoost hyperparameters were determined: six maximum depth, 1.0 minimum child weight, 0.8 subsample, 0.6 colsample by tree, 0.0 gamma, and 0.07 learning rate for sub-model (1); eight maximum depth, 1.0 minimum child weight, 0.8 subsample, 1.0 colsample by tree, 0.0 gamma, and 0.07 learning rate for sub-model (2); and 10 maximum depth, 1.0 minimum child weight, 0.8 subsample, 0.6 colsample by tree, 0.0 gamma, and 0.05 learning rate for sub-model (3). The performance of the optimized model by sub-model was then evaluated in testing and Table 3.4 shows the evaluation results. The optimized model showed reliable performance on average (avg. accuracy of 0.873, avg. weighted average F1 score of 0.876, and avg. AUC of 0.840).

Table 3.4 Evaluation result of the optimized model

Sub-model	Accuracy	Weighted average F1 score	AUC
Sub-model (1)	0.868	0.870	0.832
Sub-model (2)	0.833	0.836	0.820
Sub-model (3)	0.917	0.921	0.868
Average	0.873	0.876	0.840

3.4.2. Findings and Discussions

The results above were discussed in terms of outstanding algorithm selection, influential variables identification, model evaluation, model performance verification by region, and model expandability validation.

Outstanding Algorithm Selection

According to the results of comparing the algorithm performance based on the weighted average F1 score to select an outstanding algorithm, logistic regression (one of the statistical approaches) had the lowest performance (avg. of 0.793), and XGBoost, CNN, and DNN, which can adjust the weights of variables in training had high performance (XGBoost: avg. of 0.872, CNN: avg. of 0.857, DNN: avg. of 0.848). Here, XGBoost showed better performance than deep learning algorithms such as CNN and DNN. This result was in line with previous studies that have found that tree-based ensemble algorithms (e.g., XGBoost) have been evaluated to outperform the deep learning algorithms for tabular data (structured data) despite the rapid development of deep learning (Arik and Pfister 2021; Bansal 2018). XGBoost generates trees while adjusting the weights of misclassified samples in the boosting process to classify the data of minority classes well; as such, these findings demonstrate its strength in this study with the data imbalance

problem. On the other hand, since deep learning algorithms require a large number of parameters and complex networks, they could be overparameterized and experience difficulty with appropriate inductive bias to find optimal solutions using structured data with a few data and explanatory variables (Arik and Pfister 2021; Shavitt and Segal 2018).

Influential Variables Identification

As a result of identifying the influential variables, common variables influencing the deck condition in the three sub-models included 'bridge age,' 'first past condition grade of deck,' 'ADT,' 'annual freeze-thaw frequency,' 'bridge length,' and 'total width.' Specifically, inspection history, represented by bridge age and past condition grade of deck, were found to be the critical factors in estimating the deck condition grades in the next inspection, as many previous studies have shown. Also, ADT refers to the dominant external load of the deck, and length and width of bridge refer to the load of the bridge itself, so it could be confirmed that the internal and external bridge loads have a decisive effect on the deck, which is a main structural element of the bridge. As one of the environmental effects, repeated freezing and thawing of concrete structures (e.g., deck) is known to cause spatial cracking, spalling, and corrosion of exposed rebar, rapidly deteriorating structural durability.

For more detailed information, the author utilized Shapley additive explanation (SHAP) method proposed by Lundberg and Lee (2017). XGBoost results can be interpreted by SHAP to explain how each explanatory variable affects the model's estimation. SHAP originates from game theory and is an additive feature attribution method in which a model's output is defined as a linear addition of input variables. Thus, the explanation model, g, is defined as Equation 3.4:

$$g(z') = \phi_0 + \sum_{i=1}^{M} \phi_i z'_i \tag{3.4}$$

where z' = the vector of simplified input variables that are observed ($z' = 0$) or unknown ($z' = 1$); M = the number of input variables; and ϕ_i = the attribution value for i-th variable. The output of a conditioned tree on a variable subset, S, is represented as Equation 3.5, and SHAP values are calculated by averaging all possible conditional expectations as Equation 3.6:

$$f_x(S) = [E(f(x)|x_s] \tag{3.5}$$

$$\phi_i = \sum_{S \subseteq N \setminus \{i\}} \frac{|S|!(M-|S|-1)!}{M!} [f_x(S \cup \{i\}) - f_x(S)] \tag{3.6}$$

where $|S|$ are the non-zero entries in z and N is the set of all input variables.

Figure 3.7 illustrates SHAP summary plots for the three optimized sub-models. A SHAP summary plot demonstrates the distribution of the SHAP values and represents the corresponding influence trends for each influential variable. In the figure, the x-axis indicates the SHAP value, for which a positive value means a positive influence on the model's estimation and a negative value means the opposite influence. The y-axis also indicates up to 20 influential variables of each sub-model, ordered by the sum of the absolute values of the SHAP values. The dot indicates each sample (i.e., testing data), and the color of the dot indicates the value of the specific variable. The blue color means a small value, and the red means a large value (Feng et al. 2021).

As a result of the interpretation of Figure 3.7, the influential variables and influence trends were examined further by sub-models. For sub-model (1), the young bridge age, high past condition grade of deck, and thick deck pavement thickness influenced estimations into the less-damaged group for the deck condition (Figure 3.7 (a)). For sub-model (2), the long inspection interval affected the estimation of condition grade 'B' for the deck condition. Specifically, it is known that as bridges age, their decks have difficulty in maintaining the condition grade 'A' as the best condition, regardless of the

internal and external factors influencing the deck condition. So, a longer inspection interval can lead to a faster progression from ‘A’ to ‘B’ as the inspections are repeated. Also, with long annual heatwave days and deep water depth, the deck condition was estimated to be condition grade ‘B’ (Figure 3.7 (b)). For sub-model (3), the small value of ‘deck rebar spacing’ and the young bridge age affected the estimation of condition grade ‘C’ for the deck condition. Structurally, the deck rebar indicates a deck’s reinforcing steel bar, which is used to withstand tensile strength, and large spacing between the deck rebars could lead to serious damage that requires maintenance, such as severe cracking or corrosion of exposed rebar. The deck condition was also estimated to be condition grade ‘Under C’ with lots of ADT, short bridge length, and narrow total width (Figure 3.7 (c)).

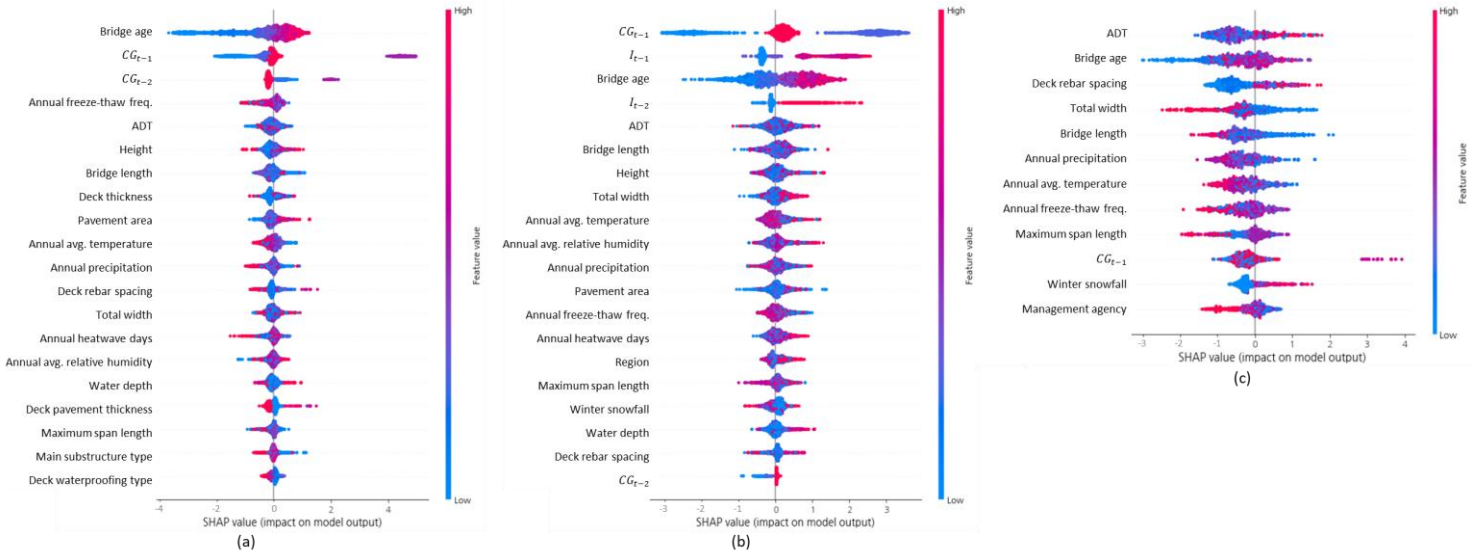

Figure 3.7 SHAP summary plot: (a) sub-model (1); (b) sub-model (2); and (c) sub-model (3)

Model Evaluation

As a result of developing an optimized deck condition estimation model using the outstanding algorithm and the influential variables, the optimized model had good performance with an average weighted average F1 score of 0.876 and an average AUC of 0.840. Nevertheless, the predictive performance of condition grades 'A' and 'B' in sub-model (2) was relatively low. In visual inspection practices in South Korea, it is known that there is not much difference between condition grades 'A' and 'B,' and the condition grades are mainly determined by the inspector's subjectivity. Since the sub-model trained the data reflecting these practices, condition grades 'A' and 'B' could easily be confused—even in the estimation result of sub-model (2). On the other hand, sub-model (3) had very high predictive power because the input data for the model had a clear difference in the values of the influential variables (e.g., 'ADT,' 'bridge age,' and 'first past condition grade') to classify condition grade 'C' and 'Under C.'

Model Performance Verification by Region

The model performance for estimating bridge elements' condition can be affected by the region since it is known that the bridge management level and environmental conditions vary depending on the region where the bridge

is located. In order to verify the proposed model's performance by region, the author developed deck condition estimation models for representative regions from the prepared KOBMS data and compared the models' performance.

The regional distribution of 4,779 concrete-girder bridges entered into the KOBMS database is shown in Figure 3.8. Gyeonggi-do accounts for the largest proportion (17%), and Gyeongsangnam-do and metropolitan cities, including Busan, Daegu, and Incheon, account for the lowest proportion (7% and 3%, respectively). Referring to this, the author selected three regions: Gyeonggi-do, which has the most concrete-girder bridges and is known to be relatively well-managed because it is located in the capital area; Gangwon-do, which has the second most concrete-girder bridges with different environmental conditions from the capital area; and Jeollanam-do, which has a relatively large number of concrete bridges despite having lower traffic volume compared to other regions.

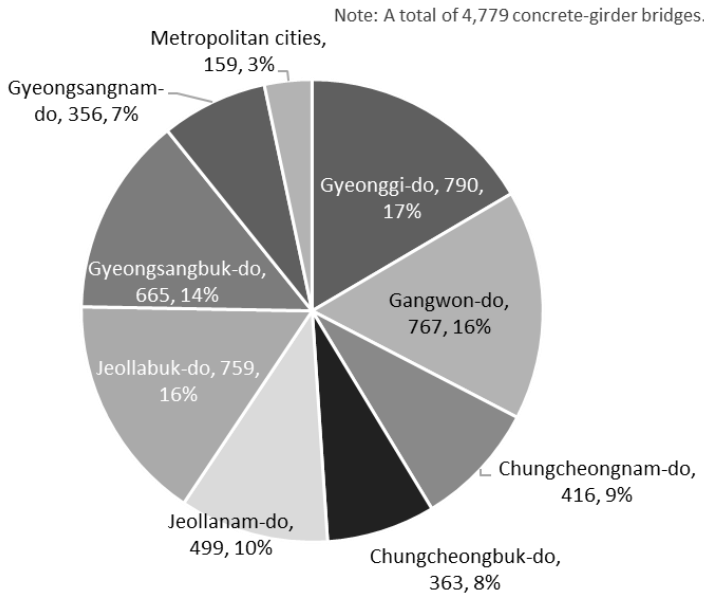

Figure 3.8 Regional distribution of concrete-girder bridges

To develop the deck condition estimation models for the three regions (i.e., the Gyeonggi model, the Gangwon model, and the Jeon-nam model), this research extracted 2,737 data for the Gyeonggi model, 2,550 data for the Gangwon model, and 2,078 data for the Jeon-nam model from the prepared 17,567 of data. The extracted data were split into training data (80%) and testing data (20%) by three sub-models, and the training data were resampled considering the data imbalance. XGBoost was then trained with optimal hyperparameters according to the grid search by using the resampled training

data by sub-models. The performance of the trained models was evaluated using testing data for each region.

As a result, Figure 3.9 shows the average performance of the sub-models for the Gyeonggi model, the Gangwon model, and the Jeon-nam model using the three regional testing data. In all three testing data, models trained with data from the same region showed the best performance, and models trained with data from other regions showed a weighted average F1 score drop of 0.1 or more. Thus, it was confirmed that the region has a critical effect on estimating the deck condition and that the estimation model developed using the BMS dataset from a specific region dataset represents outstanding performance in estimating the elements' condition of the bridges located in the region.

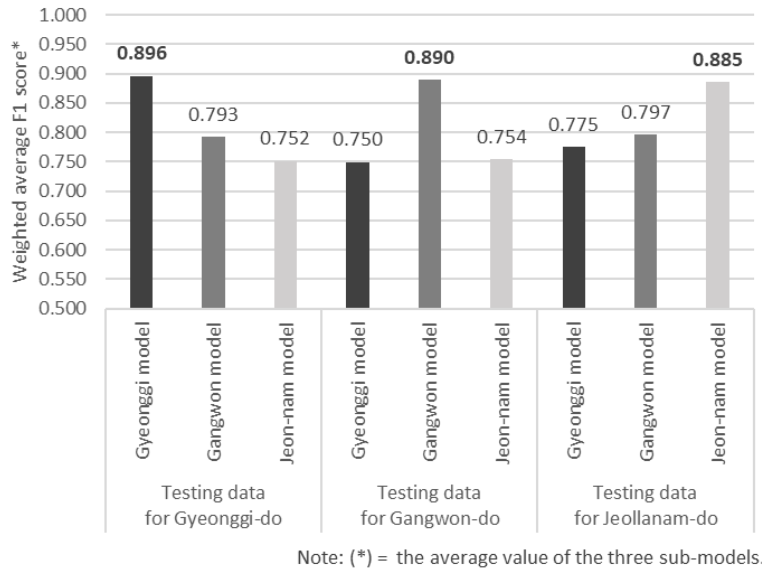

Figure 3.9 Model performance using the regional testing data

Meanwhile, except for a few regions, the number of prepared data necessary for regional models is insufficient, so there is a limit to constructing an optimized model for each region. Table 3.5 provides the evaluation results based on the weighted average F1 score for the optimized model developed without classifying the regions (i.e., the current model) and the three regional models using the testing data in the region. It was found that there was no significant difference in performance between the model without classifying the regions and the three regional models from the result of Pearson's chi-squared test at the 0.05 significance level ($p > 0.960$) (Couallier et al. 2013).

Therefore, the model without classifying the regions was verified to be acceptable until sufficient data were collected and analyzed by region.

Table 3.5 Result of model performance verification by region

Sub-model	Current model(*)	Gyeonggi model	Gangwon model	Jeon-nam model
Sub-model (1)	0.870	0.862	0.866	0.880
Sub-model (2)	0.836	0.885	0.844	0.843
Sub-model (3)	0.921	0.941	0.960	0.932
Average	0.876	0.896	0.890	0.885

Note: (*) means the optimized model developed without classifying the regions; and the numbers in the table indicate the model performance based on the weighted average F1 score.

Model Expandability Validation

To validate the expandability of the proposed method for estimating bridge element condition, the author applied the method to BMS data from other countries. The data were collected from the NBI database in the United States, which is known to be the most representative BMS data. General and structural information (e.g., highway agency district, structure length, and deck structure type), inspection information including bridge age and condition ratings of bridge components, and traffic information on highway bridges entered into the NBI are annually recorded for each of the 116 items in the NBI database. Specifically, the condition ratings are assigned on a scale of 0 (worst condition) to 9 (best condition) (FHWA 1995). The research team

also collected the inspection history containing past condition ratings of bridge components and time intervals for two past inspections. In addition, weather information by bridge and year was collected in connection with the NBI data. The information has 12 variables such as average humidity, temperature, and wind speed (FHWA 2022).

Among the collected data, a dataset of 1,034 highway bridges in California with concrete or PSC as the main span material from 1995 to 2021 was selected for analysis. As a result of the preprocessing steps, the final dataset for developing the deck condition estimation model using the NBI data consisted of 25 explanatory variables (15 numerical and 10 categorical variables), one target variable (i.e., condition rating of deck), and 20,425 of data. Meanwhile, since condition ratings 0, 1, 2, 3, 4, and 9 accounted for only 5.3% of the selected data, the condition ratings of deck were divided into four classes: fail (condition ratings 0–5; 3,426 of data), satisfactory (condition rating 6; 3,827 of data), good (condition rating 7; 11,917 of data), and very good (condition ratings 8–9; 1,255 of data). Thus, a multi-class classification was implemented to estimate the condition rating of deck.

In the data sampling part, the preprocessed data were split into training data (80%) and testing data (20%), and the training data were resampled considering the data imbalance among the four classes. The research team

then confirmed that XGBoost, which showed excellent performance on structured data such as the KOBMS data, is appropriate as an outstanding algorithm on other BMS data. As a result of performance evaluation of the algorithm trained with optimal hyperparameters according to the grid search, XGBoost represented satisfactory performance with a weighted average F1 score of 0.876. Next, to identify influential variables for estimating the condition rating of deck, the series of steps in the RFE were iterated 25 times until all explanatory variables were eliminated. As a result of the model performance comparison, iteration 16 showed the highest performance and the 16 influential variables were identified as follows: first past condition rating of deck, time of wetness, prevailing wind direction, ADTT, total precipitation, bridge age, maximum temperature, wearing surface type, second past condition rating of deck, deck width, length of maximum span, number of freeze-thaw cycles, structure length, skew angle, second past inspection interval, and main span design.

An optimized model was finally developed based on XGBoost and the 16 influential variables. According to the model training, the optimal hyperparameters were determined to be 10 maximum depth, 1.0 minimum child weight, 0.6 subsample, 0.6 colsample by tree, and 0.05 learning rate. As a result of the model evaluation in testing, the model showed a weighted

average F1 score of 0.880. It was confirmed that the NBI data were smoothly applied to the model development process and that the optimized model showed promising performance. Therefore, these results demonstrated that the proposed method based on an optimal combination of appropriate algorithms and influential variables for the BMS data given for analysis is expandable regardless of the BMS characteristics.

3.5. Summary

For the first objective of this dissertation, which is to estimate bridge elements' condition, this chapter provided a research process to develop an optimized model using data-driven approaches. To accomplish this objective, first, the author prepared general and structural information and inspection records from the KOBMS and environmental information around the bridges from external databases. Using the preprocessed dataset, the author selected the outstanding algorithm based on the results of comparing the performance of diverse algorithms and identified influential variables affecting the condition of specific elements among the collected information. An optimized estimation model was then developed by utilizing the selected algorithm and the influential variables. As a result of the deck condition estimation on concrete-girder bridges managed by the KOBMS, XGBoost was selected as the optimal algorithm, and 'bridge age,' 'first past condition grade of deck,' 'ADT,' 'annual freeze-thaw frequency,' 'bridge length,' and 'total width' were explored as representative influential variables. Finally, the optimized model showed good performance with an average weighted average F1 score of 0.876 and an average AUC of 0.840. In the model verification and validation, as a result of the model performance verification by region, the proposed model without classifying the regions was acceptable until sufficient data

were collected by region. Also, the proposed method based on an optimal combination of appropriate algorithms and influential variables for the BMS data given for analysis is expandable regardless of the BMS characteristics.

Chapter 4. Bridge Damage Size Estimation

This chapter covers the second objective of this dissertation to estimate repair-required damage size on bridge elements. As described in Section 2.3.4 "Limitations of Existing Studies," previous studies showed promising results in estimating the occurrence and severity of the damage at the damage level; but they had difficulties in providing information on damage size. The author addressed the problem with regression and classification models to estimate repair-required damage size on bridge elements based on BMS data. Figure 4.1 illustrates the proposed research process. The targets of the models were set as the damage types and size on the bridge element (e.g., $2.1m^2$ cracking on a deck) expected in the next inspection. First, BMS data, including inspection records for damage size, was collected and preprocessed. Data exploration was also conducted to understand the characteristics of the target variable (i.e., damage size by type of deck damage). Second, considering the characteristics, regression and classification models were developed using XGBoost and DNN, as representative AI-based data-driven algorithms. Last, after model evaluation, the author compared the models in terms of strength, weakness, and performance; the final estimation model was then selected.

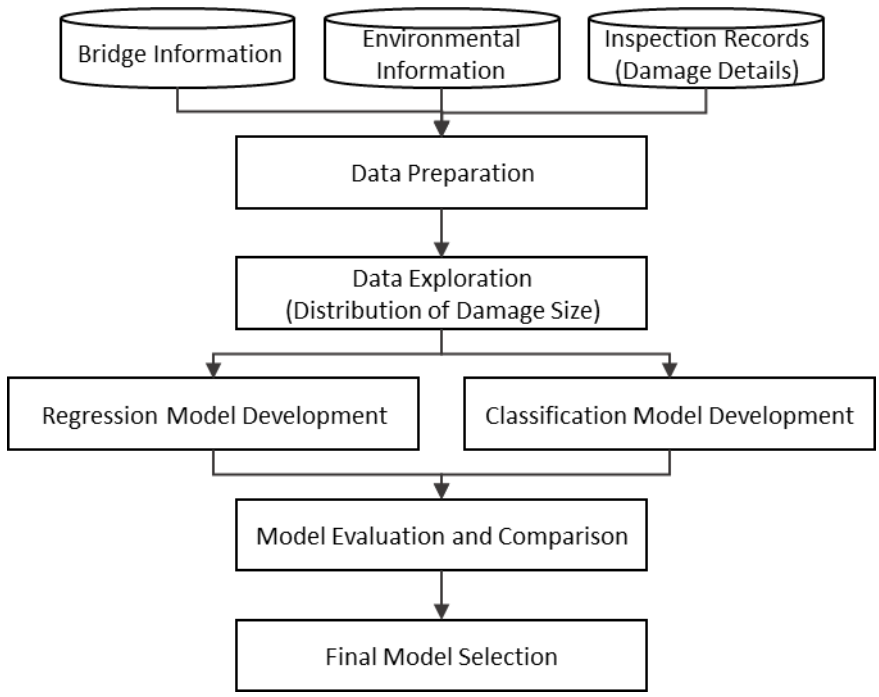

Figure 4.1 Research process of bridge damage size estimation

4.1. Data Preparation

4.1.1. Data Collection and Preprocessing

The BMS data for this chapter were also collected from the KOBMS database. The collected data include bridge information (i.e., general and structural information), inspection records, and environmental information for the bridges in South Korea. As described in Section 3.1.1 "Data Collection," the general information contains 16 variables regarding the deck (except for 'main substructure type'). The total size of the element for each element was added to the general information to consider the element size that may be damaged. The structural information contains nine variables regarding the deck. Since structural information was accumulated for each span/support, representative values (median values for numeric variables and mode values for categorical variables) were extracted for each bridge. The environmental information collected from external databases includes two types of traffic information and 11 types of weather information at the measurement point closest to the bridge location.

Among the accumulated inspection records in the KOBMS, the author extracted the damage details inspected on deck through 3,716 in-depth inspections of 1,798 concrete-girder bridges from 2011 to 2021. The inspected damage details include damage type, size, and history along with

‘inspection year,’ ‘bridge age,’ and diagnosed ‘condition grade of deck.’ There are eight types of deck damage: cracking, leakage and efflorescence, map cracking, spalling, scaling, segregation, corrosion of exposed rebar, and breakage. The detailed description of each damage type lists in Table 4.1. Figure 4.2 also shows the shape of each damage type (FHWA 2012; Korea Authority of Land & Infrastructure Safety [KALIS] 2019). The damage size by each damage type was recorded with units to two decimal places. In particular, since cracking was recorded as m and m^2 according to the inspector, the author collected data of line-craking (m) and area-cracking (m^2) separately. In addition, the author also collected damage history that contains past damage size by damage type and time intervals between past and current inspections. The damage history specifically includes the first past damage size (DS_{t-1}) by damage type, the first past inspection interval (I_{t-1}), the second past damage size (DS_{t-2}) by damage type, and the second past inspection interval (I_{t-2}).

Table 4.1 The detailed description of deck damage

Type of deck damage	Description
Cracking	A linear fracture in concrete
Leakage	Water leaking from cracks or crevices in concrete
Efflorescence	White compounds on the surface where calcium hydroxide on concrete is dissolved in water and combined with carbon dioxide in the air
Map Cracking	Inter-connected cracks (network-shaped cracks) between girders
Spalling	Falling off the surface of the concrete in a circular shape along cracks
Scaling	Gradual loss of mortar on the concrete surface
Segregation	Exposed aggregates in the form of honeycombs on the concrete surface
Corrosion of Exposed Rebar	A large amount of exposed rebar causing a chemical reaction in the air to deteriorate
Breakage	A developed spalling in losing the original shape

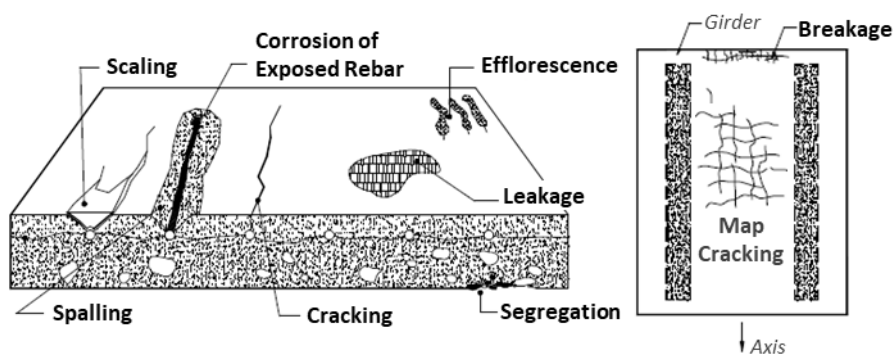

Figure 4.2 The shape of deck damage

The collected data were preprocessed based on data cleaning, integration, reduction, and transformation. In the data cleaning step, the author eliminated the inspection records with too large a damage size that are considered a recording error of the inspector. The missing values of less than 20% in the numeric variables for bridge information were replaced with the median values of the variables. In the case of variables related to the damage history, if the past inspection was not recorded, the values of the past damage size and the past inspection intervals were represented as zero. The values of the past inspection intervals over six years were substituted with the number six. Next, the data within multiple data tables were integrated to make one dataset so that the data could be input into the model.

In the data reduction step, the author removed the variables with duplicate meanings (i.e., 'construction year,' 'competent authority,' and 'inspection year'), those with a high proportion of missing values (i.e., 'pavement area' and 'deck rebar diameter'), and one of the variables with redundancies. The author examined possible variable redundancies across the integrated data in the same method described in Section 3.1.2 "Data preprocessing." For nine types of damage, one variable with a lower correlation with the target variable (i.e., damage size) was then removed. Based on the results of the Pearson's correlation coefficient analysis of the

combinations of numerical variables, 12 combinations of variables with correlation coefficients over 0.6 were investigated; e.g., 'total size of deck – bridge length (0.84),' 'annual precipitation – summer precipitation (0.79),' and 'total width – number of spans (0.72).' When the target variable was area-cracking size, the variables, including 'bridge length,' 'summer precipitation,' and 'total width,' were then removed. On the other hand, as a result of the Cramer's V coefficient calculation between categorical variables, the combinations of variables with correlation coefficients over 0.6 were 'management agency – competent authority (1.00),' and 'competent authority' was then removed. Last, the data were transformed into appropriate forms for analysis.

As a result of the preprocessing steps, the final dataset for each damage type consists of a tabular format with several explanatory variables and one target variable (i.e., damage size). Table 4.2 shows variables and the number of data included in each final dataset by nine types of deck damage. The total damage size for each final dataset is distributed as described in Figure 4.3.

Table 4.2 Variables of the final dataset by type of deck damage

Concept	Variable	LC	AC	LE	MC	SP	SC	SG	CE	BR
General information (14)	Facility class	*	*	*	*	*	*	*	*	*
	Region	*	*	*	*	*	*	*	*	*
	Management agency	*	*	*	*	*	*	*	*	*
	Bridge length									
	Total width									
	Road width								*	*
	Height	*	*	*	*	*	*	*	*	*
	Water depth	*	*	*	*	*	*	*	*	*
	Total number of lanes (up/down)	*	*	*	*	*	*	*		
	Number of spans	*	*			*	*	*		*
	Maximum span length	*	*	*	*	*	*	*	*	*
	Total size of deck			*	*				*	
	Main superstructure type	*	*	*	*	*	*	*	*	*
	Design live load	*	*	*	*	*	*	*	*	*
Structural informaion of deck (8)	Deck material	*	*	*	*	*	*	*	*	*
	Deck waterproofing type	*	*	*	*	*	*	*	*	*
	Deck thickness	*	*	*	*	*	*	*	*	*
	Deck strength	*	*	*	*	*	*	*	*	*
	Deck rebar strength	*	*	*	*	*	*	*	*	*
	Deck rebar spacing	*	*	*	*	*	*	*	*	*
	Deck pavement type	*	*	*	*	*	*	*	*	*
	Deck pavement thickness	*	*	*	*	*	*	*	*	*
	Average daily traffic (ADT)	*	*	*	*			*		
	Average daily truck traffic (ADTT)					*	*		*	*

Environ-mental information (13)	Annual freeze-thaw frequency		*							
	Annual heatwave days	*	*	*	*	*		*		
	Annual average temperature				*	*			*	
	Summer average temperature						*			*
	Winter average temperature	*		*			*	*		*
	Annual precipitation		*	*		*	*		*	
	Summer precipitation	*			*			*		*
	Winter precipitation	*	*	*	*	*	*	*	*	*
	Annual average relative humidity	*								
	Summer average relative humidity		*	*	*	*	*	*	*	*
	Winter average relative humidity		*	*	*	*	*	*	*	*
Inspection records – damage details (7)	Bridge age	*	*	*	*	*	*	*	*	*
	Condition grade of deck (CG_t)	*	*	*	*	*	*	*	*	*
	Damage size (DS_t)*	*	*	*	*	*	*	*	*	*
	First past damage size (DS_{t-1})	*	*	*	*	*	*	*	*	*
	First past inspection interval (I_{t-1})	*	*	*	*	*	*	*	*	*
	Second past damage size (DS_{t-2})	*	*	*	*	*	*	*	*	*
	Second past inspection interval (I_{t-2})	*	*	*	*	*	*	*	*	*
# of explanatory variables		33	34	33	33	33	34	34	32	33
# of data		3,713	3,707	3,710	3,701	3,709	3,712	3,711	3,712	3,707

Note: (**) = the target variable; C = categorical variable; N = numerical variable; LC = Line-Cracking (m); AC = Area-Cracking (m^2); LE = Leakage and Efflorescence (m^2); MC = Map Cracking (m^2); SP = Spalling (m^2); SC = Scaling (m^2); SG = Segregation (m^2); CE = Corrosion of Exposed Rebar (m^2); BR = Breakage (m^2); and (*) = selected as explanatory variable.

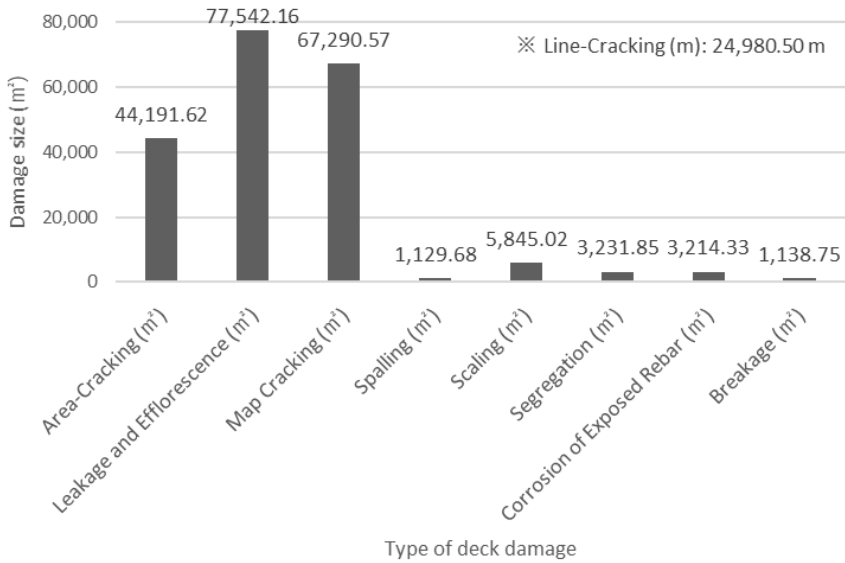

Figure 4.3 Total damage size by type of deck damage

4.1.2. Data Exploration

To construct a model for estimating the damage size, the data distribution according to the target variable, i.e., the damage size, was explored. Table 4.3 lists the damage size distribution by nine types of deck damage. All types of deck damage had a median value of zero and a very large standard deviation. The author also explored the scatter plots according to the damage size. As shown in the example of the scatter plot for the damage size of area-cracking in Figure 4.4, data with zero damage size were dominant (86%) of the total number of data, and the number of data with an enormous damage size was very rare. For nine types of deck damage, more than 80% of

the data belonged to the 'Damage=N' group with zero damage size, as visualized in Figure 4.5. As a result of data distribution exploration according to the damage size, the author found it difficult to directly implement regression analysis to estimate the exact damage size. Thus, classifying whether the damage size belonged to the 'Damage=N' group with zero damage size or the 'Damage=Y' group with non-zero damage size was required first.

Table 4.3 Damage size distribution by type of deck damage

Damage type	# of data	Mean	SD	Min	Median	Max
Line-Cracking (m)	3,713	6.73	43.25	0.00	0.00	925.80
Area-Cracking (m^2)	3,707	11.92	72.86	0.00	0.00	1,109.47
Leakage and Efflorescence (m^2)	3,710	20.90	106.80	0.00	0.00	1,585.81
Map Cracking (m^2)	3,701	18.18	103.95	0.00	0.00	1,278.00
Spalling (m^2)	3,709	0.30	2.42	0.00	0.00	52.96
Scaling (m^2)	3,712	1.57	14.29	0.00	0.00	301.38
Segregation (m^2)	3,711	0.87	8.88	0.00	0.00	215.00
Corrosion of Exposed Rebar (m^2)	3,712	0.87	4.86	0.00	0.00	113.80
Breakage (m^2)	3,707	0.31	2.38	0.00	0.00	50.76

Note: SD = standard deviation.

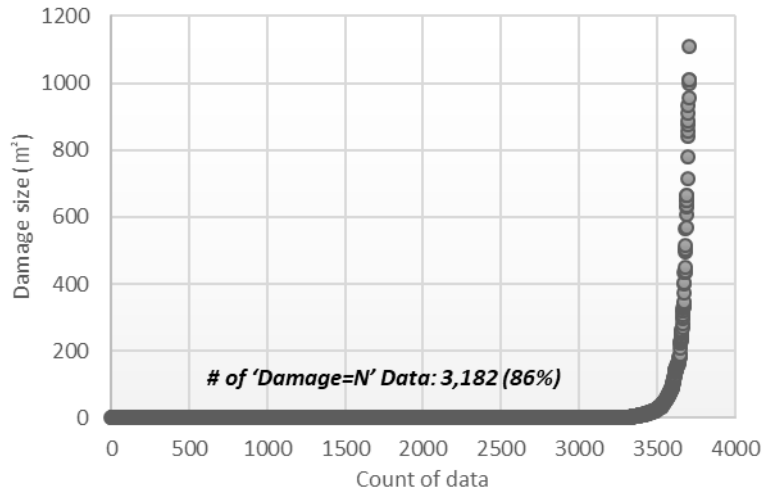

Figure 4.4 Scatter plot for the damage size of area-cracking

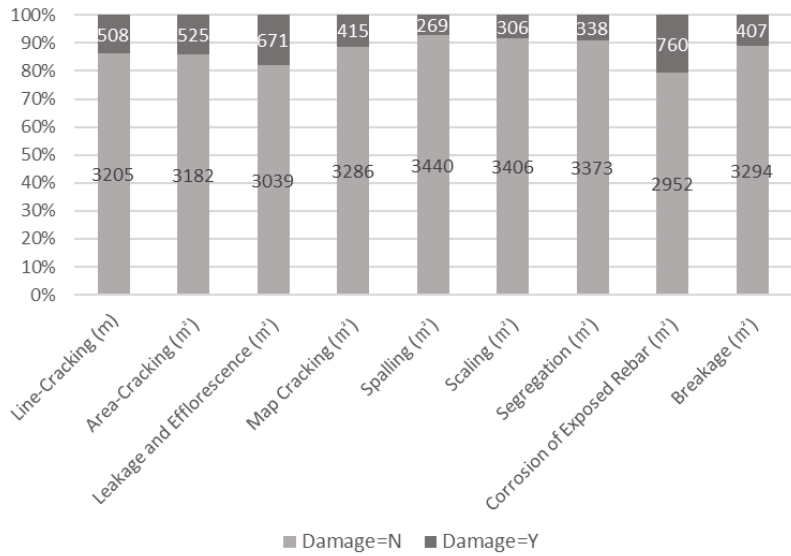

Note: 'Damage=N' group includes data with zero damage size, and 'Damage=Y' group includes data with non-zero damage size.

Figure 4.5 Data distribution ('Damage=N' group and 'Damage=Y' group) by type of deck damage

Next, a more detailed data exploration was conducted on data belonging to the ‘Damage=Y’ group with non-zero damage size. Table 4.4 lists the damage size distribution for the ‘Damage=Y’ group by nine types of deck damage. Taking area-cracking as an example, Figure 4.6 shows a general histogram for the damage size of area-cracking belonging to the ‘Damage=Y’ group. It could be seen that in 525 data with non-zero damage size, the number of data was very small as the damage size increased. In general, an enormous value in the data distribution can be defined as a value exceeding the third quartile (Q3, upper quartile) (Shmueli et al. 2010). Namely, among data belonging to the ‘Damage=Y’ group, data with enoumous values could be said to belong to the ‘Over Q3=Y’ group. However, since data belonging to the ‘Over Q3=Y’ group had a large deviation, the author found it difficult to estimate the exact damage size by utilizing regression. Therefore, after filtering out ‘Over Q3=Y’ group, the author needed to estimate the exact damage size with the data of the ‘Over Q3=N’ group with damage size of the third quartile or less.

Table 4.4 Damage size distribution of the 'Damage=Y' group by type of deck damage

Damage type	# of data	Mean	Min	Q1	Q2	Q3	Max
Line-Cracking (m)	508	49.17	0.03	2.60	9.96	41.94	925.80
Area-Cracking (m^2)	525	84.17	0.01	2.70	15.15	71.50	1,109.47
Leakage and Efflorescence (m^2)	671	115.56	0.02	2.70	19.80	113.56	1,585.81
Map Cracking (m^2)	415	162.15	0.06	6.72	37.92	182.50	1,278.00
Spalling (m^2)	269	4.20	0.02	0.41	1.20	4.29	52.96
Scaling (m^2)	306	19.10	0.01	0.75	3.00	12.00	301.38
Segregation (m^2)	338	9.56	0.01	0.40	1.20	5.57	215.00
Corrosion of Exposed Rebar (m^2)	760	4.23	0.01	0.36	1.11	3.52	113.80
Breakage (m^2)	407	2.80	0.01	0.19	0.66	2.19	50.76

Note: Q1=the first quartile (25%, lower quartile); Q2=the second quartile (50%, median); and Q3=the third quartile (75%, upper quartile).

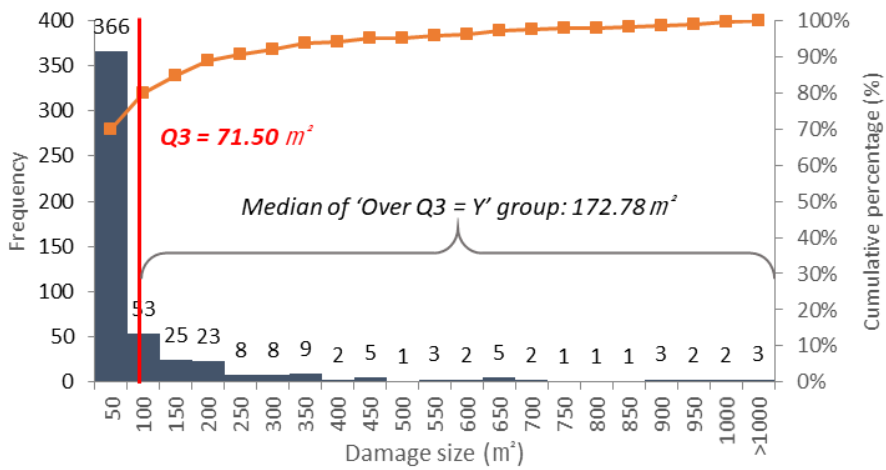

Figure 4.6 General histogram for the damage size of area-cracking belonging to the 'Damage=Y' group

In addition, since the deviation became larger at larger damage sizes, the data needed to be normalized on a log scale. Figure 4.7 shows a log-scaled histogram for the damage size of area-cracking belonging to the 'Damage=Y' group. The author could confirm that the log-scaled data was properly binned to four ranges (e.g., $0 < \text{size} \leq 1$, $1 < \text{size} \leq 10$, $10 < \text{size} \leq 100$, and $\text{size} > 100$), which have similar frequencies. Therefore, after classifying the log-scaled ranges, it was required to estimate the damage size for each range based on the median value.

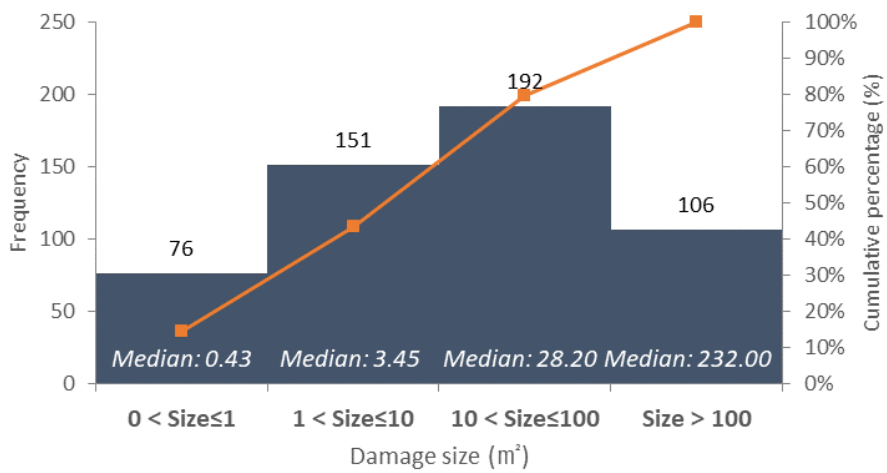

Figure 4.7 Log-scaled histogram for the damage size of area-cracking belonging to the 'Damage=Y' group

In summary, it was difficult to directly conduct regression analysis to estimate the exact damage size, so it was required to estimate the damage occurrence first, which means classifying whether the damage size belongs to the ‘Damage=N’ group with zero damage size or the ‘Damage=Y’ group with non-zero damage size. In the case of the ‘Damage=Y’ group, research methods for estimating the damage size could be considered by examining general and log-scaled histograms. First, as a result of examining the general histogram, after filtering out the ‘Over Q3=Y’ group, the author needed to estimate the exact damage size of the data of the ‘Over Q3=N’ group with damage size of the third quartile or less. Second, as a result of examining the log-scaled histogram, it was required to classify the log-scaled ranges and then estimate the damage size for each range based on a median value.

4.2. Proposed Method: Regression and Classification Models

4.2.1. Model Design

According to the results of data exploration, two models (i.e., regression model and classification model) were designed to estimate damage size for each type of deck damage, as shown in Figure 4.8. In the regression model (Figure 4.8 (a)), the damage occurrence is first estimated by 'Binary classification (1)', which means estimating whether the damage size belongs to the 'Damage=N' group or the 'Damage=Y' group. After classifying whether the data has an enoumous value, which belongs to the 'Over Q3=Y' group, by 'Binary classification (2),' the exact damage size is then estimated by 'Regression.' If classified as the 'Over Q3=Y' group, the damage size is estimated based on the median value of the 'Over Q3=Y' group. In the classification model (Figure 4.8 (b)), the damage occurrence is first estimated by 'Binary classification (1),' the same as the regression model. The four log-scaled ranges are then classified, and the damage size for each range is estimated based on a median value.

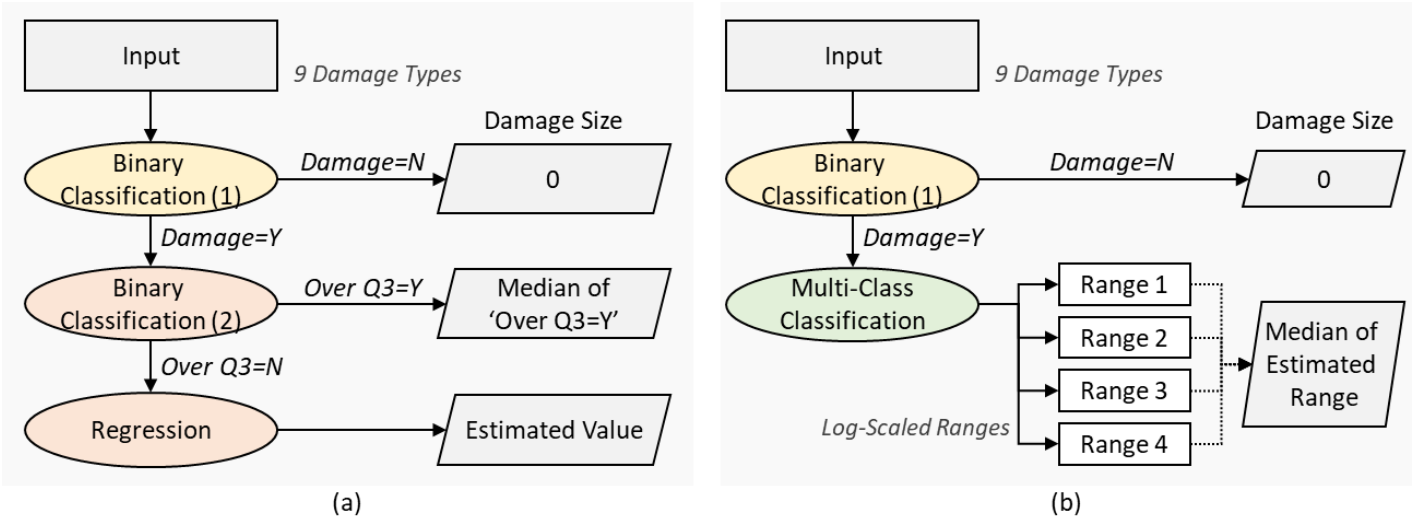

Figure 4.8 Model design for damage size estimation: (a) regression model; and (b) classification model

4.2.2. Regression and Classification Algorithms

To develop the designed two models, the author utilized XGBoost and DNN algorithms, which are known for their superior performance for regression and classification of a tabular dataset. The promising performance of the two algorithms on BMS data was also discussed in Section 3.4.2 'Findings and Discussions.' The models using these algorithms were developed by using the scikit-learn 0.24.2 and the xgboost 1.5 Python libraries, and Tensorflow version 2.0 by Google.

Extreme gradient boosting (XGBoost)

XGBoost, which was proposed by Chen and Guestrin (2016), is based on gradient boosting combined with the classification and regression trees (CARTs). Gradient boosting generates a strong classifier by tuning parameters of the weak classifiers to reduce the gradient of loss function (Friedman 2001). Figure 4.9 illustrates gradient-boosted tree architecture for regression and classification. In the general gradient-boosted tree, the output on i-th leaf, $\hat{y}_i$, can be expressed as Equation 4.1:

$$\hat{y}_i = \sum_{k=1}^{K} f_k(x_i, \theta_k), \; f_k \in F \tag{4.1}$$

where K = number of trees for boosting; f_k = output of the k-th tree in regression tree or scoring function to estimate the output of the k-th tree in classification tree; θ_k = structure of k-th tree trained from a training set (i.e., all parameters such as split and leaf nodes in Figure 4.9); and $\hat{y}_i$ = predicted value of target in regression tree or averaged or voted value by a collection F of K trees in classification tree (Lim and Chi 2019; Wang et al. 2020; Zhang et al. 2018).

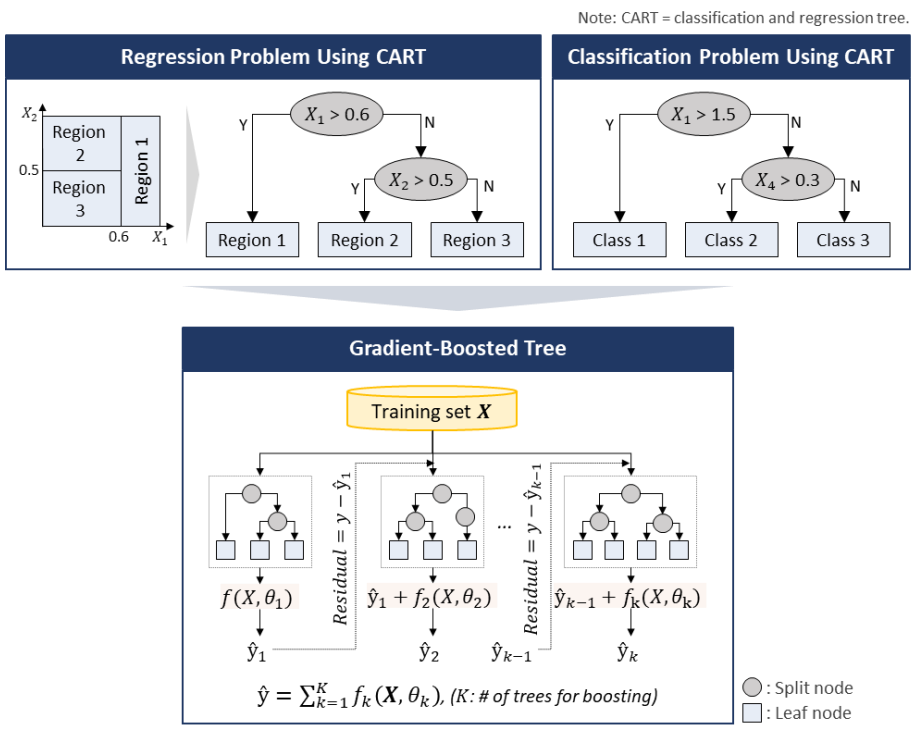

Figure 4.9 Gradient-boosted tree architecture for regression and classification

Although gradient boosting shows high performance, it has a high risk of overfitting. To avoid overfitting, Chen and Guestrin (2016) combined a regularization term with the training loss function in the general gradient-boosted tree. The regularized objective is defined as Equation 4.2, and the regularization term on k-th tree, $\Omega(f_k)$, is defined as Equation 4.3:

$$L(\theta) = \sum_{i=1}^{n} l(y_i, \hat{y}_i) + \sum_{k=1}^{T} \Omega(f_k) \tag{4.2}$$

$$\Omega(f) = \gamma T + \frac{1}{2}\lambda \sum_{j=1}^{T} w_j^2 \tag{4.3}$$

where n = number of considered samples; $l()$ = commonly training loss function (e.g., square loss in regression tree and logistic loss in classification tree); γ = complexity parameter of each leaf; T = number of leaves; λ = parameter to scale the penalty; and w = vector of scores on leaves. When the output of the i-th instance at the t-th iteration is defined as $\hat{y}_i^{(t)}$, the regularized objective can be given as in Equation 4.4.

$$L^{(t)} = \sum_{i=1}^{n} l(y_i, \hat{y}_i^{(t-1)} + f_t(x_i)) + \sum_{k=1}^{T} \Omega(f_k) \tag{4.4}$$

The second-order approximation can be used to optimize the objective in XGBoost as in Equation 4.5 and the constant terms to obtain the simplified objective as in Equation 4.6:

$$L^{(t)} \approx \sum_{i=1}^{n}[g_i w_{q(x_i)} + \frac{1}{2}(h_i w_{q(x_i)}^2)] + \gamma T + \frac{1}{2}\lambda \sum_{j=1}^{T} w_j^2 \qquad (4.5)$$

$$L^{(t)} = \sum_{j=1}^{T}[\left(\sum_{i\epsilon I_j} g_i\right) w_j + \frac{1}{2}(\sum_{i\epsilon I_j} h_i + \lambda) w_j^2] + \gamma T \qquad (4.6)$$

where $g_i = \partial_{\hat{y}^{(t-1)}} l\left(y_i, \hat{y}_i^{(t-1)}\right)$; $h_i = \partial^2_{\hat{y}^{(t-1)}} l\left(y_i, \hat{y}_i^{(t-1)}\right)$; and $I_j = \{i|q(x_i) = j\}$ as the instance set of leaf j.

Therefore, for a fixed structure, $q(x)$, the optimal weight, w_j^*, of leaf j can be calculated by Equation 4.7, and the optimal value, L^*, can be calculated by Equation 4.8:

$$w_j^* = -\frac{G_j}{H_j + \lambda} \qquad (4.7)$$

$$L^* = -\frac{1}{2}\sum_{j=1}^{T} \frac{G_j^2}{H_j + \lambda} + \gamma T \qquad (4.8)$$

where $G_j = \sum_{i \epsilon I_j} g_i$; and $H_j = \sum_{i \epsilon I_j} h_i$. When a tree splits a leaf into two leaf nodes, let assume that I_L and I_R are the instance sets of left and right nodes after the split ($I = I_L \cup I_R$). The score of gain is then given as Equation 4.9.

$$Gain = \frac{1}{2}\left[\frac{G_L^2}{H_L+\lambda} + \frac{G_L^2}{H_R+\lambda} = \frac{(G_L+G_R)^2}{H_L+H_R+\lambda}\right] - \gamma \quad (4.9)$$

The score is usually used for evaluating the split candidates (Chen and Guestrin; Lim and Chi 2019; XGBoost developers 2021).

Deep Neural Network (DNN)

A deep neural network (DNN) refers to a neural network with two or more hidden layers between the input layer and output layer. Figure 4.10 illustrates basic DNN architecture for regression and classification. A DNN consists of an input layer, several hidden layers, and an output layer. In order to predict the actual value or class of target using data with high complexity (e.g., a large number of explanatory variables on tabular data), the input signals go through the hidden layers to identify the optimal weight and bias.

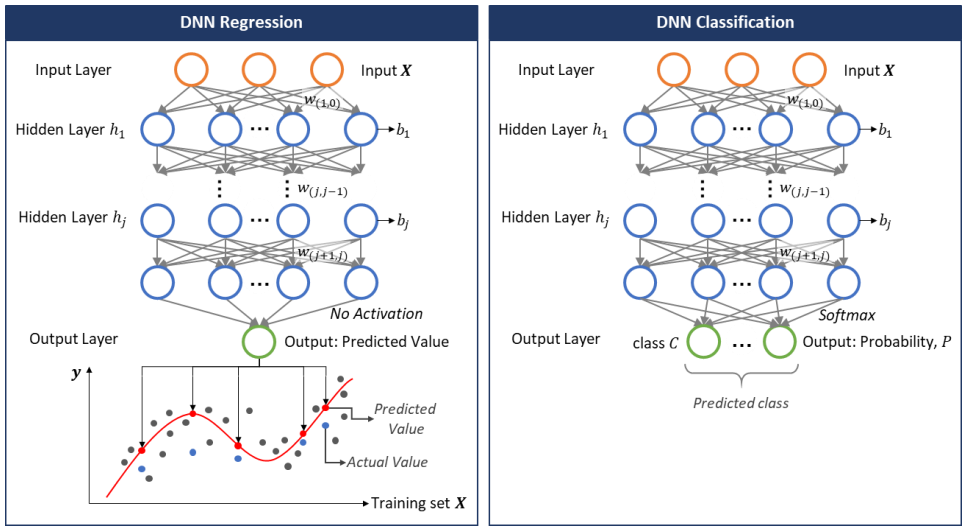

Figure 4.10 Basic DNN architecture for regression and classification

Specifically, given a training set $(x^{(i)}, y^{(i)})$, where $x^{(i)}$ is a given explanatory feature vector and $y^{(i)}$ is the actual value or class of target, the output of j-th hidden layer, $h_j(x^{(i)})$, is defined as Equation 4.10 and 4.11:

$$h_j(x^{(i)}) = f(w_{(j,j-1)}h_{j-1}(x^{(i)}) + b_j) \ (j = 2, \dots, N) \qquad (4.10)$$

$$h_1(x^{(i)}) = f(w_{(1,0)}x^{(i)} + b_1) \ (j = 1) \qquad (4.11)$$

where f = activation function (e.g., relu, sigmoid); $w_{(j,j-1)}$ = weight metrices between j-th hidden layer and $(j-1)$-th hidden layer; b_j = bias vectors of j-th hidden layer; and N = number of hidden layers ($j = 1, \dots, N$).

Next, for a DNN regression, the output layer has no activation (i.e., $f(x) = x$), so the output corresponds to the output of the last hidden layer, $h_N\left(x^{(i)}\right)$. For a DNN classification, on the other hand, the output layer utilizes a softmax function for activation. Softmax function outputs the probability of a given explanatory feature vector, P, to belong to a specific class c, as Equation 4.12:

$$P\left(c\middle|h\left(x^{(i)}\right)\right) = \frac{exp(w_l^c h_l(x^{(i)}) + b_l^c)}{\sum_{k=1}^{C} exp(w_l^k h_l(x^{(i)}) + b_l^k)} \tag{4.12}$$

where $h_l(x^{(i)})$ = the last hidden layer activation for $x^{(i)}$; C = total number of classes; and (w_l^c, b_l^c) = weights matrix and bias vector, which connect the output node for class c with the last hidden layer. Then, the class with the highest probability can be selected as the predicted class.

In regression and classification, the parameters, i.e., weight and bias, are adjusted iteratively to minimize the error between the predicted value (or class) and the actual value (or class) by considering a loss function. The loss

function can be considered as a mean absolute error (MAE) loss or a mean square error (MSE) loss for regression and a categorical cross-entropy for multi-class classification. The parameters are modified step by step via backpropagation (Bishop 2006; Lozano-Diez et al. 2017). In addition, to overcome the risk of overfitting due to the algorithm complexity for the BMS data, the author added dropout layers between the hidden layers to lower the model complexity by omitting a part of the network. Batch normalization was also applied to reduce the weight range through normalization using the mean and variance of each batch (Buduma and Lacascio 2017; Lim and Chi 2021).

4.2.3. Model Development

The regression and classification models with XGBoost and DNN were developed to estimate damage size by nine types of deck damage. Table 4.5 lists each median value of 'Over Q3=Y' group by type of deck damage in the regression models. For the classification models, the damage size by each type of deck damage was categorized into four log-scaled ranges. Table 4.6 represents the log-scaled ranges and median values of the ranges by type of deck damage.

Table 4.5 The median value of 'Over Q3=Y' group by type of deck damage

Damage type	Damage size	Median
Line-Cracking (m)	41.94–925.80	108.00
Area-Cracking (m^2)	71.50–1109.47	172.78
Leakage and Efflorescence (m^2)	113.56–1585.81	287.77
Map Cracking (m^2)	182.50–1278.00	408.18
Spalling (m^2)	4.29–52.96	8.55
Scaling (m^2)	12.00–301.38	43.02
Segregation (m^2)	5.57–215.00	13.96
Corrosion of Exposed Rebar (m^2)	3.52–113.80	7.18
Breakage (m^2)	2.19–50.76	5.34

Table 4.6 Log-scaled ranges of damage size by type of deck damage

Damage type	Range (damage size, median)			
	Range 1	Range 2	Range 3	Range 4
Line-Cracking (m)	(0, 1], 0.75	(1, 10], 3.27	(10, 100], 28.03	(100,), 187.70
Area-Cracking (m^2)	(0, 1], 0.43	(1, 10], 3.45	(10, 100], 28.20	(100,), 232.00
Leakage and Efflorescence (m^2)	(0, 1], 0.37	(1, 10], 3.81	(10, 100], 31.44	(100,), 253.03
Map Cracking (m^2)	(0, 1], 0.77	(1, 10], 4.00	(10, 100], 35.46	(100,), 300.00
Spalling (m^2)	(0, 0.1], 0.05	(0.1, 1], 0.50	(1, 10], 2.93	(10,), 17.68
Scaling (m^2)	(0, 0.1], 0.08	(0.1, 1], 0.49	(1, 10], 3.24	(10,), 37.89
Segregation (m^2)	(0, 0.1], 0.06	(0.1, 1], 0.49	(1, 10], 3.00	(10,), 24.00
Corrosion of Exposed Rebar (m^2)	(0, 0.1], 0.05	(0.1, 1], 0.48	(1, 10], 2.55	(10,), 18.90
Breakage (m^2)	(0, 0.1], 0.06	(0.1, 1], 0.32	(1, 10], 2.65	(10,), 18.66

The preprocessed data for each type of deck damage were divided into training data (80%) and testing data (20%) in accordance with the damage size distribution. To find the combination of parameters with the best performance for XGBoost and DNN, the hyperparameters were determined based on a grid search by using 5-fold cross-validation according to the grid search values described in Table 3.3. In DNN, the number of hidden layers (3–5), dropout rate (0.1–0.5, interval 0.1), and activation function (relu, sigmoid) were added for a grid search. The performance for the cross-validation was measured with a mean absolute error (MAE) index for regression and an average accuracy index for classification. MAE is defined as the mean of the absolute value of the difference between the actual value and the predicted value. Accuracy is also defined as the number of correctly predicted data among the total number of testing data. Each model was then trained with the determined optimal hyperparameters.

To evaluate and compare the performance of the trained models, the author utilized MAE, defined as Equation 4.13:

$$MAE\ \ (mean\ \ absolute\ \ error) = \frac{1}{N}\sum_{i=1}^{N} |y_i - \hat{y}_i| \qquad (4.13)$$

where N = number of testing data; y_i = actual damage size; and $\hat{y}_i$ = predicted damage size. MAE is the most popular and intuitive indicator for prediction accuracy because it is more robust to outliers than other indicators, such as MSE (mean square error) and RMSE (root mean square error). A small MAE indicates a high performance of the model because there is less error between the actual value and the predicted value.

Although MAE is useful for comparing the model performance for the same type of damage, it is difficult to compare the performance between different types of damage because the damage size by type of damage has diverse distribution, as described in Table 4.3. For this reason, the author utilized the error reduction rate to evaluate how well the models predicted the damage size compared to the standard deviation (SD) and baseline for each damage type and compare the predictive performance between damage types. The error reduction rate of the model to the SD is defined in Equation 4.14.

$$Error\ reduction\ rate\ to\ the\ SD = \frac{(MAE)-(SD)}{(SD)}\ (\%) \qquad (4.14)$$

The baseline predicts the target as a mean value of the target in the training data (Shmueli et al. 2010). That is, the baseline error can be defined as in

Equation 4.15, and the error reduction rate of the model to the baseline can be defined as in Equation 4.16:

$$Baseline\ \ error = \frac{1}{N}\sum_{i=1}^{N} |y_i - y_{mean}| \tag{4.15}$$

$$Error\ \ reduction\ \ rate\ \ to\ \ the\ \ baseline = \frac{(MAE) - (Baseline\ \ error)}{(Baseline\ \ error)}\ \ (\%) \tag{4.16}$$

where y_{mean} is a mean value of the damage size in the training data. A model with a large error reduction rate has superior predictive performance compared to the SD and baseline.

4.3. Results and Discussions

4.3.1. Model Evaluation

Model performance by type of deck damage was evaluated based on the MAE and the error reduction rate to the SD and baseline. As a result of the MAE comparison between the four models, the regression model with XGBoost showed the best performance in the eight types of damage, except for scaling (Table 4.7). Table 4.8 and Table 4.9 also list the results of the error reduction rate calculation to the SD and baseline, respectively. As a result of the error reduction rate comparison, on average, the regression model with XGBoost showed the highest performance (error reduction rate: 84.3% to the SD, 38.4% to the baseline), and the classification model with DNN showed the lowest performance (error reduction rate: 81.8% to the SD, 28.4% to the baseline). When comparing the error reduction rate to the SD of the regression model with XGBoost between the damage types, the author identified that segregation and breakage had the highest reduction rate (92.7%) and leakage and efflorescence had the lowest reduction rate (76.8%). Based on the error reduction rate results to the baseline, segregation had the highest reduction rate (53.7%), and line-cracking had the lowest reduction rate (32.4%). Finally, the regression model with XGBoost was selected to estimate the damage size.

Table 4.7 Model performance by type of deck damage (MAE)

Damage type	Regression model		Classification model	
	XGBoost	DNN	XGBoost	DNN
Line-Cracking (m)	8.84	9.86	9.81	9.14
Area-Cracking (m^2)	13.19	16.27	15.54	17.34
Leakage and Efflorescence (m^2)	24.81	25.59	28.33	27.07
Map Cracking (m^2)	19.36	25.80	23.54	22.85
Spalling (m^2)	0.41	0.50	0.47	0.51
Scaling (m^2)	1.71	1.61	1.73	1.84
Segregation (m^2)	0.65	0.83	0.76	1.05
Corrosion of Exposed Rebar (m^2)	0.84	0.85	0.97	0.88
Breakage (m^2)	0.35	0.45	0.38	0.36

Table 4.8 Model performance by type of deck damage (error reduction rate to the SD)

Damage type	SD	Regression model		Classification model	
		XGBoost	DNN	XGBoost	DNN
Line-Cracking (m)	43.25	79.6%	77.2%	77.3%	78.9%
Area-Cracking (m^2)	72.86	81.9%	77.7%	78.7%	76.2%
Leakage and Efflorescence (m^2)	106.80	76.8%	76.0%	73.5%	74.7%
Map Cracking (m^2)	103.95	81.4%	75.2%	77.4%	78.0%
Spalling (m^2)	2.42	82.9%	79.3%	80.7%	79.1%
Scaling (m^2)	14.29	88.0%	88.7%	87.9%	87.1%
Segregation (m^2)	8.88	92.7%	90.7%	91.4%	88.2%
Corrosion of Exposed Rebar (m^2)	4.86	82.7%	82.5%	80.0%	82.0%
Breakage (m^2)	4.82	92.7%	90.6%	92.2%	92.5%
Average		84.3%	82.0%	82.1%	81.8%

Note: SD = standard deviation.

Table 4.9 Model performance by type of deck damage (error reduction rate to the baseline)

Damage type	Baseline	Regression model		Classification model	
		XGBoost	DNN	XGBoost	DNN
Line-Cracking (m)	13.07	32.4%	24.6%	25.0%	30.1%
Area-Cracking (m^2)	21.85	39.7%	25.5%	28.9%	20.6%
Leakage and Efflorescence (m^2)	37.85	34.4%	32.4%	25.1%	28.5%
Map Cracking (m^2)	32.58	40.6%	20.8%	27.7%	29.9%
Spalling (m^2)	0.63	34.3%	20.6%	26.0%	19.8%
Scaling (m^2)	2.68	36.3%	40.0%	35.6%	31.4%
Segregation (m^2)	1.40	53.7%	40.8%	45.6%	25.0%
Corrosion of Exposed Rebar (m^2)	1.39	39.5%	38.7%	30.0%	37.0%
Breakage (m^2)	0.54	35.0%	16.5%	30.6%	33.2%
Average		38.4%	28.9%	30.5%	28.4%

Additionally, Table 4.10 represents the testing results of the regression model with XGBoost, which showed the best performance. In the first row of area-cracking and corrosion of exposed rebar, the damage size was estimated to be zero, the same as the actual value. In the third row of each damage, the model estimated close to the actual size (a difference of $0.19m^2$ for area-cracking and a difference of $0.04m^2$ for corrosion of exposed rebar). In the fourth row of are-cracking, the model classified the damage size as belonging to the 'Over Q3=Y' group and estimated the damage size to be the median value of $172.78m^2$, which was underestimated by $8.37m^2$ from the actual value. As shown in the fourth row of corrosion of exposed rebar, the damage

size was classified into the 'Over Q3=Y' group and estimated to be the median value of 7.18m^2, which was estimated by 1.02m^2 over the actual size.

Table 4.10 Example of damage size estimation result using the regression model with XGBoost

Damage type	Bridge No.	Inspection year	Condition grade	Estimated (m^2)	Actual (m^2)	Difference (m^2)
Area-Cracking	026234	2020	B	0.00	0.00	0.00
	000763	2017	C	0.00	1.50	-1.50
	025717	2018	C	8.78	8.97	-0.19
	031399	2019	C	172.78	181.15	-8.37
Corrosion of Exposed Rebar	032784	2014	B	0.00	0.00	0.00
	000148	2019	C	0.58	0.00	0.58
	000039	2018	C	0.89	0.85	0.04
	115740	2018	C	7.18	6.16	1.02

4.3.2. Model Comparison

Although the regression model showed the best performance for all types of damage, the regression model and classification models for estimating the damage size could be compared for the model training process and estimation results, as summarized in Table 4.11.

Table 4.11 Summary of model comparison results

Category	Regression model	Classification model
Model complexity	High	Low
Robustness to outliers	Low	High
Model performance	High	Low
Information about small damage	Large	Small
Information about large damage	Small	Large

First, in the model training process, the regression model showed higher model complexity than the classification model. As described in Figure 4.8, the classification model trained one multi-class classifier after training a binary classifier that estimates damage occurrence. On the other hand, the regression model trained the first binary classifier that estimates damage occurrence, the second binary classifier that estimates enormous damage, and the regressor that estimates the exact damage size. The high complexity of the regression model resulted in the low efficiency of model training.

Second, in the training process, the classification model can be more robust to outliers, which are data with an enormous damage size, than the regression model. Because the classification model classifies fixed ranges of damage, the outliers containing training data are difficult to influence model training significantly. On the other hand, in the regression model, the third quartile, Q3, and the median value of the ‘Over Q3 = Y’ group are changed by the outliers, so the model training process is less robust to the outliers.

Third, in terms of the estimation results of the models, the performance of the regression model was superior to that of the classification model, as described in Section 4.3.1 “Model Evaluation.” Last, the regression model can provide managers with more detailed information about small damage with a size of the third quartile, Q3, or less. It is because the regression model estimates the exact value for damage size below Q3 (e.g., $8.78m^2$ for the area-cracking on a deck) using the regressor. The classification model, however, is difficult to provide specific information about the damage size because it utilizes the median value of each range to estimate the damage size. Meanwhile, for large damage with a size greater than third quartile, Q3, the classification model can provide more information to the manager than the regression model. For example, in breakage, the regression model estimates the damage size as greater than $2.19m^2$ to be $5.34m^2$, while the classification model estimates the damage size to be $2.65m^2$ for less than $10m^2$ and $18.66m^2$ for more than $10m^2$, providing specific information about the damage size.

4.4. Summary

For the second objective of this dissertation, which is to estimate repair-required damage size on bridge elements, this chapter proposed regression and classification models using BMS data. To accomplish this objective, BMS data, including damage details for concrete-girder bridges' decks, was collected and preprocessed. Data exploration was then implemented to examine the characteristics of the damage size by nine types of deck damage drawing scatter plots and histograms. Based on the results of data exploration, regression and classification models were designed and developed utilizing XGBoost and DNN. As a result of model evaluation based on MAE, the regression model with XGBoost showed the best performance on average for nine types of damage (84.3% error reduction rate to the standard deviation and 38.4% to the baseline). In addition, a model comparison was conducted in terms of the model training process and estimation results. Although the regression model had superior performance, the classification model had lower model complexity and higher robustness to outliers than the regression model.

Chapter 5. Bridge Repair Cost Estimation

This chapter covers the third objective of this dissertation to estimate bridge repair costs for repair-required damage. As described in Section 2.3.4 "Limitations of Existing Studies," previous studies tried to estimate the repair costs based on the bridge condition changes and environmental effects; but they had difficulties in deriving accurate repair costs considering repair-required damage size according to the construction cost calculation method. To address the problem, the author proposed a research process to estimate bridge repair cost according to damage size and unit cost by repair method using BMS data, as described in Figure 5.1. First, the author estimated the damage size and portion by repair method utilizing data exploration on inspection records and damage portion classification by repair method. Second, unit cost information was collected from repair records, and the appropriate unit cost for each repair method was identified based on the similarity between data for the selected influential variables. The total repair cost was then calculated by multiplying the estimated damage size and unit cost by each repair method.

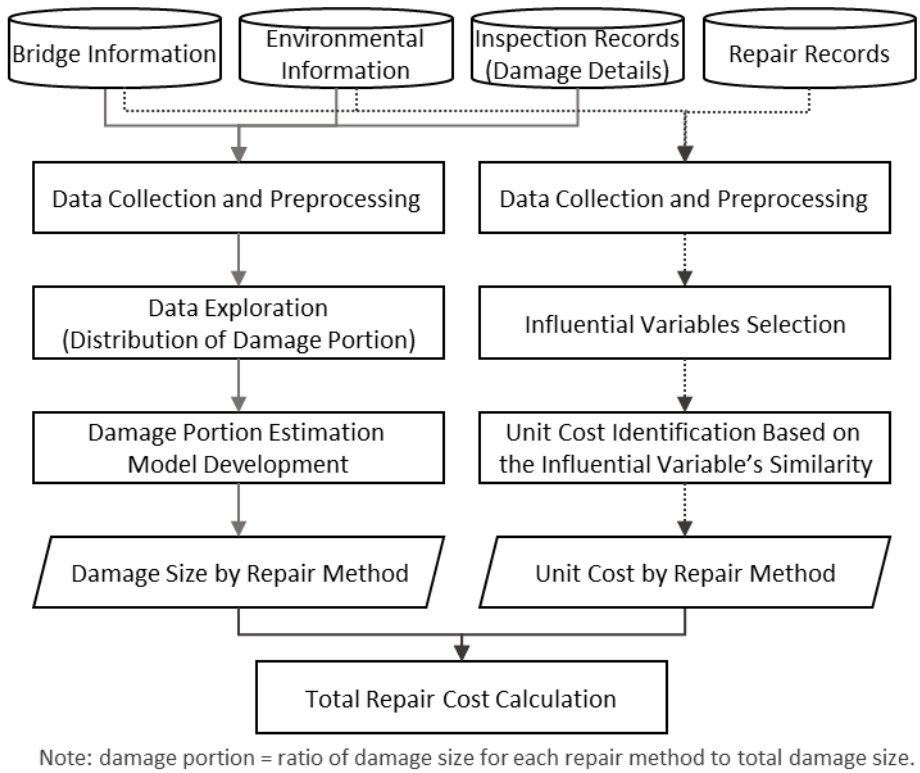

Figure 5.1 Research process of bridge repair cost estimation

5.1. Damage Size Estimation by Repair Method

5.1.1. Data Collection and Preprocessing

The BMS data for this section were collected from the KOBMS database in the same way as described in Section 4.1.1 “Data Collection and Preprocessing.” The collected data include general information with 17 variables, structural information with nine variables regarding the deck, and environmental information with 13 variables. The author extracted the inspection records inspected on deck through 3,716 in-depth inspections of 1,798 concrete-girder bridges from 2011 to 2021. The extracted records contain damage details, including the damage size for nine types of deck damage and the expected repair method for each damage, along with the inspection year, bridge age, and diagnosed condition grade of deck.

The expected repair methods for concrete deck damage include three major methods: grouting, surface repair, and section repair. The repair-required damage size for the three major methods accounted for more than 99% of the total damage size in the collected inspection records. The detailed description of each repair method on deck lists in Table 5.1 (MOLIT 2019).

Table 5.1 The detailed description of the major repair methods on deck

Repair method	Description
Grouting	It means a method of integrating concrete by injecting epoxy-based resin and cement-based materials into crackings. It prevents deterioration and corrosion by increasing the water-tightness of concrete.
Surface Repair	It means a method of improving waterproofness and durability by constructing a coating film on tiny damage. It can strengthen the surface in a simple way. However, it is difficult to deal with internal damage and advanced cracking.
Section Repair	It means a method of partially removing concrete damage and constructing materials (e.g., mortar). It is mainly used for repairing chemical corrosion, spalling, scaling, corrosion of exposed rebar, and breakage. Depending on the degree of damage and construction conditions, it is difficult to select materials and specific construction methods.

However, for one damage type inspected on the same bridge deck, several types of repair methods can be expected by the inspector. In this case, the author added a damage portion for each repair method, which is the ratio of the damage size for each repair method to the total damage size, along with the damage size for each repair method. Table 5.2 shows an example of the inspection records extracted for estimating damage size by repair method.

Table 5.2 Example of inspection records for damage size estimation by repair method

Bridge No.	Bridge age	Condition grade of deck (CG_t)	Damage type	Damage size (DS_t)	Grouting		Surface repair		Section repair	
					Damage size	Damage portion	Damage size	Damage portion	Damage size	Damage portion
000001	33	C	Line-Cracking (m)	51.00	35.40	0.7	15.60	0.3	-	-
000039	25	C	Line-Cracking (m)	9.23	9.23	1.0	-	-	-	-
000039	25	C	Scaling (m^2)	0.94	-	-	-	-	0.94	1.0
000148	28	C	Line-Cracking (m)	0.60	-	-	0.60	1.0	-	-
000095	33	C	Segrega-tion (m^2)	0.75	-	-	-	-	0.75	1.0
032818	27	C	Breakage (m^2)	2.42	-	-	-	-	2.42	1.0

Note: damage portion means the ratio of the damage size for each repair method to the total damage size.

The collected data were then preprocessed based on data cleaning, integration, reduction, and transformation. In the data cleaning step, the author eliminated the inspection records with zero size of damage because it means that the damage size for all repair methods is zero. The damage size data expected by non-major repair methods (e.g., deck waterproofing repair) were also deleted to consider only the three major repair methods; the total damage portion for the three main repair methods became 1.0. The missing values of less than 20% in the numeric variables for bridge information were replaced with the median values of the variables. Next, the data within multiple data tables were integrated to make one dataset so that the data could be input for analysis. In the data reduction step, the author removed the variables with duplicate meanings (i.e., construction year, competent authority, and inspection year) and those with a high proportion of missing values (i.e., pavement area and deck rebar diameter).

As a result of the preprocessing steps, the preprocessed datasets were constructed in tabular format for nine types of deck damage. The dataset for each type of deck damage contains 14 variables for general information, eight variables for structural information, and 13 variables for environmental information, as represented in Table 4.2. For inspection records, the dataset also includes nine variables, i.e., bridge age, condition grade of deck, damage

size, and damage size and portion by major repair methods (target variables), as represented in Table 5.2.

5.1.2. Proposed Method: Data Exploration and Damage Portion Estimation

This section explains the research method to estimate damage size for the three repair methods using the preprocessed dataset for nine types of deck damage. The author implemented data exploration to identify the data distribution according to the damage size and portion for the repair methods. When several repair methods were expected at the same time, a damage portion estimation model was developed to estimate the final damage size for each repair method.

Data Exploration

The data distribution according to the damage size for each repair method was explored using the preprocessed datasets for each type of deck damage. Table 5.3 describes the number of data, total damage size, and damage size by the major repair methods. Specifically, in spalling, scaling, corrosion of exposed rebar, and breakage, the expected repair method was only section repair. That is, the damage size for these four types of deck

damage was expected to be the damage size for section repair. For the remaining damage types, two main repair methods were expected at the same time. Among them, in area-cracking, leakage and efflorescence, and map cracking, surface repair accounted for more than 98% of the inspected damage size. Thus, the damage size for these three types of deck damage could be estimated as the damage size for surface repair. On the other hand, in line-cracking and segregation, none of the damage methods accounted for the overwhelming majority of the inspected damage size. Grouting and surface repair could be expected in line-cracking, and surface repair and section repair could be expected in segregation.

Table 5.3 Damage size distribution by repair method for nine types of deck damage

Damage type	# of data	Total damage size	Damage size by main repair method	
			Repair method	Damage size (ratio)
Line-Cracking (m)	508	24,980.50	Grouting	10,739.99 (43%)
			Surface Repair	14,056.92 (56%)
Area-Cracking (m^2)	525	44,191.62	Surface Repair	43,358.33 (98%)
			Section Repair	533.11 (1%)
Leakage and Efflorescence (m^2)	671	77,542.16	Surface Repair	75,931.46 (98%)
			Section Repair	1,610.70 (2%)
Map Cracking (m^2)	415	67,290.57	Surface Repair	65,805.17 (98%)
			Section Repair	1,485.40 (2%)
Spalling (m^2)	269	3,019.12	Section Repair	3,019.12 (100%)
Scaling (m^2)	306	9,473.75	Section Repair	9,473.75 (100%)
Segregation (m^2)	338	3,231.85	Surface Repair	1,552.00 (48%)
			Section Repair	1,679.85 (52%)
Corrosion of Exposed Rebar (m^2)	760	6,333.84	Section Repair	6,333.84 (100%)
Breakage (m^2)	407	3,353.54	Section Repair	3,353.54 (100%)

Note: ratio = ratio of the damage size for repair method to the total damage size.

Next, the data distribution according to the damage portion for each repair method was explored for line-cracking and segregation where two repair methods could be expected. As shown in Figure 5.2 (a), in line-cracking, the damage portion for grouting and surface repair was distributed from zero to one. The data on line-cracking could be categorized into three classes; grouting class (‘grouting portion = 1.0’ and ‘surface repair portion = 0.0’), surface repair class (‘grouting portion = 0.0’ and ‘surface repair portion =

1.0'), and mixed class ('grouting portion ≠ 0.0' and 'surface repair portion ≠ 0.0'). In segregation, as shown in Figure 5.2 (b), the damage portion for surface repair and section repair was mainly distributed as zero or one. The data on segregation could be categorized into two classes; surface repair class ('surface repair portion = 1.0' and 'section repair portion = 0.0') and section repair class ('surface repair portion = 0.0' and 'section repair portion = 1.0'). Table 5.4 shows the data distribution by damage portion class for line-cracking and segregation.

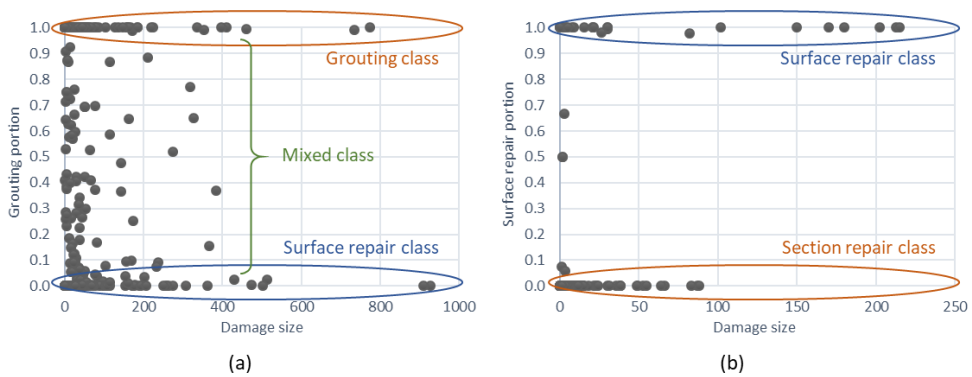

Figure 5.2. Damage portion distribution by repair method: (a) line-cracking; and (b) segregation

Table 5.4 Data distribution by damage portion class for line-cracking and segregation

Damage type	Total number of data	Damage portion class	# of data (ratio)
Line-Cracking (m)	508	Grouting class	280 (55%)
		Mixed class	79 (16%)
		Surface repair class	149 (29%)
Segregation (m^2)	330	Surface repair class	32 (10%)
		Section repair class	298 (90%)

Note: ratio = ratio of the number of data for damage portion class to the total number of data.

Damage Portion Estimation Model Development

In line-cracking and segregation, a model was developed to estimate damage portion for each repair method. According to the results of data exploration (Figure 5.2), the data on line-cracking and segregation could be categorized into two or three classes based on the damage portion for two repair methods. Thus, the damage portion estimation models were designed as described in Figure 5.3. Multi-class classification for line-cracking estimates the damage portion class (i.e., grouting class, mixed class, or surface repair class) (Figure 5.3 (a)), and binary-class classification for segregation estimates the damage portion classes (i.e., surface repair class or section repair class) (Figure 5.3 (b)). As discussed in Chapter 3 “Bridge Element Condition Estimation” and Chapter 4 “Bridge Damage Size

Estimation," the author also utilized XGBoost algorithm, which showed the best performance in classification for tabular data, such as BMS data.

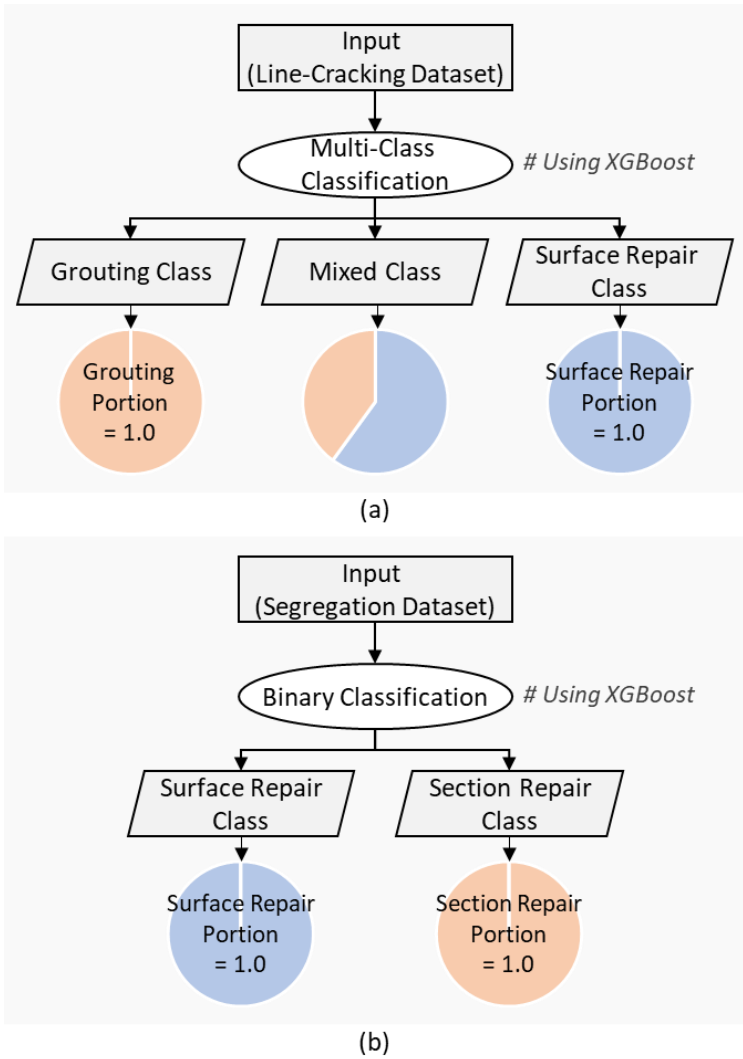

Figure 5.3 Model design for damage portion estimation: (a) line-cracking; and (b) segregation

To develop each classification model, the preprocessed datasets for line-cracking and segregation were prepared as represented in section 5.1.1 “Data Collection and Preprocessing.” Additionally, the author examined possible variable redundancies across the preprocessed data and removed one variable with a lower correlation with the target variable (i.e., damage portion) in the same way as described in Section 3.1.2 “Data preprocessing.” As a result of the redundant variable removal, the final data for line-cracking consisted of a total of 508 rows with 29 explanatory variables and one target variable (i.e., damage portion class), and the final data for segregation consisted of a total of 330 rows with 28 explanatory variables and a target variable (i.e., damage portion class), as listed in Table 5.5.

Table 5.5 Variables of the final dataset for damage portion estimation (line-cracking and segregation)

Damage type	Concept	Variable
Line-Cracking (m)	General information (10)	Facility class, Region, Management agency, Total width, Height, Water depth, Maximum span length, Total size of deck, Main superstructure type, Design live load
	Structural information for deck (7)	Deck waterproofing type, Deck thickness, Deck strength, Deck rebar strength, Deck rebar spacing, Deck pavement type, Deck pavement thickness
	Environ-mental information (8)	ADTT, Annual freeze-thaw frequency, Annual heatwave days, Summer average temperature, Summer precipitation, Winter precipitation, Summer average relative humidity, Winter average relative humidity
	Inspection records (4)	Bridge age, Condition grade of deck (CG_t), Damage size (DS_t), Damage portion class*
Segregation (m^2)	General information (10)	Facility class, Region, Management agency, Total width, Height, Water depth, Maximum span length, Total size of deck, Main superstructure type, Design live load
	Structural information for deck (7)	Deck waterproofing type, Deck thickness, Deck strength, Deck rebar strength, Deck rebar spacing, Deck pavement type, Deck pavement thickness
	Environ-mental information (7)	ADTT, Annual freeze-thaw frequency, Annual heatwave days, Annual average temperature, Winter precipitation, Summer average relative humidity, Winter average relative humidity
	Inspection records (4)	Bridge age, Condition grade of deck (CG_t), Damage size (DS_t), Damage portion class*

Note: (*) = the target variable; and ADTT = average daily truck traffic.

The final data for line-cracking and segregation were then divided into training data (80%) and testing data (20%) in accordance with the data distribution by classes of the target variable. Next, in consideration of the severity of the data imbalance between the two or three classes in the training data, the data in the minority class were generated using borderline-SMOTE as described in Section 3.2.1 “Proposed Method: Comparison of Classification Algorithms.” To find the combination of parameters with the best performance for XGBoost in the classification model, the hyperparameters were then determined based on a grid search by using 5-fold cross-validation according to the grid search values described in Table 3.3. The performance for the cross-validation was measured with an average accuracy index for classification. Finally, the trained models with optimal hyperparameters were evaluated based on the weighted average F1 score achieved in testing. A detailed explanation of the classification model development using XGBoost is described in Section 3.2.1. The model was also developed by using the scikit-learn 0.24.2 and the xgboost 1.5 Python libraries.

5.1.3. Results and Discussions

As a result of the classification model evaluation, the model for line-cracking showed a weighted average F1 score of 0.802, and the model for segregation showed a weighted average F1 score of 0.938. Specifically, for line-cracking, it was difficult to show outstanding performance due to the small number of data despite the multi-class classification problem of estimating the one actual class of the three classes. For segregation, on the other hand, the difference in characteristics between the two classes was remarkable despite significant data imbalance between classes. For example, if the damage size of segregation was $100m^2$ or more, the surface repair was expected to repair the damage.

When line-cracking damage was estimated as a mixed class by the multi-class classification model, various combinations of grouting portion and surface repair portion could be distributed, as illustrated in Figure 5.2 (a). Thus, the author calculated the mean absolute error (MAE) of the model when considering the nine combinations of damage portion, which means the grouting portion from 0.1 to 0.9 (interval 0.1) and the surface repair portion from 0.9 to 0.1 (interval 0.1). According to the calculation results, the optimal damage portion with the least MAE among the nine combinations was determined as the representative damage portion in the mixed class. The MAE

in the damage portion estimation model is defined as the mean of the absolute value of the difference between the actual damage size for grouting and the predicted damage size for grouting. As a result, the model with the grouting portion of 0.4 and the surface repair portion of 0.6 in the mixed class had the least MAE, 0.161 (m), as shown in Figure 5.4. The optimal damage portion in the mixed class was then determined to be 0.4 for the grouting portion and 0.6 for the surface repair portion. It can be practically acceptable because the MAE, 0.161 (m), for grouting means an average error of 14,000 won per bridge when converted into repair costs.

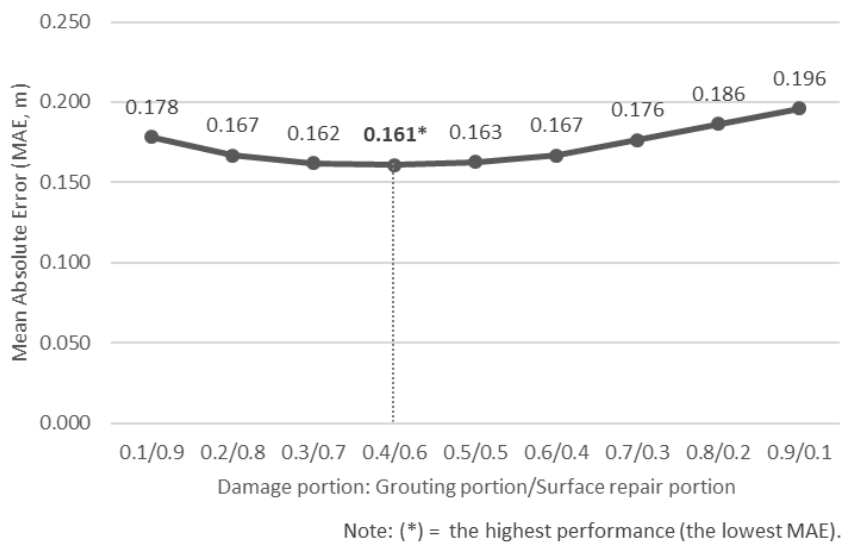

Figure 5.4 Result of the optimal combination of damage portion in mixed class for line-cracking

Consequently, Table 5.6 represents an example of the testing results of the damage size estimation for line-cracking and segregation. In the first row of line-cracking, the damage portion class was estimated to be mixed class by the damage portion estimation model, and the damage portions of grouting and surface repair were estimated to be 0.4 and 0.6, respectively. When the damage size (51.00m) was multiplied by the estimated damage portion, the damage size for grouting and surface repair was estimated to be 20.40m and 30.60m, respectively. In the second row of segregation, for instance, the damage portion class was estimated to be section repair class by the damage portion estimation model, and the damage size of 0.60m^2 was estimated as the damage size for section repair.

Table 5.6 Example of damage size estimation result by repair method

Damage type	Bridge No.	Inspection year	Condition grade	Damage size	Estimated damage size (damage portion)		
					Grouting	Surface Repair	Section Repair
Line-Cracking (m)	000001	2019	C	51.00	20.40 (0.4)	30.60 (0.6)	-
	000039	2018	C	9.23	9.23 (1.0)	-	-
	000148	2019	C	0.60	-	0.60 (1.0)	-
Segregation (m^2)	000005	2014	D	30.14	-	30.14 (1.0)	-
	033130	2020	C	0.60	-	-	0.60 (1.0)
	000179	2017	C	180.00	-	180.00 (1.0)	-

5.2. Unit Cost Analysis by Repair Method

Bridge maintenance practices have used unit cost by repair method estimated based on the market inflation rate and the standard construction cost in each country (Gordian 2022; MOLIT 2022a). For example, in South Korea, management agencies that perform repair construction have provided guidelines that introduce unit costs for bridge repair and reinforcement activities to estimate the repair cost and allocate the repair construction budget in each agency. However, since the unit cost differed depending on the repaired damage size, environmental effects on repair construction, and bridge specifications, the practices had a limitation in estimating accurate unit cost by repair method. In this section, therefore, the author aimed to identify the appropriate unit cost for each repair method by using the actual repair records collected from BMS.

5.2.1. Data Collection and Preprocessing

The BMS data for this section cover repair records collected from the KOBMS database to analyze unit cost by repair method. The repair records were accumulated through 2,970 repair constructions of 4,186 bridges in South Korea from 2012 to 2021. According to this dissertation scope, the author extracted the repair records of decks on 525 repair constructions of 701

concrete-girder bridges. The repair records include ‘repair construction start/end date,’ ‘bridge age,’ ‘repair method for deck,’ ‘repaired damage size,’ and ‘construction cost’ for each span of bridge. The unit cost by each repair method was calculated by dividing the construction cost by the repaired damage size. In addition, the author used the construction cost index to convert the unit cost by construction year into present value. The construction cost index is defined as an index that measures the price fluctuations of direct construction costs (including material cost, labor cost, and expense) for each month as of December 2014, which is announced by the KICT (KICT 2022a). Thus, ‘unit cost by repair method’ was derived by applying the ‘construction cost conversion index’ calculated as of December 2021, based on the construction cost index. Table 5.7 shows an example of the repair records extracted for analyzing unit cost by repair method.

Table 5.7 Example of repair records for unit cost analysis by repair method

Bridge No.	Span No.	Repair construction end date (month/year)	Bridge age	Repair method	Repaired damage size	Construction cost (1,000won)	CCCI	Unit cost (1,000won)
025657	1	12/2012	19	Section Repair (m^2)	0.50(m^2)	253	0.696	727.0(/m^2)
028681	5	12/2018	6	Surface Repair (m^2)	26.87(m^2)	1,244	0.821	56.4(/m^2)
010044	1	12/2017	26	Grouting (m)	1.00(m)	97	0.784	123.7(/m)
002618	4	11/2021	29	Surface Repair (m^2)	50.10(m^2)	4,588	0.996	91.9(/m^2)
033679	1	06/2013	10	Section Repair (m)	1.00(m)	107	0.699	153.1(/m)

Note: CCCI = construction cost conversion index as of December 2021.

The collected data also include bridge information, structural information regarding the deck, and environmental information with two types of traffic information affecting the unit cost, in the same way as described in Section 3.1.1 “Data Collection.” Among the data, the author extracted data for the 701 concrete-girder bridges with repair construction details in the repair records.

The extracted data were then preprocessed based on data cleaning, integration, and reduction. In the data cleaning step, the unit cost data by non-major repair methods (e.g., deck waterproofing repair) were deleted to consider only the three main repair methods. The author eliminated the repair records with too large construction costs that are considered recording errors of bridge managers. The repair records with fewer than two years of bridge age were also eliminated because they were considered repair records for defects during construction, not repair records for damages caused by use in the management stage. The missing values of less than 20% in the numeric variables for bridge information were replaced with the median values of the variables. Next, the data within multiple data tables were integrated to make one dataset so that the data could be input for analysis. In the data reduction step, the author removed the variables with duplicate meanings in the same way as described in Section 3.1.2 “Data Preprocessing.” For example, ‘repair

construction start/end date' and 'construction year,' which were variables that had duplicate meanings with 'bridge age,' were removed because 'bridge age' is defined as the difference between 'repair construction end year' and 'construction year.' 'Construction cost' and 'construction cost conversion index,' which were variables that had duplicated meanings with 'unit cost,' were also removed. The numerical variables with more than 20% missing values, such as 'pavement area' and 'deck rebar diameter,' were removed.

As a result of the preprocessing steps, the preprocessed dataset for analyzing unit cost by repair method consisted of a tabular format with the repair records; i.e., repair method, repaired damage size, and unit cost (target variable), bridge information, and traffic information. The dataset was also composed of a total of 4,328 data on 491 repair constructions of 661 concrete-girder bridges and a total repair construction cost of 24,059,237 thousand won. Table 5.8 lists the repair cost and the number of data by repair method.

Table 5.8 Repair cost distribution by repair method of deck

Repair method	Repair cost (1,000won) (ratio)	# of data
Grouting (m)	483,112 (2.0%)	415
Surface Repair (m^2)	17,672,418 (73.5%)	2,179
Surface Repair (m)	31,857 (0.1%)	22
Section Repair (m^2)	5,871,850 (24.4%)	1,712
Total	24,059,237 (100%)	4,328

Note: ratio = ratio of the repair cost for the repair method to the total repair cost.

In addition, the distribution of unit cost by each repair method was explored, as represented in Table 5.9. In all repair methods, the mean value was larger than the median value, and the data were widely distributed toward the larger value, as the histogram shown in Figure 5.5. Through the data distribution, the author confirmed that there was a limit to applying the representative unit cost (e.g., mean and median value) by repair method to all repair construction.

Table 5.9 Unit cost distribution by repair method

Repair method	# of data	Mean	SD	Min	Q1	Q2	Q3	Max
Grouting (m)	415	108.3	52.2	42.6	75.8	85.5	130.3	307.8
Surface Repair (m^2)	2,179	143.8	54.3	7.0	112.7	136.8	158.9	837.2
Surface Repair (m)	22	86.0	57.6	34.3	35.5	35.8	153.1	154.5
Section Repair (m^2)	1,712	606.5	374.1	9.6	411.8	530.9	702.2	3,866.4

Note: SD = standard deviation; Q1=the first quartile (25%, lower quartile); Q2=the second quartile (50%, median); and Q3=the third quartile (75%, upper quartile).

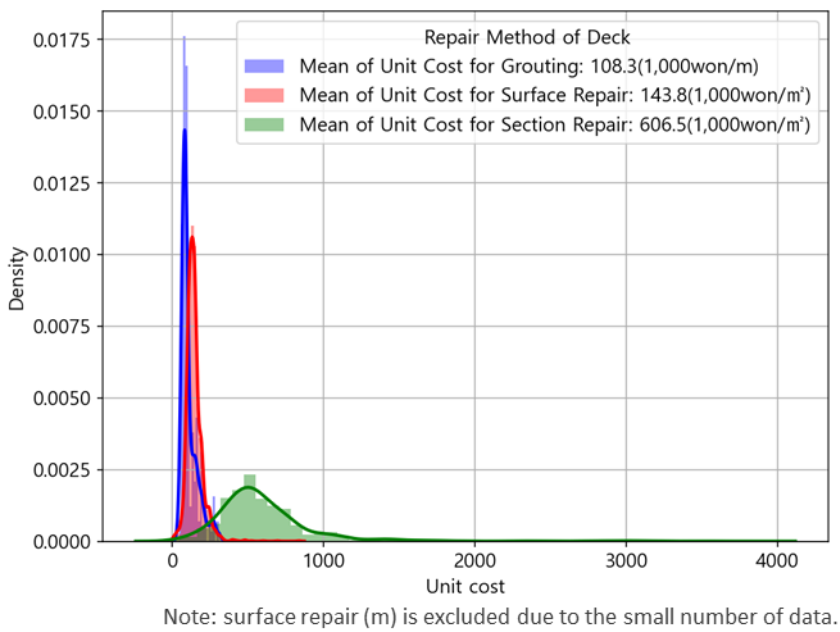

Figure 5.5 Unit cost distribution (histogram) by repair method

5.2.2. Proposed Method: Unit Cost Identification Based on the Influential Variable's Similarity

This section explains the research method to identify unit cost by the three repair methods using the preprocessed dataset. First, the author selected influential variables affecting the unit cost among several explanatory variables. Then, the expected unit cost by repair method was identified based on the unit cost in the case of having the same or similar values for the selected influential variables. The specific method is represented below.

Influential Variable Selection

To select influential variables that affect the unit cost for repair construction, an expert interview was conducted to apply empirical and substantive domain knowledge. The interviewees consisted of four industry practitioners in the areas of bridge operation and maintenance, KOBMS, and big-data analytics with more than 10 years of working experience. In the interview, the interviewees scrutinized the variables collected from KOBMS and considered repair construction specifications, environmental information on repair construction, and bridge information that could affect the bridge repair cost among these variables. They also suggested that the influential variable selection process needs to consider distinct characteristics of bridge

maintenance practice in South Korea and the type or range of variables covered by the KOBMS.

Influential Variable's Similarity Calculation

The similarity between the input data and other data included in the dataset was calculated differently according to the types of the selected influential variables. Similarity for each categorical variable was defined as one if the category was the same and zero otherwise. For numerical variables, after the variables were scaled by min-max normalization, similarity for the scaled numerical variables was defined as the Euclidean distance (Han et al. 2010; Lattin et al. 2003). Taken together, the similarity between the input data, X^{in}, and other data, X, for the selected influential variables is given as Equation 5.1 and 5.2:

$$Similarity_{(X^{in},X)} = C_1 \times \ldots \times C_k \times \{1 - \sqrt{\frac{1}{l}\sum_{j=1}^{l}\left(x_{n,j}^{in} - x_{n,j}\right)^2}\} \quad (5.1)$$

$$C_i = 1 \ \left(if \ \ x_{c,i}^{in} = x_{c,i}\right) \ or \ \ 0 \ \ (otherwise) \quad (5.2)$$

where $X^{in} = \left(x_{c,1}^{in}, \ldots, x_{c,k}^{in}, x_{n,1}^{in}, \ldots, x_{n,l}^{in}\right)$; $X = (x_{c,1}, \ldots, x_{c,k}, x_{n,1}, \ldots, x_{n,l})$; $x_{c,i}$ = i-th categorical variable ($i = 1, \ldots, k$); $x_{n,j}$ = j-th scaled numerical variable ($j = 1, \ldots, l$); and C_i = similarity for i-th categorical variable ($i = 1, \ldots, k$). The high similarity means that the values of the selected variables between the two data are very similar.

Based on the calculated similarity for the influential variables, the unit cost of input data was estimated as the average unit cost of the N data with the highest similarity. The author performed a sensitivity analysis to find the optimal number of similar data by repair method. When all data in the dataset were set as input data, a mean absolute error (MAE) between the actual unit cost and the estimated unit cost was calculated. N with the lowest MAE was derived as the optimal value.

5.2.3. Results and Discussions

As a result of the expert interview for influential variables selection, first, ‘damage size’ and ‘management agency’ was selected regarding repair construction specifications. It was experientially known that the unit cost is lower as the repaired damage size is larger. ‘Management agency’ could also influence the repair construction cost since the management agencies have

different characteristics, such as the number of managed bridges, region, and repair construction experience.

Second, environmental information on repair construction includes several factors, such as traffic information, weather information, and construction market conditions. The traffic information (i.e., 'ADT') was only selected because weather information is difficult to predict in bridge maintenance practice, and construction market conditions are not covered by the KOBMS. According to the interviewee in the area of bridge operation and maintenance, in practice, bridges with high traffic volume tended to have a high repair construction cost due to traffic control and construction delays.

Last, among various types of bridge information in the KOBMS, the interviewees selected 'bridge age,' 'bridge length,' 'height,' and 'main superstructure type' as conventional bridge information used in bridge maintenance practice. In particular, the deck material is major information in the deck repair works, but it was excluded from this research since all concrete-girder bridges have RC or PSC decks. Consequently, the author selected five numerical variables and two categorical variables: 'damage size,' 'ADT,' 'bridge age,' 'bridge length,' and 'height' for numerical variables and 'management agency' and 'main superstructure type' for categorical variables.

The relationship between these seven influential variables and the unit cost by repair method was confirmed using the preprocessed dataset. Figure 5.6 illustrates the unit cost distribution for surface repair according to the influential variables. The negative correlation between 'damage size' and the unit cost and the positive correlation between 'ADT' and the unit cost was in line with the expert interview's result, as shown in Figure 5.6 (a) and (b). 'Bridge age' and 'bridge length' represented a weak negative correlation with the unit cost (Figure 5.6 (c) and (d)), and 'height' showed a weak positive correlation with the unit cost (Figure 5.6 (e)). While examining the distribution of the unit cost by each category of the two categorical variables, the unit cost was low on average in Gyeonggi and Daejeon and high on average in Gangwon (Figure 5.6 (f)). Among the main superstructure types, PSCB had a high unit cost on average (Figure 5.6 (g)).

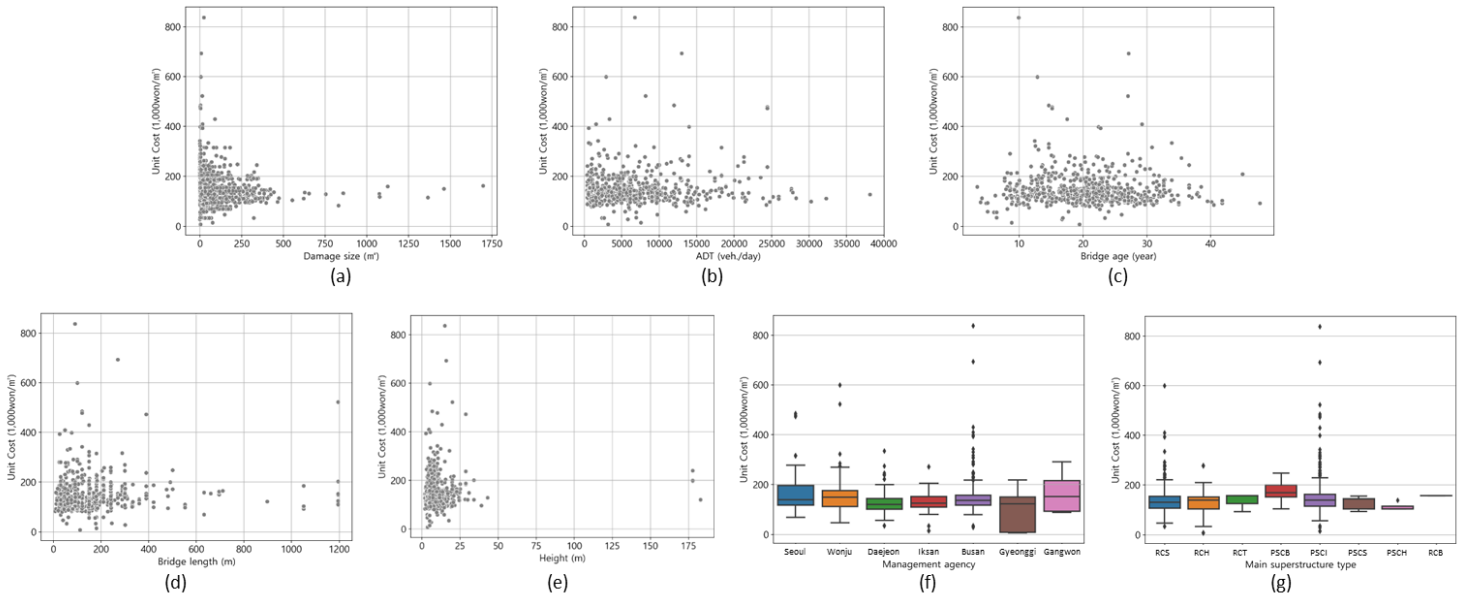

Figure 5.6 Unit cost distribution for surface repair according to seven influential variables: (a) damage size; (b) ADT; (c) bridge age; (d) bridge length; (e) height; (f) management agency; and (g) main superstructure type

The author then conducted the sensitivity analysis ($N = 1, \dots, 9$) for three repair methods (i.e., grouting, surface repair, and section repair) using the seven influential variables and unit cost extracted from the preprocessed dataset. As a result, Table 5.10 represents the MAE according to N by the three repair methods. The optimal N was derived as three for grouting, surface repair, and section repair.

Table 5.10 MAE by repair method according to the number of similar data

N	MAE by repair method (1,000won)		
	Grouting (m)	Surface Repair (m^2)	Section Repair (m^2)
1	19.6	21.2	179.9
2	15.7	17.7	173.6
3	15.5*	16.6*	171.0*
4	16.4	18.9	180.9
5	16.6	19.7	186.2
6	17.3	20.7	185.3
7	18.6	21.5	192.7
8	20.6	23.7	201.4
9	22.2	24.3	205.1

Note: N = # of similar data; and (*) = the MAE in the optimal N (the lowest MAE).

To verify the research method for unit cost identification, the author calculated the error reduction rate to the standard deviation (SD). The MAE based on the research method was also compared with the MAE based on the baseline when the median value was expected as the estimated unit cost. Table 5.11 provides the verification results of unit cost identification. The error

reduction rate to the SD was the largest in grouting and the smallest in section repair and showed an average of 64.7%. When compared to the baseline, the error reduction rate represented an average of 42.5%. Here, surface repair (m) was excluded from the analysis due to the very small number of data, and the unit cost for surface repair (m) was estimated by the mean value.

Table 5.11 Verification results of unit cost identification

Repair Method	MAE*	SD	MAE based on the baseline	ERR to the SD	ERR to the baseline
Grouting (m)	15.5	52.2	33.6	70.3%	53.8%
Surface Repair (m^2)	16.6	54.3	35.4	69.5%	53.2%
Section Repair (m^2)	171.0	374.1	215	54.3%	20.5%
Average				64.7%	42.5%

Note: (*) = the MAE based on the research method; SD = standard deviation; and ERR = error reduction rate (%).

5.3. Calculation of Total Repair Cost

Finally, the repair cost by repair method was calculated by multiplying the damage size and unit cost estimated in Section 5.1 “Damage Size Estimation by Repair Method” and Section 5.2 “Unit Cost Analysis by Repair Method.” The total repair cost at the individual bridge level (i.e., project level) was then estimated as the sum of the estimated repair costs for repair methods. Table 5.12 shows an example of a total deck repair cost estimation. For each bridge, the damage portion and size by repair method for nine types of deck damage were estimated, and the unit cost was identified based on the similarity between data for the selected influential variables. The total cost was estimated by adding up the repair cost by repair method.

Table 5.12 Example of total deck repair cost estimation

Bridge No.	YR_{t+1}	CG_{t+1}	Damage type	Damage size	Repair cost by repair method					Total cost (1,000won)*
					Method	Portion	Size	Unit cost (/1,000won)	Cost (1,000won)	
025717	2023	C	LC (m)	17.08	Grouting	0.4	6.83	81.5	556.6	10,344.5
					Surface Repair	0.6	10.25	86.0	881.5	
			AC (m^2)	8.78	Surface Repair	1.0	8.78	102.0	895.6	
			LE (m^2)	12.01	Surface Repair	1.0	12.01	102.0	1,225.0	
			MC (m^2)	0.00	Surface Repair	-	-	-	-	
			SP (m^2)	7.03	Section Repair	1.0	7.03	578.5	4,066.9	
			SC (m^2)	0.00	Section Repair	-	-	-	-	
			SG (m^2)	0.00	Surface Repair	-	-	-	-	
					Section Repair	-	-	-	-	
			CE (m^2)	4.70	Section Repair	1.0	4.70	578.5	2,719.0	
			BR (m^2)	0.00	Section Repair	-	-	-	-	

Note: $(t+1)$ = future time to be repaired; YR_{t+1}= year at $(t+1)$; CG_{t+1}= condition grade of deck at $(t+1)$; LC = Line-Cracking (m); AC = Area-Cracking (m^2); LE = Leakage and Efflorescence (m^2); MC = Map Cracking (m^2); SP = Spalling (m^2); SC = Scaling (m^2); SG = Segregation (m^2); CE = Corrosion of Exposed Rebar (m^2); BR = Breakage (m^2); and (*) = cost as of December 2021.

5.4. Summary

For the third objective of this dissertation, which is to estimate bridge repair cost, this chapter provided a research process to calculate the repair cost according to the estimated damage size and unit cost by repair method using BMS data. To accomplish this objective, first, the author explored data distribution according to the damage size and portion by repair method for nine types of deck damage. Using line-cracking and segregation data that could be categorized into several classes based on the damage portion for two repair methods, classification models with XGBoost were then developed to estimate the damage portion by repair method. As a result of model evaluation, the model for line-cracking showed a weighted average F1 score of 0.802, and the model for segregation showed a weighted average F1 score of 0.938. Second, influential variables affecting the unit cost by repair method were selected by conducting an expert interview. The unit cost by repair method was then identified based on the similarity between data for the selected seven variables: 'damage size,' 'ADT,' 'bridge age,' 'bridge length,' 'height,' 'management agency,' and 'main superstructure type.' The proposed research method showed an average error reduction rate of 64.7% compared to the standard deviation. Last, the total repair cost was calculated by multiplying the estimated damage size and unit cost by each repair method.

Chapter 6. Experimental Results and Discussions

This chapter provides experimental processes, results, and discussions to verify and validate this study. The experiment aimed to conduct performance verification and validate the superiority in providing predictive maintenance information by comparison with existing approaches. The existing approaches include a practical method based on the estimated condition grade of deck and a repair cost estimation model on deck. The comparison focused on the types of predictive information and repair cost estimation performance. For the experiment, input data were collected for 100 concrete-girder bridges widely distributed across Gyeonggi-do, Gangwon-do, Jeolla-do, and Gyeongsang-do. As illustrated in Figure 6.1, the data contain bridge information and inspection records with the latest inspection record for the deck in 2018 (t) extracted from the KOBMS database and environmental information acquired from external databases. The author also collected inspection and repair records in 2020 ($t + 1$) for the 100 bridges as the ground truths from the KOBMS database. The results and discussions of the experiment using the input data and ground truths are explained in the following sections.

Bridge No.	Bridge Information		Environmental Information		Inspection Records						
	Bridge Length	...	ADT	...	Bridge Age	CG_t	DS_t	I_t	CG_{t-1}	DS_{t-1}	I_{t-1}
025132	120.0	...	32,270.2	...	18.6	B	(0, 0, ..., 0, 0)	2	B	(0, 0, ..., 0, 0)	2
027148	120.0	...	7249.7	...	12.6	B	(0, 0, ..., 0, 0)	2	A	(0,0, ..., 0, 0)	2
031058	120.0	...	1,373.8	...	21.6	C	(34.8, 0, ..., 0, 0)	2	B	(0,0, ..., 0, 0)	2
...	...	...	...	...	...	...	...	...	...	...	...

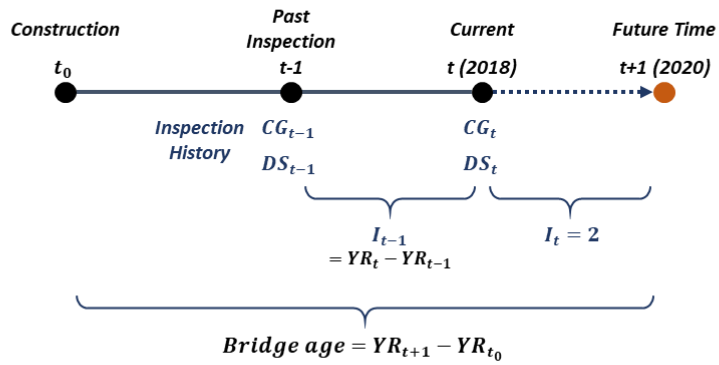

Note: CG_t = condition grade of deck at t; $DS_t = (DS_t^{LC}, ..., DS_t^i, ..., DS_t^{BR})$, DS_t^i = damage size by i-th type of deck damage at t, i = (Line-Cracking (m), Area-Cracking (m²), Leakage and Efflorescence (m²), Map Cracking (m²), Spalling (m²), Scaling (m²), Segregation (m²), Corrosion of Exposed Rebar (m²), Breakage (m²)); and YR_t = year at t.

Figure 6.1 Description of input data for the experiment

6.1. Results of Performance Verification

To verify the performance of the proposed methodology, the author derived the condition grade, damage size, and repair cost on each bridge deck expected in the next inspection ($t + 1 = 2020$) by putting the input data into the developed models, as shown in Figure 6.2. As a result, the condition grades and damage size were successfully estimated with a weighted average F1 score of 0.845 and an error reduction rate to the SD of 85.0%, respectively. The unit cost by each repair method for estimating deck repair cost was estimated with an error reduction rate to the SD of 64.2%. Finally, the repair cost based on the expected damage size and unit cost by repair method was estimated with an MAE of 6,996.3 thousand won compared to the ground truths (i.e., actual repair cost for each bridge's deck). The estimation performance is about 20% of the average deck repair cost per concrete-girder bridge (35,104.8 thousand won) entered into the KOBMS and is similar to the section repair cost of $11m^2$ deck based on the average unit cost of section repair (606.5 thousand won).

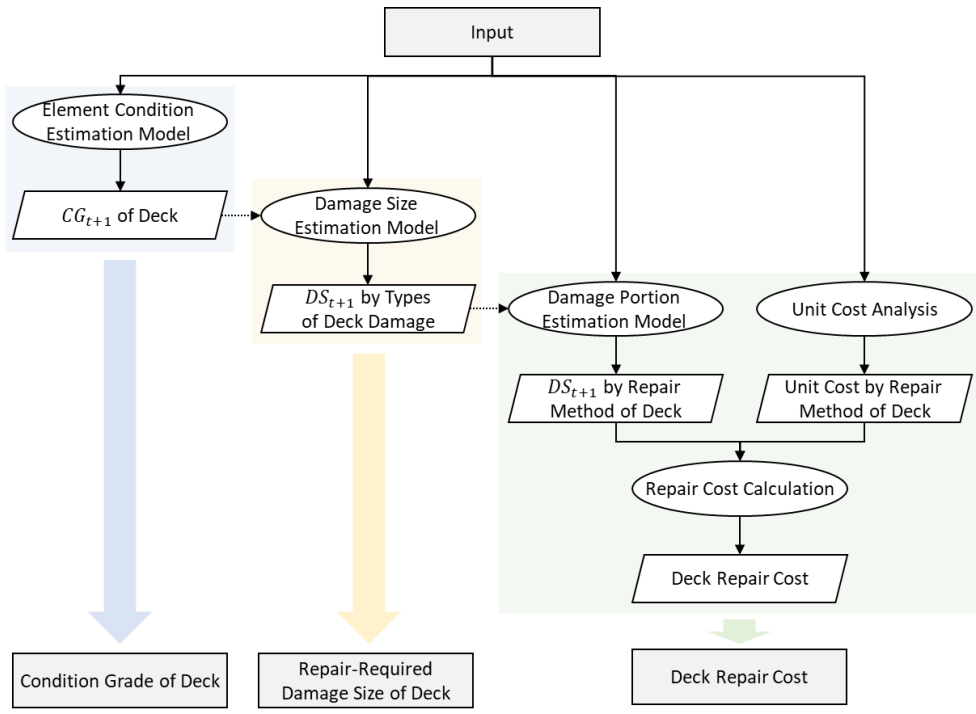

Note: CG_{t+1}= condition grade of deck at future time; DS_{t+1}= damage size by nine types of deck damage at future time.

Figure 6.2 The estimation process based on the proposed methodology

Table 6.1 shows the estimated results and ground truths for condition grade, damage size, and repair cost on deck in detail through three cases. In the case of 'Case #1: Bridge No. 027148,' the deck was estimated to be condition grade 'C' with damage such as map cracking and spalling. The damage size and unit cost for surface repair and section repair were estimated, respectively, and the final repair cost was then estimated at 1,787.1 thousand won. In the actual records (i.e., ground truths), although the deck was

inspected as condition grade ‘B’ with no repair-required damage in 2020, a $5.0m^2$ section repair work was performed with 1,655.4 thousand won, which had a very slight difference from the estimated one (131.7 thousand won). Meanwhile, in the case of ‘Case #2: Bridge No. 025132,’ the unit cost for each repair method was well estimated, but there was a considerable difference between the estimated and actual repair cost (about 60 million won) because the area-cracking size was underestimated. In the case of ‘Case #3: Bridge No. 031058,’ although the condition grade and damage size had a satisfactory estimation, the actual repair construction for the deck was not performed, resulting in a difference of more than 50 million won between the estimated and actual repair cost.

Table 6.1 Estimated result and ground truth for condition grade, damage size, and repair cost of deck

Case #1: Bridge No. 027148														
Category	CG	Damage size									(Damage size) × (Unit cost)			Repair cost (1,000won)
		LC	AC	LE	MC	SP	SC	SG	CE	BR	Grouting	Surface repair	Section repair	
Estimated result	C	-	-	-	3.83	0.36	0.94	-	0.61	-	-	(3.83) ×(228.0)	(1.91) ×(409.5)	1,787.1
Ground truth	B	-	-	-	-	-	-	-	-	-	-	-	(5.00) ×(357.4)	1,655.4
Case #2: Bridge No. 025132														
Category	CG	Damage size									(Damage size) × (Unit cost)			Repair cost (1,000won)
		LC	AC	LE	MC	SP	SC	SG	CE	BR	Grouting	Surface repair	Section repair	
Estimated result	D	-	172.78	-	-	8.55	-	-	0.55	0.58	-	(172.78) ×(115.2)	(9.68) ×(576.5)	25,484.8
Ground truth	D	-	606.45	-	-	4.42	-	-	3.65	0.98	-	(766.00) ×(110.9)	(1.00) ×(506.5)	85,479.4
Case #3: Bridge No. 031058														
Category	CG	Damage size									(Damage size) × (Unit cost)			Repair cost (1,000won)
		LC	AC	LE	MC	SP	SC	SG	CE	BR	Grouting	Surface repair	Section repair	
Estimated result	C	11.55	6.42	-	408.18	-	-	-	0.70	-	(11.55) ×(147.4)	(414.60) ×(124.0)	(0.70) ×(586.2)	53,523.2
Ground truth	C	39.60	0.45	-	344.64	-	-	-	0.84	-	-	-	-	0.0

Note: CG = condition grade of deck in 2020; LC = Line-Cracking (m); AC = Area-Cracking (m^2); LE = Leakage and Efflorescence (m^2); MC = Map Cracking (m^2); SP = Spalling (m^2); SC = Scaling (m^2); SG = Segregation (m^2); CE = Corrosion of Exposed Rebar (m^2); BR = Breakage (m^2); and repair methods include grouting (m), surface repair (m), surface repair (m^2), and section repair (m^2).

In addition, to demonstrate the expandability of the proposed methodology, the author conducted a case study to estimate predictive information about consecutive future points in time. Based on the current point in the input data ($t = 2018$), the condition grades, damage size, and repair costs on decks were estimated for the next six years until 2024. The past inspection history, which changes over time, was input into the expected condition grade and damage size at the last time. Figure 6.3 shows an example of estimation results for 'Bridge No 027147.' The condition grade was estimated to decline to grade 'C' after one year (Figure 6.3 (a)). As represented in Figure 6.3 (b), the author could confirm the damage pattern over time. Map cracking, scaling, and corrosion of exposed rebar were expected to be inspected after one year, and area-cracking and breakage were expected to be inspected after three years. After four years, it was expected that a large area of leakage and efflorescence would be inspected. Meanwhile, after five years, it was estimated that the damage size of corrosion of exposed rebar would increase rapidly instead of decreasing the size of leakage and efflorescence. A sharp increase in repair cost was estimated with an increase in damage size after four years (Figure 6.3 (a)).

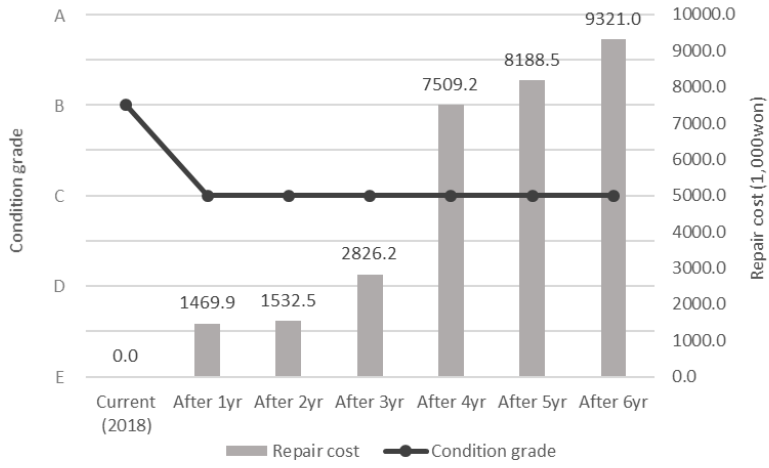

(a)

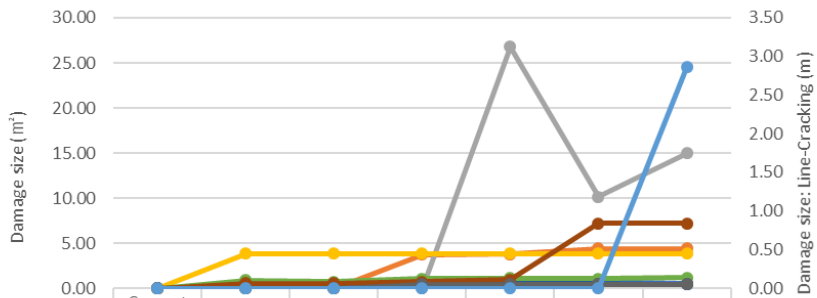

	Current (2018)	After 1yr	After 2yr	After 3yr	After 4yr	After 5yr	After 6yr
AC (m²)	0.00	0.00	0.00	3.76	3.79	4.42	4.42
LE (m²)	0.00	0.00	0.00	0.00	26.81	10.13	15.00
MC (m²)	0.00	3.83	3.83	3.83	3.83	3.83	3.83
SP (m²)	0.00	0.28	0.31	0.55	0.49	0.74	0.52
SC (m²)	0.00	0.90	0.74	1.04	1.11	1.07	1.18
SG (m²)	0.00	0.00	0.00	0.51	0.48	0.48	0.46
CE (m²)	0.00	0.56	0.56	0.73	0.96	7.18	7.18
BR (m²)	0.00	0.00	0.00	0.47	0.47	0.47	0.47
LC (m)	0.00	0.00	0.00	0.00	0.00	0.00	2.86

Note: LC=Line-Cracking (m); AC= Area-Cracking (m²); LE=Leakage and Efflorescence (m²); MC=Map Cracking (m²); SP=Spalling (m²); SC=Scaling (m²); SG=Segregation (m²); CE=Corrosion of Exposed Rebar (m²); and BR=Breakage (m²)

(b)

Figure 6.3 Example of the estimation results for consecutive future points:

(a) condition grade and repair cost; and (b) damage size

6.2. Superiority Validation for Predictive Bridge Maintenance

6.2.1. Experimental Results of Existing Approaches

The proposed methodology was compared with two existing approaches: a practical method based on deck condition estimation and a repair cost estimation model on deck. Each approach was developed using the KOBMS data and evaluated using the input data for the experiment.

Practical method

In the practical method, the future repair cost on each bridge element was calculated, as represented in Equation 6.1:

$$Repair\ \ cost = (Unit\ \ repair\ \ cost) \times (Element\ \ size) \div (CCCI) \quad (6.1)$$

where unit repair cost indicates an average unit repair cost according to the estimated condition grade on each element; and CCCI refers to the construction cost conversion index based on repair construction time. For the experiment, the future condition grade on deck was estimated by the element condition estimation model developed by the Seoul National University research team using the KOBMS data, and the unit repair cost was input based on the average values provided in Table 2.1. The calculated cost was then

converted into a repair cost as of December 2021 using the construction cost conversion index. As a result of the evaluation using the input data, the deck repair cost was estimated with an MAE of 26,603.1 thousand won compared to the ground truths.

Repair cost estimation model on bridge element

This dissertation developed a repair cost estimation model on deck using the KOBMS data collected in Section 5.2.1 “Data Collection and Preprocessing.” In the preprocessing process, the collected data were composed of a total of 837 data by summing up the deck repair costs at the bridge level. In order to consider the deck condition before repair, the author linked the condition grade of deck before each repair work to the collected data from the inspection records. In the data reduction step, the author removed the variables with duplicate meanings in the same way as described in Section 3.1.2 “Data Preprocessing.” As a result, the preprocessed dataset for estimating the future deck repair cost consisted of a tabular format with 22 explanatory variables (13 numerical variables and nine categorical variables) and one target variable (i.e., deck repair cost). Table 6.2 lists the variables used in the model development.

Table 6.2 Variables of the final dataset for deck repair cost estimation

Concept	Variable
General information (9)	Facility class*, Management agency*, Deck Size, Total width, Height, Water depth, Main superstructure type*, Main substructure type*, Design live load*
Structural information (8)	Deck waterproofing type*, Deck thickness, Deck strength, Deck rebar diameter, Deck rebar spacing, Deck pavement thickness, Deck material*, Deck pavement type*
Environmental information (1)	Average daily traffic (ADT)
Inspection records (2)	Condition grade of deck before repair work*, Interval between inspection and repair
Repair records (2)	Bridge age, Deck repair cost**

Note: (*) = categorical variable; and (**) = target variable.

In the model development process, the author utilized XGBoost, which showed excellent performance for regression in Section 4.3.1 “Model Evaluation.” XGBoost was tuned using the preprocessed data according to the grid search, as provided by Table 3.3. At the same time, five-fold cross-validation was conducted to find the optimal hyperparameter combination with the highest average accuracy. The model was then trained with the optimal hyperparameters: eight maximum depth, 5.0 minimum child weight, 0.8 subsample, 0.6 colsample by tree, 0.0 gamma, and 0.5 learning rate. As a result of the model evaluation using the input data, the repair cost was estimated with an MAE of 11,925.5 thousand won compared to the ground truths.

6.2.2. Comparison Results and Discussions

Table 6.3 shows the comparison results between the proposed methodology and existing approaches focusing on the types of predictive information and repair cost estimation performance for predictive maintenance. In terms of the types of predictive information, the proposed methodology provides the future condition grade, damage size, unit cost by repair method, and repair cost on deck at a future point. On the other hand, since the practical method utilizes the deck condition estimation model that has already been developed by the Seoul National University research team, the future deck condition can be provided, and the deck repair cost is estimated based on the estimated deck condition. A repair cost estimation model has limitations in estimating the deck condition and damage because it directly estimates the deck repair cost. In terms of the repair cost estimation performance, the proposed methodology showed the highest performance (MAE: 6,996.3), and the practical method showed the lowest performance (MAE: 26,603.1). Figure 6.4 illustrates an example of the estimation process and result comparison between the three approaches. In summary, compared to the existing approaches, the proposed methodology provided all estimated information about the deck condition, damage size, and repair cost and showed outstanding performance in estimating deck repair cost for predictive

maintenance. Specifically, it was confirmed that the proposed methodology had 73.7% improved performance compared to the practical method and 41.3% improved performance compared to the repair cost estimation model.

Table 6.3 Comparison results between the proposed methodology and existing approaches

Type of predictive information	Proposed methodology	Existing approach	
		Practical method	Repair cost estimation model
Deck condition	* (F1 score 0.845)	**	
Damage size on deck	* (ERR 85.0%)		
Unit cost by repair method	* (ERR 64.2%)		
Deck repair cost	* (MAE: 6,996.3)	* (MAE: 26,603.1)	* (MAE: 11,925.5)

Note: (*) indicates the approach provides the predictive information; (**) indicates the predictive information is provided by the model that has already been developed; F1 score = weighted average F1 score; and ERR = error reduction rate to the SD.

● *Bridge No. 027148*

[Ground Truth (Repair Record)]

(Damage Size) × (Unit Cost) by Repair Method			Deck Repair Cost (1,000won)
Grouting (m)	Surface Repair (㎡)	Section Repair (㎡)	
		(5.00) × (357.4)	1,655.4

[Proposed Methodology]

Condition Grade	Damage Size								
	LC	AC	LE	MC	SP	SC	SG	CE	BR
C	0	0	0	3.83	0.36	0.94	0	0.61	0

(Damage Size) × (Unit Cost) by Repair Method			Deck Repair Cost (1,000won)	Difference from Ground Truth
Grouting (m)	Surface Repair (㎡)	Section Repair (㎡)		
	(3.83) × (228.0)	(1.91) × (409.5)	1,787.1	**131.7 (1,000won)**

[Practical Method]

Condition Grade	Unit Repair Cost	Total Size of Deck	CCCI (as of Dec. 2021)	Deck Repair Cost (1,000won)	Difference from Ground Truth
C	14.45 (1,000won/㎡)	1,320 (㎡)	0.951	20,056.8	**18,401.4 (1,000won)**

[Repair Cost Estimation Model]

INPUT	→ XGBoost Regression →	Deck Repair Cost 4,354.4(1,000won)	Difference from Ground Truth
			2,699.0 (1,000won)

Note: LC=Line-Cracking (m); AC= Area-Cracking (㎡); LE=Leakage and Efflorescence (㎡); MC=Map Cracking (㎡); SP=Spalling (㎡); SC=Scaling (㎡); SG=Segregation (㎡); CE=Corrosion of Exposed Rebar (㎡); BR=Breakage (㎡); and CCCI=construction cost conversion index.

Figure 6.4 Example of the estimation processes and results for the proposed methodology and existing approaches

6.3. Industrial Applications

The experimental results showed that the proposed methodology had superior performance in estimating specific information (i.e., the condition grades, damage size, and repair cost) on bridge elements for predictive maintenance compared to the existing approaches. Through the developed methodology, the damage size and unit cost by repair method at a future time when maintenance will be performed can be estimated in detail. In line with the construction cost calculation method, the repair costs on elements estimated based on this information can be more concrete and precise than the estimated costs in practice.

The predictive information can be used as a basis for bridge managers to prepare details and costs for repair works in advance and establish a reasonable repair plan, including repair methods, priorities, and budgets. Bridge managers can also obtain a reasonable range for damage size and repair costs that may occur on bridge elements in the future from the predictive information. This can also help restrict unnecessary repair activities and prevent exorbitantly high repair costs in bridge maintenance practice.

In addition, it was confirmed that the developed methodology could estimate the condition, damage size, and repair cost on bridge elements for

consecutive future points in time. This predictive information can be utilized by managers to examine element deterioration patterns in the mid to long-term rather. It can also help managers plan efficient repair times and costs by providing information on future points when a sharp increase in repair costs is expected. The change in damage size over time can be useful for discovering the patterns by types of damage, such as the rate of increase in damage size and the relationship between damage types.

Chapter 7. Conclusions

This chapter summarizes and discusses the objectives, achievements, and contributions of this research. Recommendations for future research are also provided.

7.1. Summary of Research Objectives and Achievements

The primary objective of this research presented in this dissertation was to provide bridge managers with integrated predictive maintenance information based on element condition, damage size, and repair cost estimation. To accomplish this objective, the specific objectives were (1) bridge element condition estimation based on outstanding algorithm selection and influential variables identification to provide information on where to undertake repair, (2) bridge damage size estimation on elements through a comparison of the regression model and the classification model to provide information on how much repair-required damage there will be, and (3) bridge repair cost estimation on elements according to damage size and unit cost by repair method to provide information on what the repair cost will be. To address the research objectives, this research achieved the results and findings as follows:

(1) The author developed an optimized model to estimate bridge elements' condition by utilizing the outstanding algorithm and the influential variables. XGBoost was selected as the optimal algorithm, and 'bridge age,' 'first past condition grade of deck,' 'ADT,' 'annual freeze-thaw frequency,' 'bridge length,' and 'total width' were explored as representative influential variables. The optimized model showed satisfactory performance with an average weighted average F1 score of 0.876 and an average AUC of 0.840.

(2) The author developed and compared regression and classification models using XGBoost and DNN to estimate repair-required damage size by type of element's damage. As a result of model evaluation, the regression model with XGBoost showed the best performance with an error reduction rate of 84.3% to the standard deviation. Although the regression model had superior performance, the author also found that the classification model had lower model complexity and higher robustness to outliers than the regression model.

(3) To estimate damage size by repair method, the author explored data distribution according to the damage size and portion by repair

method and then developed classification models using XGBoost to estimate the damage portion by repair method. The models showed a weighted average F1 score of 0.802 and 0.938 for respectively line-cracking and segregation of deck. To identify unit cost by repair method, influential variables affecting the unit cost were selected by conducting an expert interview, and the unit cost was expected based on the similarity between data for the selected seven variables (i.e., ‘damage size,’ ‘ADT,’ ‘bridge age,’ ‘bridge length,’ ‘height,’ ‘management agency,’ and ‘main superstructure type’) The total repair cost could be calculated by multiplying the estimated damage size and unit cost by repair method.

To validate the proposed methodology, the author implemented the experiment to conduct performance verification and demonstrate the superiority in providing predictive maintenance information by comparing with existing approaches. The proposed methodology could estimate predictive maintenance information (i.e., the condition grade, damage size, and repair cost on bridge elements) in line with the construction cost calculation method. In estimating deck repair costs, 73.7% and 41.3% performance improvement was shown compared to the practical method and

the repair cost estimation model, respectively. Consequently, the research methodology enabled predictive bridge maintenance to respond to future maintenance demand in advance by estimating element condition, repair-required damage size, and repair cost.

7.2. Research Contributions

The main contributions of this research include the following: (1) determining three specific types of information about predictive bridge maintenance; (2) identifying data-driven approaches that fit the BMS data to derive three specific types of information; (3) utilizing predictive information for bridge managers in bridge maintenance practice, and (4) reducing bridge life-cycle costs and realizing a safe society. This research specifically contributed to the body of knowledge by doing the following:

(1) This research determined three specific types of predictive maintenance information about a future time—where to undertake repair, how much repair-required damage there will be, and what the repair cost will be—for predictive bridge maintenance, according to the construction cost calculation method. The information supports bridge managers in making maintenance decisions to respond to future maintenance demands ahead of time.

(2) This research identified data-driven approaches for element condition, damage size, and repair cost estimation to derive these three types of predictive information. For each step of the proposed methodology,

the author developed an estimation model with an optimal algorithm and combination of variables that fit BMS data. The proposed methodology provides bridge managers with predictive information that integrates the three types of information estimated by the developed models.

(3) In bridge maintenance practice, utilizing predictive information enables bridge managers to maintain proper bridge condition by proactively preparing for future condition, damage, and repair works on bridge elements (e.g., details and costs based on the damage size and unit cost by repair methods). In addition, bridge managers can obtain from the predictive information a reasonable range for damage size and repair costs that may occur on elements in the future. This can help restrict unnecessary repair activities and prevent exorbitantly high repair costs in bridge maintenance practice.

(4) This research assists in reducing bridge life-cycle costs by discovering influential factors that affect the bridge condition and damage in the management field and reflecting them in the bridge's life-cycle (i.e., design, construction, and management). It eventually

contributes to making society safer by preventing bridge safety accidents through predictive maintenance.

7.3. Recommendations for Future Research

Even so, there are still opportunities for improvements and future research that would further enhance this research. In order to validate the further applicability and improve the performance of this research, the recommendations for future research should be followed:

(1) To improve the performance of this research, additional data should be accumulated in the BMS database and used for data analysis and model training. In particular, it was confirmed that the insufficient number of data at the damage level and the biased data distribution (e.g., damage size distribution biased toward small values) adversely affected the model performance; thus, a large amount of evenly distributed data can help improve the model performance. Furthermore, enhancing the collected data's reliability by supplementing the collection and verification systems for BMS data helps improve the developed model's performance and practical applicability. In addition, this research had limitations in directly considering the repair history to estimate element condition and damage size. The model's reliability can be improved by linking inspection and repair records and utilizing the repair information as

an explanatory variable for estimating element condition, damage size, repair cost.

(2) To validate the further applicability of this research, additional research should be conducted to expand the research scope. The proposed research methodology can be applied to several bridge types (e.g., steel bridges), other bridge elements (e.g., girder and pavement), and BMS data from other countries. Specifically, comparing the model performance by region or country and examining which characteristics cause performance differences can suggest practical insights for bridge maintenance to managers. Furthermore, the proposed methods can be utilized to other urban infrastructures (e.g., tunnels and a water distribution system). This will enable predictive maintenance across various types of infrastructures by providing managers with information such as condition, repair-required damage size, and repair cost by component.

(3) To improve practical applicability, the author recommends future research to establish a smart bridge management system in which the proposed research framework is implemented. In the system, the

bridge information, inspection records, and repair records accumulated in the BMS database can be automatically collected and preprocessed at the level of the bridge, element, and damage, and environmental information can be updated by linking with external databases. The system can utilize the preprocessed data to estimate element condition, damage size, and repair cost at a specific future time set by the bridge manager and enables preemptive notification of such predictive information. 3D modeling and object-based building information modeling can also help with the ease of information storage and visualization.

Bibliography

AASHTO (American Association of State Highway and Transportation Officials). (1997). *Guide for Commonly Recognized (CoRe) Structural Elements*. Washington, D.C.: AASHTO.

AASHTO (American Association of State Highway and Transportation Officials). (2010). *AASHTO Bridge Element Inspection Guide Manual.* Washington, D.C.: AASHTO.

AASHTO (American Association of State Highway and Transportation Officials). (2021). *Guide to bridge preservation actions.* Washington, D.C.: AASHTO.

Agrawal, A. K., Kawaguchi, A., and Chen, Z. (2010). "Deterioration Rates of Typical Bridge Elements in New York." *Journal of Bridge Engineering*, 15(4), 419–429.

Ali, G., Elsayegh, A., Assaad, R., and El-Adaway, I. H. (2020). "Deck, Superstructure, and Substructure Deterioration Prediction for Bridges Using Deep Artificial Neural Networks." In *Proc., Construction Research Congress 2020*, 135–144. Reston: American Society of Civil Engineers (ASCE).

Alsharqawi, M., Zayed, T., and Abu Dabous, S. (2018). “Integrated condition rating and forecasting method for bridge decks using Visual Inspection and Ground Penetrating Radar.” *Automation in Construction*, 89, 135–145.

Arik, S. Ö., and Pfister, T. (2021). “TabNet: Attentive Interpretable Tabular Learning.” In *Proc., the AAAI Conference on Artificial Intelligence,* 6679–6687. Palo Alto: Association for the Advancement of Artificial Intelligence (AAAI).

Assaad, R., and El-Adaway, I. H. (2020). “Evaluation and Prediction of the Hazard Potential Level of Dam Infrastructures Using Computational Artificial Intelligence Algorithms.” *Journal of Management in Engineering*, 36(5), 04020051.

Bansal, S. (2018). “Data Science Trends on Kaggle.” Accessed April 1, 2022. https://www.kaggle.com/code/shivamb/data-science-trends-on-kaggle/notebook.

Bektas, B. A., Carriquiry, A., and Smadi, O. (2013). “Using Classification Trees for Predicting National Bridge Inventory Condition Ratings.” *Journal of Infrastructure Systems*, 19(4), 425–433.

Bishop, C. M. (2006). *Pattern Recognition and Machine Learning.* New York: Springer.

Bolukbasi, M., Mohammadi, J., and Arditi, D. (2004). “Estimating the Future Condition of Highway Bridge Components Using National Bridge Inventory Data.” *Practice Periodical on Structural Design and Construction*, 9(1), 16–25.

Breiman, L., Friedman, J. H., Olshen, R. A., and Stone, C. J. (1984). *Classification And Regression Trees*. New York: Taylor & Francis.

Bu, G. P., Lee, J. H., Guan, ; H, Loo, Y. C., and Blumenstein, M. (2015). “Prediction of Long-Term Bridge Performance: Integrated Deterioration Approach with Case Studies.” *Journal of Performance of Constructed Facilities*, 29(3), 04014089.

Buduma, N., and Lacascio, N. (2017). *Fundamentals of Deep Learning: Designing Next-Generation Machine Intelligence Algorithms*.Sebastopol: O’Reilly Media.

Cesare, B. M. A., Santamarina, C., Members, A., Turkstra, C., and Vanmarcke, E. H. (1993). “Modeling Bridge Deterioration with Markov Chains.” *Journal of Transportaion Engineering*, 118(6), 820–833.

Chang, K., and Chi, S. (2019). “Bridge Clustering for Systematic Recognition of Damage Patterns on Bridge Elements.” *Journal of Computing in Civil Engineering*, 33(5), 04019028.

Chang, M., Maguire, M., and Sun, Y. (2019). “Stochastic Modeling of Bridge Deterioration Using Classification Tree and Logistic Regression.” *Journal of Infrastructure Systems,* 25(1), 04018041.

Chawla, N. V., Bowyer, K. W., Hall, L. O., and Kegelmeyer, W. P. (2002). “SMOTE: Synthetic Minority Over-sampling Technique.” *Journal of Artificial Intelligence Research,* 16, 321–357.

Chen, T., and Guestrin, C. (2016). “XGBoost: A Scalable Tree Boosting System.” In *Proc., the 22nd ACM SIGKDD International Conference on Knowledge Discovery and Data Mining,* 785–794, New York: Association for Computing Machinery.

Chen, X., and Jeong, J. C. (2007). “Enhanced Recursive Feature Elimination.” In *Proc., Sixth International Conference on Machine Learning and Applications,* 429–435. New Jersey: Institute of Electrical and Electronics Engineers (IEEE).

Couallier, V., L. Gerville-Réache, C. Huber-Carol, N. Limnios, and M. Mesbah. (2013). *Statistical models and methods for reliability and survival analysis.* Hoboken: Wiley.

Darmatasia, and Arymurthy, A. M. (2016). “Predicting the status of water pumps using data mining approach.” In *Proc., 2016 International*

Workshop on Big Data and Information Security, IWBIS 2016, 57–64. New Jersey: Institute of Electrical and Electronics Engineers (IEEE).

Ellingwood, B. R. (2010). "The role of structural aging in achieving life-cycle performance goals of civil infrastructure." In *Proc., the 2010 Structures Congress*, 2803–2808. Reston: American Society of Civil Engineers (ASCE).

Feng, D.-C., Wang, W.-J., Mangalathu, S., and Taciroglu, E. (2021). "Interpretable XGBoost-SHAP Machine-Learning Model for Shear Strength Prediction of Squat RC Walls. " *Journal of Structural Engineering*, 147(11), 04021173.

FHWA (Federal Highway Administration). (1995). *Recording and Coding Guide for the Structure Inventory and Appraisal of the Nation's Bridges*. Washington, D.C.: FHWA.

FHWA (Federal Highway Administration). (2012). *Bridge inspector's reference manual, FHWA NHI 12-049*. Washington, D.C.: FHWA.

FHWA (Federal Highway Administration). (2018). *Bridge preservation guide*. Washington, D.C.: FHWA.

FHWA (Federal Highway Administration). (2022). "LTBP InfoBridge: Data." Accessed September 20, 2022. https://inforbridge.fhwa.dot.gov/Data.

Fisher, A., Rudin, C., and Dominici, F. (2019). “All Models are Wrong, but Many are Useful: Learning a Variable’s Importance by Studying an Entire Class of Prediction Models Simultaneously.” *Journal of Machine Learning Research*, 20, 1–81.

Frangopol, D. M., and Kong, J. S. (2000). “Expected Maintenance Cost of Deteriorating Civil Infrastructures.” In *Proc., the 1st US-Japan Workshop on Life-Cycle Cost Analysis and Design of Civil Infrastructure Systems*, 304, 22–47. Reston: American Society of Civil Engineers (ASCE).

Friedman, J. H. (2001). “Greedy function approximation: a gradient boosting machine.” *Annals of statistics*, 1189–1232.

Ghahari, S. A., Volovski, M., Alqadhi, S., and Alinizzi, M. (2019). “Estimation of annual repair expenditure for interstate highway bridges.” *Infrastructure Asset Management*, 6(1), 40–47.

Ghodoosi, F., Soliman A. S., Mehran Z., and Zayed, T. (2017). “Maintenance Cost Optimization for Bridge Structures Using System Reliability Analysis and Genetic Algorithms.” *Journal of Construction Engineering and Management*, 144(2), 04017116.

Gong, C., and Frangopol, D. M. (2020). "Condition-Based Multiobjective Maintenance Decision Making for Highway Bridges Considering Risk Perceptions." *Journal of Structural Engineering*, 146(5), 04020051.

Goodfellow, l., Bengio, Y., and Courville, A. (2016). *Deep learning*. Cambridge: MIT Press.

Gordian (2022). "RSMeans data: Construction Cost Estimating Software." Accessed August 30, 2022. https://www.rsmeans.com.

Gralund, M. S., and Puckett, J. A. (1996). "System for Bridge Management in a Rural Environment." *Journal of Computing in Civil Engineering*, 10(2), 97–105.

Hadjidemetriou, G. M., Herrera, M., and Parlikad, A. K. (2021). "Condition and criticality-based predictive maintenance prioritisation for networks of bridges. " *Structure and Infrastructure Engineering*, 18(8), 1207-1221.

Han, H., Wang, W. Y., and Mao, B. H. (2005). "Borderline-SMOTE: A new over-sampling method in imbalanced data sets learning." In *Proc., International Conference on Intelligent Computing 2005: Advances in Intelligent Computing*, 878–887. Berlin: Springer.

Han, J., Kamber, M., and Pei, J. (2011). *Data mining : concepts and techniques*. Waltham : Morgan Kaufmann.

He, H., and Ma, Y. (2013). *Imbalanced Learning: Foundations, Algorithms, and Applications*. New Jersey: Wiley-IEEE Press.

Hsu, H. H., and Hsieh, C. W. (2010). "Feature Selection via Correlation Coefficient Clustering." *Journal of Software*, 5(12), 1371–1377.

Huan, L., and Yu, L. (2005). "Toward integrating feature selection algorithms for classification and clustering." *IEEE Transactions on Knowledge and Data Engineering*, 17(4), 491–502.

Huang, R. Y., Mao, I. S., and Lee, H. K. (2010). "Exploring the deterioration factors of RC bridge decks: A rough set approach." *Computer-Aided Civil and Infrastructure Engineering*, 25(7), 517–529.

Huang, Y. H. (2010). "Artificial Neural Network Model of Bridge Deterioration." *Journal of Performance of Constructed Facilities*, 24(6), 597–602.

Huang, J., Huang, N., Zhang, L., and Xu, H. (2012). "A method for feature selection based on the correlation analysis." In *Proc., 2012 International Conference on Measurement, Information and Control*, 529–532. New Jersey: Institute of Electrical and Electronics Engineers (IEEE).

Jootoo, A., and Lattanzi, D. (2017). "Bridge Type Classification: Supervised Learning on a Modified NBI Data Set." *Journal of Computing in Civil Engineering*, 31(6), 04017063.

Kim, Y. J., and Yoon, D. K. (2010). “Identifying Critical Sources of Bridge Deterioration in Cold Regions through the Constructed Bridges in North Dakota.” *Journal of Bridge Engineering*, 15(5), 542–552.

KALIS (Korea Authority of Land & Infrastructure Safety). (2019). *Detailed Explanation of Guidelines for Maintenance and Performance Assessments - Bridge*. Jinju: KALIS.

KICT (Korea Institute of Civil Engineering and Building Technology). (2021). *Final Report: 2021 Information Cost and Performance Analysis.* Goyang: KICT.

KICT (Korea Institute of Civil Engineering and Building Technology). (2022a). “Construction Cost Management Center.” Accessed March 3, 2022. https://cost.kict.re.kr.

KICT (Korea Institute of Civil Engineering and Building Technology). (2022b). *Education of Bridge and Tunnel Management System Practice*. Goyang: KICT.

Kong, J. S., and Frangopol, D. M. (2003). “Life-Cycle Reliability-Based Maintenance Cost Optimization of Deteriorating Structures with Emphasis on Bridges.” *Journal of Structural Engineering*, 129(6), 818–828.

Korea Meteorological Administration (KMA) National Climate Data Center. (2022). “KMA Weather Data Service: Open MET Data Portal.” Accessed January 2, 2022. https://data.kma.go.kr.

Lattin, J., Carroll, J. D., Green, P. E. (2003). *Analyzing Multivariate Data.* Belmont: Cengage Learning.

Lim, S. (2019). “Bridge Damage Identification and Its Severity Estimation Using Artificial Intelligence.” Ph.D’s Thesis. Seoul, South Korea: Seoul National University.

Lim, S., and Chi, S. (2019). “Xgboost application on bridge management systems for proactive damage estimation.” *Advanced Engineering Informatics*, 41, 100922.

Lim, S., and Chi, S. (2021). “Damage Prediction on Bridge Decks considering Environmental Effects with the Application of Deep Neural Networks.” *KSCE Journal of Civil Engineering*, 25(2), 371–385.

Lim, S., Chung, S., and Chi, S. (2017). “Developing a pattern model of damage types on bridge elements using big data analytics.” In *Proc., the 34th International Symposium on Automation and Robotics in Construction*, 849–855. London: International Association for Automation and Robotics in Construction (IAARC).

Liu, H., and Zhang, Y. (2020). “Bridge condition rating data modeling using deep learning algorithm.” *Structure and Infrastructure Engineering*, 16(10), 1447–1460.

Liu, M., and Frangopol, D. M.. (2005). “Balancing Connectivity of Deteriorating Bridge Networks and Long-Term Maintenance Cost through Optimization.” *Journal of Bridge Engineering*, 10(4), 468–481.

Lozano-Diez, A., Zazo, R., Toledano, D. T., and Gonzalez-Rodriguez, J. (2017). “An analysis of the influence of deep neural network (DNN) topology in bottleneck feature based language recognition.” *PLoS ONE*, 12(8).

Lundberg, S. M., and Lee, S.-I. (2017). “A unified approach to interpreting model predictions.” In *Proc., 31st Conference on Neural Information Processing Systems*, 4765–4774. Red Hook: Curran Associates.

Martinez, P., Mohamed, E., Mohsen, O., and Mohamed, Y. (2020). “Comparative Study of Data Mining Models for Prediction of Bridge Future Conditions.” *Journal of Performance of Constructed Facilities*, 34(1), 04019108.

Mirzaei, Z., Adey, B. T., Klatter, L., and Kong, J. S. (2014). *Overview of existing Bridge Management Systems - Report by the IABMAS Bridge*

Management Committee. International Association for Bridge Maintenance and Safety (IABMAS).

MOLIT (Ministry of Land, Infrastructure and Transport). (2019). "Korean bridge and tunnel management system." Accessed December 21, 2019. https://nbms.kict.re.kr/nbms/index.jsp.

MOLIT (Ministry of Land, Infrastructure and Transport). (2021). *Guidelines for Maintenance and Performance Assessments.* Sejong: MOLIT.

MOLIT (Ministry of Land, Infrastructure and Transport). (2022a). S*tandard market unit cost for construction works in the first half of 2022.* Sejong: MOLIT.

MOLIT (Ministry of Land, Infrastructure and Transport). (2022b). "Traffic Monitoring System." Accessed January 2, 2022. https://road.re.kr.

Morcous, G. (2005). "Modeling Bridge Deck Deterioration by Using Decision Tree Algorithms." *Transportation Research Record: Journal of the Transportation Research Board*, 509–516.

Morcous, G. (2006). "Performance Prediction of Bridge Deck Systems Using Markov Chains." *Journal of Performance of Constructed Facilities*, 20(2), 146–155.

Morcous, G., Rivard, H., and Hanna, A. M. (2002). “Modeling Bridge Deterioration Using Case-based Reasoning.” *Journal of Infrastructure Systems*, 8(3), 86–95.

NTSB (National Transportation Safety Board). (2008). *Collapse of I-35W Highway Bridge Minneapolis, Minnesota August 1, 2007*. Washington D.C.: NTSB.

Reddy, M. C., Balasubramanyam, P., and Subbarayudu, M. (2013). “An Effective Approach to Resolve Multicollinearity in Agriculture Data.” *International Journal of Research in Electronics and Computer Engineering*, 1(1), 27–30.

Scherer, W. T., and Glagola, D. M. (1994). “Markovian models for bridge maintenance management.” *Journal of Transportation Engineering*, 120(1), 37–51.

Shan, Y., Contreras-Nieto, C., and Lewis, P. (2016). “Using Data Analytics to Characterize Steel Bridge Deterioration.” In *Proc., Construction Research Congress 2016: Old and New Construction Technologies Converge in Historic San Juan,* 1691–1699. Ruston: American Society of Civil Engineers (ASCE).

Shavitt, I., and Segal, E. (2018). “Regularization learning networks: deep learning for tabular datasets.” *Advances in Neural Information Processing Systems*, 31.

Shi, X., Zhao, B., Yao, Y., and Wang, F. (2019). “Prediction Methods for Routine Maintenance Costs of a Reinforced Concrete Beam Bridge Based on Panel Data.” *Advances in Civil Engineering*, 2019, 5409802.

Shmueli, G., Patel, N. R., and Bruce, P. C. (2010). *Data Mining for Business Intelligence: Concepts, Techniques, and Applications in Microsoft Office Excel with XLMiner*. New Jersey: Wiley.

Wang, M.-X., Huang, D., Wang, G., and Li, D.-Q. (2020). “SS-XGBoost: A Machine Learning Framework for Predicting Newmark Sliding Displacements of Slopes." *Journal of Geotechnical and Geoenvironmental Engineering*, 146(9), 04020074.

Wu, B., Zhang, L., and Zhao, Y. (2014). “Feature selection via Cramer’s V-test discretization for remote-sensing image classification.” *IEEE Transactions on Geoscience and Remote Sensing*, 52(5), 2593–2606.

XGBoost developers. (2021). “XGBoost.” Accessed April 3, 2002. https://xgboost.readthedocs.io.

Zhang, D., Qian, L., Mao, B., Huang, C., Huang, B., and Si, Y. (2018). “A Data-Driven Design for Fault Detection of Wind Turbines Using Random Forests and XGboost.” *IEEE Access*, 6, 21020–21031.

Zhao, J., and Tonias, D. (2013). *Bridge Engineering*. New York: McGraw-Hill Education.

Zhao, Z., and Chen, C. (2002). “A fuzzy system for concrete bridge damage diagnosis.” *Computers and Structures*, 80, 629–641.

국문 초록

교량의 스마트 유지관리를 위한 부재상태, 손상크기, 보수비용 추정

장태연

서울대학교 대학원
건설환경공학부

교량을 적절한 상태로 유지하기 위해, 관리자는 각 부재의 상태와 손상을 주기적으로 점검하고 예산 내에서 알맞은 유지보수 계획을 수립한다. 이 과정에서 공사 물량과 단가의 곱으로 정의되는 건설공사비 계산 방법을 고려할 때, 구체적으로 어떤 부재에서 얼마나 많은 손상에 대한 보수가 필요한지 아는 것은 중요하다. 그러나, 부재 손상의 양상은 공용년수, 제원, 최근 점검이력 등 교량의 특성에 따라 다양하게 나타나기 때문에, 유지보수가 수행될 미래 시점에서 보수가 필요한 손상의 크기와 보수비용을 확인하는 데에 어려움이 있다. 따라서, 교량 관리자에게 유지보수가 수행되는 특정 미래 시점에서의 세 가지 예측 정보(‘어떤 부재를 보수해야 하는지’, ‘보수가 필요한 손상이

얼마나 있는지', '보수하는 데에 얼마의 비용이 드는지')를 제공하는 것은 필요하다. 이를 위해 다수의 연구에서는 교량유지관리시스템 데이터를 활용하여 교량의 향후 부재상태와 손상의 발생여부 및 심각도를 추정하고 향후 보수비용을 분석했다. 기존 연구의 성과에도 불구하고, 향후 예상되는 손상크기에 기반하여 정확한 보수비용을 추정하는 데에는 여전히 한계점이 존재한다.

이를 해결하기 위해, 본 연구는 교량 부재상태, 손상크기, 보수비용 추정에 기반하여 관리자에게 스마트 유지관리를 위한 예측 정보를 제공하고자 한다. 첫 째로, 교량정보, 환경정보, 점검기록을 활용하여 최적 알고리즘 선택 및 영향변수 도출에 기반한 최적의 교량 부재상태 추정모델을 개발한다. 둘 째로, 보수가 필요한 손상크기를 추정하기 위해 교량정보, 환경정보, 손상점검내역을 활용하여 분류모델과 회귀모델을 구축하고 비교한다. 셋 째로, 예상되는 손상에 대한 보수비용을 추정하기 위해 교량정보, 환경정보, 손상점검내역, 보수공사내역을 활용하여 보수 공법별 손상크기와 단가를 추정하는 방법을 제안한다.

제안된 방법론을 검증하기 위해 본 연구는 추정 가능한 정보의 유형 및 모델 성능 측면에서 기존 방법들과의 비교 분석을 수행했다. 검증 결과, 제안된 방법론은 스마트 교량 유지관리를

위해 필요한 세 가지 예측 정보를 구체적으로 제공할 수 있으며 보수비용을 더 정확하게 추정할 수 있음을 확인했다.

결론적으로, 본 논문은 교량의 스마트 유지관리를 위한 부재상태, 손상크기, 보수비용 추정 방법론을 제안했다. 특히, 본 연구는 교량 관리자의 유지보수 의사결정을 지원하기 위한 세 가지 예측 정보를 정의하고, 이러한 정보를 도출하기 위해 교량유지관리시스템 데이터에 잘 맞는 데이터 기반 접근법을 제안했다. 이는 교량의 스마트 유지관리 및 예방적 유지관리에 있어 구체적인 손상크기를 추정하고 공법별 손상크기와 단가를 활용해 향후 보수비용을 제공하는 것에 대한 선구적인 시도이다. 제안된 방법론은 교량 유지관리 실무에서 부재의 상태 저하와 손상을 사전에 파악하고 보수조치를 준비함으로써 교량을 적절한 상태로 유지하는 데에 도움을 줄 수 있다. 또한 교량 관리자에게 향후 발생할 수 있는 손상크기와 보수비용의 합리적인 범위를 제공하여 불필요한 보수공사나 과도한 보수비용을 제한하는 데에 활용될 수 있다. 궁극적으로 본 연구는 교량의 생애주기 비용 감소와 안전한 사회 구현에 기여할 것이다.

주요어: 시설물 유지관리; 스마트 유지관리; 교량유지관리시스템; 상태 추정; 교량 손상크기; 교량 보수비용; 보수공법별 단가; 데이터 기반 접근법

학번: 2017-27720